2006

GROUP 13 CHELATES IN PHOSPHATE DEALKYLATION

Amitabha Mitra
University of Kentucky, amitra2@yahoo.com

ABSTRACT OF DISSERTATION

Amitabha Mitra

The Graduate School
University of Kentucky
2006

GROUP 13 CHELATES IN PHOSPHATE DEALKYLATION

ABSTRACT OF DISSERTATION

A dissertation submitted in partial fulfillment of the requirements for the degree of Doctor of Philosophy in the College of Arts and Science at The University of Kentucky

By

Amitabha Mitra

Lexington, Kentucky

Director: Dr. David A. Atwood, Professor of Chemistry

Lexington, Kentucky

ABSTRACT OF DISSERTATION

GROUP 13 CHELATES IN PHOSPHATE DEALKYLATION

A series of mononuclear boron halides of the type LBX_2 (LH = N-phenyl-3,5-di-*t*-butylsalicylaldimine, X = Cl (**2**), Br (**3**)) and LBX (LH_2 = N-(2-hydroxyphenyl)-3,5-di-*t*-butylsalicylaldimine, X = Cl (**7**), Br (**8**); LH_2 = N-(2-hydroxyethyl)-3,5-di-*t*-butylsalicylaldimine, X = Cl (**9**), Br (**10**); LH_2= N-(3-hydroxypropyl)-3,5-di-*t*-butylsalicylaldimine, X = Cl (**11**), Br (**12**)) were synthesized from their borate precursors $LB(OMe)_2$ (**1**) (LH = N-phenyl-3,5-di-*t*-butylsalicylaldimine) and LB(OMe) (LH_2 = N-(2-hydroxyphenyl)-3,5-di-*t*-butylsalicylaldimine (**4**), N-(2-hydroxyethyl)-3,5-di-*t*-butylsalicylaldimine (**5**), N-(3-hydroxypropyl)-3,5-di-*t*-butylsalicylaldimine (**6**)). The borate precursors, **1**, **4** - **6**, in turn, were prepared by refluxing the corresponding ligands LH or LH_2 with excess $B(OMe)_3$. The boron halide compounds were air- and moisture-sensitive and compound **7** on hydrolysis gave the oxo-bridged compound **13** that contained two seven-membered boron heterocycles. The boron halide compounds dealkylated trimethyl phosphate in stoichiometric reactions to produce methyl halide and unidentified phosphate materials. Compounds **8** and **12** were found to be the most effective dealkylating agents. Compound **8** on reaction with *t*-butyl diphenyl phosphinate produced a unique boron phosphinate compound $LB(O)OPPh_2$ (**14**) containing a terminal phosphinate group. Compounds **1**-**14** were characterized by ^{1}H, ^{13}C, ^{11}B, ^{31}P NMR, IR, MS, EA and MP. Compounds **5**, **6**, **11**, **12** and **13** were also characterized by single-crystal X-ray diffraction.

The alkane elimination reaction between Salen(^{t}Bu)H_2 ligands and diethylaluminum bromide was used to prepare the four Salen aluminum bromide compounds, salen(^{t}Bu)AlBr (**15**) (salen = *N,N′*-ethylenebis(3,5-di-*tert*-butylsalicylideneimine)), salpen(^{t}Bu)AlBr (**16**) (salpen = *N,N′*-propylenebis(3,5-di-*tert*-butylsalicylideneimine)), salben(^{t}Bu)AlBr (**17**) (salben = *N,N′*-butylenebis(3,5-di-*tert*-butylsalicylideneimine)) and salophen(^{t}Bu)AlBr (**18**) (salophen = *N,N′*-*o*-phenylenenebis(3,5-di-*tert*-

butylsalicylideneimine)). The compounds contained five-coordinate aluminum either in a distorted square planar or a trigonal bipyramidal environment. The bromide group in these compounds could be displaced by triphenylphosphine oxide or triphenyl phosphate to produce the six-coordinate cationic aluminum compounds [salen(^{t}Bu)Al($Ph_3PO)_2$]Br (**19**), [salpen(^{t}Bu)Al($Ph_3PO)_2$]Br (**20**), [salophen(^{t}Bu)Al($Ph_3PO)_2$]Br (**21**) and [salophen(^{t}Bu)Al{$(PhO)_3PO\}_2$]Br (**22**). All the compounds were characterized by ^{1}H, ^{13}C, ^{27}Al and ^{31}P NMR, IR, mass spectrometry and melting point. Furthermore, compounds **15**, **16**, **17**, **18**, **20, 21** and **22** were structurally characterized by single-crystal X-ray diffraction. Compounds **15, 17** and **18** dealkylated a series of organophosphates in stoichiometric reaction by breaking the ester C─O bond. Also, they promoted the dealkylation reaction between trimethyl phosphate and added boron tribromide. Stoichiometric reaction of compound **15** with trimethyl phosphate produced the aluminophosphinate compound salen(^{t}Bu)AlOP(O)Ph_2 (**23**). Compound **16** on reaction with tributyl phosphate produced the aluminophosphate compound [salpen(^{t}Bu)AlO]$_2$[$(BuO)_2PO]_2$ (**24**). Compounds **23** and **24** were characterized by single-crystal X-ray diffraction and spectroscopically.

KEYWORDS: Aluminum, Boron, Dealkylation, Salen, Phosphate

Amitabha Mitra
June 14, 2006

GROUP 13 CHELATES IN PHOSPHATE DEALKYLATION

By

Amitabha Mitra

Dr. David A. Atwood

(Director of Dissertation)

Dr. Mark S. Meier

(Director of Graduate Studies)

RULES FOR THE USE OF DISSERTATIONS

Unpublished dissertations submitted for the Doctor's degree and deposited in the University of Kentucky Library are as a rule open for inspection, but are to be used only with due regard to the rights of the authors. Biblio-graphical references may be noted, but quotations or summaries of parts may be published only with the permission of the author, and with the usual scholarly acknowledgments.

Extensive copying or publication of the dissertation in whole or in part also requires the consent of the Dean of The Graduate School of the University of Kentucky.

DISSERTATION

Amitabha Mitra

The Graduate School

University of Kentucky

2006

GROUP 13 CHELATES IN PHOSPHATE DEALKYLATION

DISSERTATION

A dissertation submitted in partial fulfillment of the requirements for the degree of Doctor of Philosophy in the College of Arts and Science at The University of Kentucky

By

Amitabha Mitra

Lexington, Kentucky

Director: Dr. David A. Atwood, Professor of Chemistry

Lexington, Kentucky

2006

Dedicated to

my parents and sister, and to the memory of my grandmothers

Acknowledgments

I am indebted to a number of people for making this dissertation work possible. The list begins with my advisor, Prof. David A. Atwood, for his guidance, constant motivation and insight, and for not letting my shoulders drop down even when the project was going through difficult phases at times. I am very grateful for the tremendous amount of independence that he allowed me in his laboratory, and I also must thank him for teaching me the art of publication writing. I thank my committee members, Professors John Selegue, Folami Ladipo, Mark Keane, and Barbara Knutson, for keeping me on the right track with their knowledge, experience, criticism, and very helpful ideas. I cannot thank Dr. Sean Parkin enough for his help with X-ray crystallography. Thanks to John Layton for all his help with the NMR instrument. I am grateful to three undergraduate researchers, Lauren DePue, Jeffrey Struss and Bijal Patel, who worked with me at different stages of this project and contributed a good amount to the experimental work. I appreciate the help of former Atwood group members, Drs. Yuzhong Wang, Burl Yearwood and Timothy Keizer for training me during my beginning days in the Atwood lab. I thank the entire Atwood research group for their support and help in the lab, sharing their ideas and skills, and also for making the lab a very enjoyable workplace. I am thankful to Dr. Richard Eaves for his insights and useful discussions. Thanks to Yuvonne and all the office staff for their excellent support and help. I acknowledge the funding from the Kentucky Science and Engineering Foundation, Merloc Chemical Company, Inc., and Tracy Farmer Center for the Environment. Thanks also to the Department of Chemistry for supporting me throughout my Ph.D. career.

Finally, I want to thank my parents and my sister. After all, I would not be where I am today without their love, support, encouragement and patience.

Table of Contents

List of Tables

List of Figures

Chapter 1

Introduction and Background

1.1. Group 13 chelates

Since the first use of $AlCl_3$ in what later became known as the Friedel-Craft reaction in 1877, [1] Group 13 Lewis acids have been widely used for catalytic and synthetic applications. This was advanced significantly by Ziegler in 1955 by the discovery that organoaluminum reagents polymerized olefins. [2] Extensive research in this area during the past few decades has lead to the discovery of group 13 compounds with interesting structures and a wide range of coordination environments for the metal. [3] Chelated group 13 compounds are becoming increasingly popular with the use of ligands with tailor-made structures. Many of these chelate compounds have far superior air and moisture stability compared to traditional unchelated group 13 Lewis acids. These compounds are finding applications in fields which have normally been dominated by transition metal compounds. Examples include important areas, such as asymmetric catalysis and oxirane polymerizations.

The chelate effect [4, 5] refers to the increased stability of a complex formed from multidentate ligands compared to a similar complex containing monodentate ligands. Thus a complex containing a chelate ring has a higher formation constant compared to a similar one containing no chelate ring. One common example is:

$Ni^{2+}(aq) + 6NH_3(aq) = [Ni(NH_3)_6]^{2+}(aq)$ $\quad \log\beta = 8.61$

$Ni^{2+}(aq) + 3en(aq) = [Nien_3]^{2+}(aq)$ $\quad \log\beta = 18.28$

There are two concepts that have been invoked to explain the higher stability of chelate complexes compared to complexes with individual ligands. According to one concept, which is based on thermodynamic considerations, the increased stability is due to the increased entropy resulting from the net increase of the number of unbound molecules released when the chelate is formed. According to the other concept, which is based on geometrical consideration, the stability is due to the increased proximity of the other ligand atom(s) of the chelate once the first metal ligand bond is formed. This second concept implies that when one end of a multidentate ligand binds to a metal ion, the other ends stay in close proximity to the ion creating a high local concentration of the ligand atoms while a monodentate ligand can diffuse away from the metal ion. The first example of a group 13 chelate is probably tris(acetylacetonate) aluminum, first reported in 1887. [6] In this compound aluminum has an octahedral geometry. Group 13 elements form a variety of stable chelates particularly with combinations of nitrogen and oxygen ligands. Of particular stability is the complex of EDTA with aluminum (stability constant = 16.3). In solution EDTA displaces aqua or hydroxo ligands from $[Al(H_2O)_x(OH)_y]^{n+}$.

1.2 Schiff base ligands

Schiff base [7] ligands were first synthesized in 1864 and contain the azomethine group (-RC=N-). They are formed by the condensation of an amine with an aldehyde (Figure 1.1). However, the first Schiff base-metal complex, bis(salicylaldimino)Cu(II), [8] was isolated in 1840 from the combination of cupric acetate, salicylaldehyde, and aqueous ammonia. Schiff base ligands have played a very important role in transition metal [9] and main group [10-15] coordination chemistry. They are easy to prepare and are of great synthetic flexibility and structural variability. This provides the ability to control the

coordination environment of the coordinated metal center. Condensation between aldehydes and amines can be effected in different conditions and in different solvents. The presence of a dehydrating agent, usually $MgSO_4$, favors the formation of Schiff bases. They are generally purified by recrystallization since chromatography using silica gel can cause decomposition of the product. They can be characterized by conventional organic techniques. The presence of the C=N group gives a strong IR absorption in the region between 1680 and 1603 cm^{-1}. The UV spectra are characterized by bands in the range 235-272 nm for the unconjugated C=N chromophore. However, conjugation with alkenic or aryl groups causes a change in the spectrum. The presence of keto-amine tautomerism can be observed by NMR.

Schiff base ligands usually contain both N and O as the donor atoms. The most widely studied types of these ligands are derivatives of salicylaldimines (Figure 1.2(a)). The most popular of these are the "Salen" class of ligands (Figure 1.2(b)) which are formed from the condensation of two moles of salicylaldehyde with one mole of a diamine. These are tetradentate, potentially dianionic ligands with two coordinate-covalent and two covalent sites. They are similar to porphyrin ligands but are less expensive and easier to synthesize. Also the "open front" of the Salen compounds can be utilized in catalytic reactions. These ligands provide a wide range of options in terms of varying the steric and electronic properties around the metal center. For example, a variety of organic groups can be incorporated into the ligand "backbone". Moreover, their solubility can be varied by incorporating appropriate substituent groups on the phenyl rings. Salen(^{t}Bu) ligands are more appealing compared to unsubstituted Salen(H_2) ligands because of their

better solubility in organic solvents and hence better scope of characterizing their solution-state properties.

Salen ligands have been used to prepare both mono- and binuclear compounds.[10] Besides tetradentate Salen ligands containing two N and two O as donor atoms (N_2O_2), Schiff base ligands having denticities of two, three and higher are also common. Some of the examples include N-phenylsalicylideneimine (NO), N-phenylsalicylidene-*o*-aminophenol (NO_2) and Phensal(^{t}Bu)H_3 (N_2O)(where Phensal(^{t}Bu)H = salicylidene(1-iminophenylene-2-amine) ligands.

Group 13 elements, specially boron and aluminum, are known to form various mononuclear (1:1 ligand to metal) and binuclear (1:2 ligand to metal) chelate complexes with many Schiff base ligands, especially Salen type ligands. In most cases the bonding occurs through the oxygen or nitrogen atoms of the chelating ligands. This may be ascribed to high B-O (809 kJmol^{-1}), B-N (390 kJmol^{-1}), Al-O (511 kJmol^{-1}) and Al-N (298 kJmol^{-1}) bond energies. [16]

While aluminum and gallium form both mono- and binuclear chelates of the type LMX and L(MX_2)$_2$ (M=Al or Ga; X= alkyl, alkoxide, aryloxide, siloxide group), respectively, depending on ligand to metal stoichiometry used, boron mainly forms binuclear chelates of the type L(MX_2)$_2$ or L(MXX')$_2$ (M=Al or Ga; X,X'= alkyl, alkoxide, aryloxide, siloxide group) even with excess ligand. This is because of the tendency of boron to adopt a four-coordinate tetrahedral geometry which is not possible with mononuclear compounds with Salen ligands. In addition to neutral compounds, cationic five- and six-coordinate aluminum [17-22] and four coordinate boron [23] compounds of Schiff base ligands have been synthesized recently.

1.3. Group 13 complexes for Lewis acid catalysis

The Lewis acidic property of group 13 compounds stems from the electron deficiency around the metal center. This is dependent upon the extent of the interaction of the available *p* orbital of the metal with unshared or π-electrons of the ligand system. From an electronegativity consideration only, the Lewis acidity of group 13 compounds should decrease along the series B>Al>Ga>In>Tl. However other factors such as size of the metal, interaction of the metal *p* orbital with the unshared electrons of the ligand already present and steric factors could alter the trend. One advantage of group 13 chelated complexes over simple group 13 compounds like BCl_3 or $AlCl_3$ is the ability to tune their structure by varying the coordinated ligands, and, thus, prepare 'designer Lewis Acids.' Moreover, the ligand does not participate in the reaction. Both neutral and cationic group 13 chelate complexes find various applications as Lewis acids. These include Aldol transfer reaction, [24] Tishchenko reactions [24] Diels-Alder reactions [25-30], oligomerization of oxiranes [17, 18, 23] and lactides, [31, 32] and dealkylation of organophosphate esters. [33-35]

1.4. Organophosphate compounds

The esters of orthophosphoric acid can be classified into phosphate monoesters, diesters and triesters (Fig. 1.3). Mono- and di-esters have ionizable hydrogen atoms that can be replaced by cations. Triesters are covalent compounds and they do not exist naturally; they must be synthesized. Phosphate esters contain one or more P-O-C linkages where the P-O (~359 KJ mol^{-1}) and C-O (~355 KJ mol^{-1}) bonds are of comparable energy. [36]

Organophosphate esters are a commercially important class of compounds finding applications in various areas. [37, 38] For example, tri-n-butyl phosphate is used for the

selective extraction of metals, particularly uranium compounds, and as a hydraulic fluid in aircraft. Tris(2-ethylhexyl) phosphate is used as a plasticizer in polymers and is a flame retardant. Triaryl phosphates are used as additives for gasoline, plasticizers, lubricants, coolants, hydraulic fluids, and flame retardants. Various organophosphate compounds are used in pesticides. The first laboratory synthesis of an organophosphate ester was reported in 1820 from the reaction of phosphoric acid and ethanol [39] However, the first large-scale use of organophosphate esters was developed during the 1930s for potential use in nerve gas agents. [37]

The phosphate ester bond is very important in living systems. It appears in many biological molecules [40] such as DNA and RNA, and ATP (Fig. 1.4). Also, many coenzymes are esters of phosphoric acid. It participates in storage and transfer of genetic information, carries chemical energy and regulates the activity of enzymes and signaling molecules in the cell.

1.5. Organophosphate toxicity

Organophosphate esters are active components of chemical warfare agents and pesticides. They can enter the body by inhalation, through skin or orally. They function by irreversibly blocking the serine hydroxy group in the enzyme acetylcholinesterase by phosphorylation (Figure 1.5). [41-43] Acetylcholinesterase is responsible for the hydrolysis of the neurotransmitter acetylcholine (Figure 1.5). Loss of the activity of this enzyme causes buildup of acetylcholine in the synapse and as a result the neural signal to the muscle is not terminated. This overstimulation leads to muscular paralysis and death. This occurs in seconds to minutes after the exposure and is the basis of the extreme neurotoxicity of nerve gas agents and pesticides.

Common antidotes for nerve gases are pyridine aldoxime (e.g., Pralidoxime), Atropine and Valium (Figure 1.6). Aldoxime reacts with inhibited acetyl cholinesterase and regenerates the active enzyme from the phosphorylated form. Atropine acts as an antagonist for the acetylcholine receptor in the synapse. It binds to the receptor and thus prevents transmission of the signal created by the binding of acetylcholine to the synapse. It thus gives protection from the build up of excess acetylcholine that results from the inhibition of acetylcholinesterase by the nerve agent. Anticonvulsants such as Valium protect against convulsions and the resulting brain damage.

Today, organophosphate pesticides are the most widely used type of pesticides and have replaced organochlorine pesticides, which are more persistent in the environment. Despite their potential environmental problems the use of organophosphate pesticides has been increasing and is predicted to increase in the future because of the lack of suitable substitutes. [44] Decontamination of nerve gases is required in battlefields, laboratories, storage and destruction sites. Long-lived pesticides pose a threat when they spread beyond their intended application. Examples of some nerve gas agents and pesticides are shown in Figure 1.7. All of these compounds possess a P-O-C linkage in their structure. The cleavage of the P-O-C bond has been targeted as a means of deactivating these toxic agents. [45, 46] This is convenient due to the nucleophilicity of the phosphorus and polar nature of the P─O and the C─O bonds.

Nerve gases can be destroyed by bleach, through oxidation to less toxic inorganic phosphates, and alkali, through hydrolysis of the P-O or P-S bonds. [45, 46] One disadvantage of using bleach is that a large excess is required. Also the active chlorine content of bleach solutions decreases with time. Moreover, bleach is indiscriminately

corrosive to any surface or compound it comes into contact with. Base hydrolysis also has some limitations such as the requirement of large quantities to maintain a high pH level. Also VX has low solubility in alkaline solution and reacts with base very slowly. Catalytic hydrolyses involving metal ions (e.g., Cu^{2+}, Ag^{+}, Hg^{2+}) [45, 47-49] and enzymes (e.g., organophosphorus acid anhydrases) [45, 50-54] have been proposed but they also have their limitations. For example, Cu(II) has limited capability for hydrolysis of VX whereas Ag^{+} is too expensive and Hg^{2+} is too toxic to be used as a decontamination agent. The enzyme organophosphorus hydrolase (OPH) is highly efficient for the hydrolysis of organophosphorus pesticides (k_{cat} is up to 3800 s^{-1}) but has much lower efficiency for the hydrolysis of VX (k_{cat} = 0.3 s^{-1}). [55]

1.6. Phosphate ester cleavage in biology

In biology, the hydrolytic cleavage of phosphate esters is catalyzed by a number of enzymes. These reactions have been the subject of much attention [56-60] and can be divided into two types: associative and dissociative (Figure 1.8). A dissociative path proceeds through a hydrated metaphosphate ion PO_3^-, and an associative path goes through a five-coordinate phosphorus intermediate. Inversion of configuration around the phosphorus atom generally takes place in the associative mechanism.

Currently, it is thought that in solution the hydrolysis of di- and triesters follows a more associative-like pathway whereas that of monoesters proceeds through a dissociative mechanism. [61-63] This has been proposed to explain the higher reactivity of monoesters compared to di- and triesters. However, this is being debated. The enzymes catalyzing the hydrolytic cleavage contain metal ions and use the functional group of the amino acids and/or the Lewis acidity of the metal ions. A number of recent reviews have

been published on this subject. [64, 65] These enzymes can be divided into three classes depending on the phosphate containing substrate. These are, phosphate monoesterase, diesterase and triesterase. Important monoesterase enzymes are glucose-6-phosphatase, alkaline phosphatase, and purple acid phosphatase. Phosphate diesterases are exemplified by P1 nuclease, phospholipase C and 3'-5' exonuclease from the Klenow fragment of DNA polymerase I. [66] Examples of phosphotriesterases are parathion hydrolase and DFPase.

1.6.1. Alkaline phosphatase

Alkaline phosphatase (AP) [64, 65, 67-70] is probably the most widely studied enzyme of the metallohydrolases. It shows low substrate specificity and optimal activity in alkaline conditions (pH 7.5) and is found in prokaryotes and eukaryotes. The most extensively studied of these enzymes is that from *E. coli*. This is a homodimeric protein (94kDa) that contains two Zn^{2+} ions and one Mg^{2+} ion in each active site. The hydrolysis proceeds through a phosphorylated intermediate formed by the nucleophilic attack of Ser-102 on the phosphate monoester. This intermediate is subsequently attacked by an adjacent Zn-OH group (Figure 1.9). [71] A retention of configuration at the phosphorus center is observed which implies a dissociative mechanism. The two Zn^{2+} ions are important for the activity of AP, but the Mg^{2+} ion plays only an ancillary role. One or two of the Zn^{2+} ions can be substituted by Mg^{2+}, Mn^{2+} or Co^{2+} but this results in a considerable reduction in activity. [70] This is probably related to either intrinsic chemical properties of the metal ions, slight change induced in the conformation of protein side chain at the active center or change in interaction between the Ser-102 residue and the metal. [72, 73]

1.6.2. Purple acid phosphatase

Purple acid phosphatases (PAPs) [74-77]are a group of phosphomonoesterases that catalyze phosphate ester hydrolysis under acidic conditions (pH optima at 4.9 - 6.0), resist inhibition by tartrate and exhibit a characteristic intense purple color. They contain two irons or one iron and another dipositive cation (Fig.1.10). Most of the enzymes having the Fe^{III}-Fe^{II} couple are isolated from bovine spleen [78] or porcine uterine fluid. [79] PAPs isolated from kidney beans [80] generally contain one iron and one zinc or manganese.

1.6.3. P1 nuclease

P1 nuclease [81] is a phosphodiesterase that preferentially cleaves the bond between the 3'-hydroxy and 5'-phosphate group of single stranded RNA and DNA. It requires the presence of three zinc ions [82] per molecule and the hydrolysis causes inversion of configuration at phosphorus . [83]

1.6.4. Phospholipase C

Phospholipase C (PLC) enzymes catalyze the hydrolysis of various phospholipids, for example, phosphatidylinositol and phosphatidylcholine. The PLC [84, 85] from soil bacterium *B. Cereus* contain two tightly bound Zn(II) ions (Zn1 and Zn2) per molecule, whereas a third more weakly bound zinc(II) ion (Zn3) was revealed in its X-ray crystal structure. [86] All of the zinc ions are in trigonal-bipyramidal coordination environments. Zn1 and Zn2 are 3.3 Å apart and bridged by Asp122 and a water. Zn3 has a lower site occupancy and is located 6.0 and 4.7 Å from the other two zinc ions. Other metal ions

like cobalt, magnesium and manganese can replace zinc in some PLC enzymes, however, this results in reduced activity and altered substrate specificity. [87-89]

1.6.5. Phosphate triesterase

Phosphate triesterases (PTEs) [90] catalyze the hydrolysis of organophosphate triesters. The triesters do not occur in nature but they are released into nature by the use of pesticides and insecticides. The best characterized phosphotriesterase is the enzyme from soil bacteria *Pseudomonas diminuta* which is a monomeric metalloprotein that hydrolyzes P-O, P-F, P-CN, and P-S bonds between the phosphorus and the leaving group. [91-93] The native enzyme contains two Zn^{2+} ions in the active site but they can be substituted with Cd^{2+}, Co^{2+}, Ni^{2+}, or Mn^{2+} without affecting catalytic activity. [94]

1.7. Phosphate ester cleavage using models of biological catalysts

To elucidate the role of the metal ions in the hydrolysis of phosphate esters extensive studies have been conducted during the last several years. [66, 95, 96] Besides kinetic and structural studies of the original enzymes, several well-defined model compounds have been developed to understand the process of the cleavage. Besides understanding the mechanism of phosphate ester cleavage, studies of metal containing model compounds are also relevant to the synthesis of artificial metallohydrolases. These model compounds use d- and f-block metals such as cobalt, [97, 98] zinc, [99-103] copper, [104-106] and lanthanides. [107-115] The systems include mono-, bi- (Fig. 1.11) and trinuclear metal compounds. Binuclear compounds have been found to be much more active than the mononuclear counterparts. For example, the hydrolysis rate of bis(*p*-nitrophenyl) phosphate (BNP) increases almost ten-fold for the binuclear $[Zn_2\mathbf{L1}(OH)_2]^+$ (**L1**=

[30]aneN_6O_4] complex with respect to the mononuclear **L2**-Zn-OH^+ (**L2**=[15]aneN_3O_2). [116] This was determined by comparing the second order rate constants k_{BNP} for the mono- and binuclear species. k_{BNP} was determined from the slope of the plot of hydrolysis rate vs. BNP^- concentration. The rate of hydrolysis was monitored by visible spectroscopy. The higher reactivity with binuclear systems is attributed to the double Lewis acidic activation from the coordination of two phosphoryl oxygen atoms with two metal centers as shown for a peroxide bridged lanthanide binuclear complex in Figure 1.12.

1.8. Phosphate ester cleavage with various agents

1.8.1. Phosphate ester cleavage with metal halides and thiophenoxides

Alkali metal iodides have been studied for catalytic dealkylation of phosphates and phosphinates. [117] The order of effectiveness was found to be $Li^+ > Na^+ > K^+$. The reaction is thought to proceed through a S_N2 transition state (associative) (Fig.1.13). Fluoride salts MF (M= Na, K, Cs, Me_4N) catalyze the hydrolysis of phosphate esters. [118] The cleavage of phosphate esters with fluoride ion is fully regiospecific and involves exclusively homolytic P-OAr bond cleavage. It does not have any effect on the P-OMe bond in trimethyl phosphate. However, the catalytic effect is much weaker when the metal ion is Li^+. The cleavage is thought to proceed through the initial formation of a phosphorofluoridate, which then undergoes further hydrolysis (Figure 1.14). Thiophenoxide salts, PhS^-M^+ ($M^+ = Me_4N^+$, K^+, Na^+, Li^+) in methanol can dealkylate phosphate esters (Figure 1.15). [119] The reaction was thought to proceed through a solvent-separated ion pair. Trimethyl phosphate can be dealkylated in a stepwise manner with phenylthiotrimethylsilane, $PhSSiMe_3$ in the presence of catalytic PhS^- (Figure 1.16). [120] This works for other phosphate triesters of the type $(RO)_3PO$, $ROP(O)(Me)_2$,

$PhOP(O)(OR)_2$ and $(PhO)_2P(O)OR$ (R=Me, Et, n-Pr and Ph). The ease of cleavage is in the order of Me, Et, n-Pr. However, no cleavage occurs with phenyl.

1.8.2. Dealkylation with organosilicon compounds

Bromo- and chloro- trialkysilanes react with alkyl phosphates or phosphonates to give the corresponding alkylsilyl esters. [121-123] Use of bromotrimethylsilane was found to be superior to the chloro compounds. Chlorotrimethylsilane in conjunction with a metal halide in acetonitrile has been used to dealkylate dialkyl vinyl phosphate (Figure 1.17). Iodotrimethylsilane is more reactive to phosphate and phosphonate esters and transforms them to the corresponding trimethylsilyl ester and alkyl iodide rapidly and quantitatively at room temperature (Figure 1.18). [124] However, the reaction is not catalytic.

1.8.3. Phosphate cleavage with hypervalent iodine compounds

o-Iodosyl- and o-iodoylcarboxylate derivatives have been widely studied for the degradation of organophosphate substrates. [125] They have been found to be rapid catalysts for the hydrolysis of *p*-nitrophenyl diphenyl phosphate (PNDPP) (with a second order rate constant as high as 10^{-4} $M^{-1}.s^{-1}$) and fluorophosphonate nerve gas agents in presence of micellar reagents. In the catalytic cycle, IBA (IBA = *o*-iodosylbenzoate) is thought to function in a two-step sequence in which the first step involves the attack of the nucleophilic $I\text{-}O^-$ moiety on the phosphoryl group forming a phosphorylated intermediate (Figure 1.19).

1.8.4. Dealkylation with quaternary ammonium salts and micelles

Quaternary pyridinium aldoximes e.g., 1-methyl-2-hydroxyiminomethylpyridinium iodide, can catalytically cleave 4-nitrophenyl diphenyl phosphate (PNDPP) in neutral or

slightly basic aqueous solution (Figure 1.20). [126] This reaction becomes considerably faster in comicelles with the inert cationic tenside, cetyltrimethylammonium bromide (CTAB). Cationic surfactants, [127-129] micellar, [130-132] metallomicellar [105, 133] and reverse micellar [128] systems have been widely studied to catalyze the cleavage of P-O bond.

1.8.5. Phosphate ester cleavage using polymers and nanoparticles

Metalated hybrid polymers, e.g., CPPPL-Zn (Figure 1.21) have been found to catalytically cleave 2-(hydroxypropyl)-*p*-nitrophenyl phosphate (HPNP). [134] Zn(II)-based functional gold nanoparticles formed by self-assembly of triazacyclononane-functionalized thiols on the surface of gold nanoparticles have been reported to be very effective catalyst for the cleavage of HPNP. [135] Initial research indicates that during the catalytic process there is cooperativity between Zn(II) ions bound to the functionalized gold nanoparticles. These catalyst have also been found to be fairly active in the cleavage of the phosphate bond in RNA dinucleotides.

1.9. Phosphate ester cleavage with group 13 chelates

1.9.1. Phosphate ester cleavage using chelated boron compounds

One advantage of chelated boron complexes over simple boron Lewis acidic compounds like BCl_3 is the ability to tune their structure by varying constituents in the ligand environment. Chelated mononuclear (1:1 ligand to metal) boron compounds have been known for a long time. Some of the recent examples of these include β-diketonates, [136] β-diketiminate, [137] substituted anthracene, [138] polysaccharides, [139] L-cysteine, [140] nitroles, [141, 142] tropolonates [143] and salilcylaldimines. [23] Recently, binuclear (1:2 ligand to metal) boron compounds [33-35, 144-150] have attracted attention due to their potential use as

two-point Lewis acids. Most of these binuclear compounds are derived from Salen ligands.

1.9.1.1. Binuclear boron alkoxides and borosiloxides

Binuclear boron alkoxides [146] can be prepared by the alcohol elimination reaction between Salen ligands and corresponding alkyl borates (Figure 1.22(a)). The resulting compounds show interesting extended structures due to intra- and intermolecular hydrogen bonding of the alkoxide oxygens with the imine protons. The compounds form readily even in the presence of excess ligand. This is in contrast to aluminum that forms both mono- and binuclear compounds depending on the metal to ligand ratio. This is due to the smaller size of boron and its preference for a four-coordinate tetrahedral geometry. Similar binuclear boron compounds can be prepared by the condensation of boronic acids with the Salen ligands. [150] They can further be derivatized to bimetallic boron siloxides (Figure 1.22 (b)). [148]

1.9.1.2. Binuclear boron halides

Although the bimetallic boron alkoxides and siloxides are interesting from a fundamental standpoint, they are not ideal for use as precursors to two-point Lewis acids. For example, the bimetallic borate compounds do not dealkylate trimethyl phosphate. [35] This is probably due to the high strength of the B─O bond (~ 809 kJ mol^{-1}). [16] One step towards this goal was the synthesis of binuclear boron bromides and chlorides of the type $L[BX_2]_2$ [33-35] opening the possibility of creating cations through salt elimination reactions. Binuclear boron chlorides can be prepared in almost quantitative yield by combining the

corresponding Salen(^{t}Bu)[B(OMe$_2$)$_2$] reagents with BCl_3 in stoichiometric ratio at room temperature (Figure 1.23). Similarly, binuclear boron bromides can be prepared using BBr_3 instead of BCl_3. However, one difference in the synthesis of boron chlorides is that the reaction for chloride remains unaffected with addition of excess BCl_3 whereas for bromides with addition of excess BBr_3, one B-Br bond is cleaved to produce an additional product L[BBr_2(BBr)$^+$]BBr_4^-. [35] This was the first indication of the lability of B-Br bonds in these compounds. It was further evident by the formation of a cation upon the addition of THF. [35] In these compounds the boron atoms are in a distorted tetrahedral geometry and trans to one another.

In addition to binuclear boron tetrahalides of the type L[BX_2]$_2$, Salen aryl boron bromide compounds L[B(*p*-tolyl)Br]$_2$ [33] can be prepared from Salen (^{t}Bu)[(*p*-tolyl)B(OMe)]$_2$ and BBr_3 (Figure 1.24).

1.9.1.3. Phosphate dealkylation with binuclear boron halide chelates

The binuclear boron halide chelate compounds can dealkylate a wide range of phosphates at ambient temperature (Tables 1.1 and 1.2). [33-35] For example, salpen(^{t}Bu)[BBr_2]$_2$ dealkylates $(MeO)_3P(O)$ by 89% and $(^nBuO)_3P(O)$ by 99% in only 30 minutes in stoichiometric reactions. [33] This is significant considering the fact that BCl_3 or BBr_3 alone is not very effective for phosphate dealkylation. In the dealkylation reaction MeCl or MeBr is produced along with a yet unidentified phosphate material. The reaction can be monitored by comparing the ^{1}H NMR peak integration of methyl halide to that of the original phosphate.

The active species in this type of reaction is thought to be a cation formed through the heterolytic cleavage of a B-X bond. The cation then coordinates to the phosphate, thereby

activating the ester carbon (Figure 1.25). This is supported by the formation of this type of cation by the simple addition of a Lewis base to $L[BX_2]_2$ [35] When THF was added to a solution of salpen(^{t}Bu)$[BBr_2]_2$ in $CDCl_3$ in a NMR tube the ^{11}B NMR shifted downfield by 4.85 ppm, indicating the displacement of Br^- by THF and formation of a cation.

The coordination of the P=O bond to the boron atom makes the P-O-R bonds susceptible to nucleophilic attack by the halide anion (Figure 1.26). A similar type of activation of an alkyl group is found during the dealkylation of phosphoramidates in strongly acidic medium [151] and also during the dealkylation of phosphonates with boron tribromide [152] All of the alkoxy bonds are cleaved in the process to produce three moles of RX and an as yet uncharacterized boron phosphate material. The process could be made catalytic in the Salen boron bromide compounds by conducting the reaction in the presence of excess BBr_3. [33, 35] In general, bromide compounds were found to be more active compared to chloride analogues, which is in accordance with the weaker B-Br bond strength (396 kJ. mol $^{-1}$) in comparison to B-Cl (511 kJ. mol $^{-1}$). None of the chelate compounds could dealkylate $(ArO)_3P(O)$. However, this could be anticipated by the fact that phenylthiotrimethyl silane ($PhSSiMe_3$) also cannot dealkylate arylphosphates. [120] Also, the aryl C-O bond strength is higher compared to alkyl C-O (e.g., $D(CH_3O—Ph)$ = 424 kJ. mol^{-1}, $D(CH_3O—CH_3)$ = 349 kJ. mol^{-1}). [153]

It was also observed that Salen compounds with longer “backbones” (the connection between the two nitrogens) were more efficient than those with shorter backbones probably due to unfavorable interaction between two boron centers. Thus salpen$[BBr_2]_2$, having a propylene backbone, and salben$[BBr_2]_2$, having a butylene backbone, were more efficient than salen$[BBr_2]_2$ having an ethylene backbone. Also, the dealkylation activity

of the Salen boron bromide compounds decreased with the branched phosphates such as $(PhO)_2((2\text{-Et})hexylO)P(O)$. It was also found that one mononuclear boron chelate complex, LBX_2 (L= ^{t}Bu Sal(^{t}Bu), X= Br) could dealkylate trimethyl phosphate at 92% conversion. [33] Thus, it seems that the presence of two boron centers may not be necessary for the dealkylation to occur. If this is the case then this will be in contrast with biological phosphate ester cleavage by enzymes and many binuclear d-block and lanthanide compounds where the presence of two metal centers increases the phosphate cleavage rate. Also, with these compounds, the cleavage involves the direct attack of a nucleophile (water or hydroxide) on the phosphorus atom which is not the case with the boron chelates where the attack occurs at the ester carbon of the phosphate.

1.9.2. Phosphate ester cleavage with aluminum compounds

Aluminum hydroxyphosphate sulfate has been reported to catalyze the hydrolysis of the P-O bonds in phosphate esters. [154, 155] Allyl phosphates can be heterolytically cleaved by various organoaluminum reagents of the type R_3Al (R = Me, Et and *i*-Bu) and R_2AlX (R = Me, X = S-^{t}Bu, SPh, NHPh, OPh) through a cross-coupling reaction in a stereospecific manner at low temperature (Figure 1.27(a)). [156] More selective production of the cyclized product is obtained by the use of dimeric aluminum reagents of the type $R_2AlXAlR_2$ (X = S, PhN, and O) in which the reaction is thought to proceed through the formation of a chelated anionic complex with the phosphate residue (Figure 1.27(b)).

Phosphoric acid triesters with Me, Et, n-Bu and $SiMe_3$ groups react with aluminum and gallium amides, $[M(NMe_2)_3]_2$ (M = Al, Ga) to form amorphous metal phosphate (MPO_4) solid state materials in aprotic solvents (Figure 1.28). [157] $AlCl_3$ also reacts similarly. Trimethyl phosphate was found to be more reactive than the other phosphates.

Gallium amides were less reactive than aluminum amides. Unlike alkyl and silyl phosphates, triphenyl phosphate undergoes a ligand scrambling reaction. The driving force in these reactions is the bond energy difference between Al-O and Al-N (585 kJ mol^{-1} vs. 280 kJ mol^{-1}). For alkyl and silyl substituents the C-O bond of the phosphate is preferentially cleaved whereas for phenyl esters the P-O bond instead of the C-O bond is formed. This is responsible for the prevention of formation of the aluminophosphate. Trialkyl phosphates $P(O)(OR)_3$ (R = Me, Et, Ph, $SiMe_3$) react with $AlMe_3$, $AlEt_3$ and $GaMe_3$ to form the adducts $Me_3Al{\bullet}OP(OR)_3$ (R = Me, Et, Ph, $SiMe_3$), $Et_3Al{\bullet}OP(OR)_3$ (R = $SiMe_3$), and $Me_3Ga{\bullet}OP(OR)_3$ (R = Me, Si Me_3) (Figure 1.29). [158] The trimethylsilyl ester adducts further undergo thermally induced dealkylsilylation to form cyclic alumino and gallophosphate dimers, $[R'_2M(\mu_2\text{-}O)_2P(SiMe_3)_2]_2$ (R'_2M = Me_2Al, Et_2Al and Me_2Ga). The phosphate adducts could also undergo reaction with Me_2NH to form aluminophosphate (Figure 1.30).

Alumazene $[2,6\text{-}(i\text{-}Pr)_2C_6H_3NAlMe]_3$ has been reported to undergo dealkylsilylation reaction with the tris(trimethylsilyl) ester of phosphoric acid to form a heteroadamantane molecule $(MeAl)[2,6\text{-}(i\text{-}Pr)_2C_6H_3N]_3\{Al[OP(OSiMe_3)_3]\}_2(O_3POSiMe_3)$ [159] In this reaction the phosphate ester is first thought to form an adduct with the aluminum. From this adduct the formation of a bicyclic intermediate with a bridging $O_2P(OSiMe_3)_2$ takes place through dealkylsilylation (Figure 1.31). This bicyclic intermediate then undergoes a second dealkylsilylation to give the final adamantane-like product.

1.10. Goals of this research

The effectiveness of binuclear boron Schiff base halide compounds, Salen(^{t}Bu)$[BBr_2]_2$ for dealkylation of organophosphate esters opened up a means of using a mild, soft route

for dealkylation of organophosphates. This finding was significant in the wake of recent concern for organophosphate nerve agent and pesticide destruction and decontamination.[160-162] For understanding the full utility and scope of this finding it is necessary to expand this study to other comparable systems. One preliminary step would be to investigate mononononuclear boron Schiff base compounds. Mononuclear cationic boron complexes with N-salicylidene-*o*-aminophenol have been found to catalyze the polymerization of oxiranes, [23] but so far mononuclear boron chelates have not been examined in detail for the dealkylation of phosphates. Previous work indicates that stoichiometric combinations of LBX_2 (L= ^{t}Bu Sal(^{t}Bu), X= Br) and trimethyl phosphate leads to phosphate cleavage.[33] A detailed study of a series of mononuclear boron complexes for phosphate dealkylation would determine if the presence of two boron centers in the same compound is necessary for the dealkylation.

The high activity of boron halide Schiff base chelate complexes towards phosphate dealkylation demands a similar study with aluminum chelates since aluminum centers in these compounds may also act as Lewis acids and thus facilitate the initial coordination of the Lewis basic oxygen of phosphate esters. Both neutral and cationic Schiff base complexes of aluminum have been found to catalyze the polymerization of oxiranes, a reaction that has been attributed to the Lewis acidic property of the aluminum. [17, 18] Lewis acids such as $AlCl_3$ [157] can dealkylate phosphates but only with long reaction times (2 days) and under reflux in THF. Compounds with Al-Br bonds, such as Salen(^{t}Bu)AlBr, are expected to be more active compared to the chloride analogues due to the weaker bond strength. Synthesizing Salen(^{t}Bu)AlBr compounds and exploring their phosphate dealkylation activity will be an important goal of this research.

Thus this research will focus on synthesis and characterization of new mononuclear boron and aluminum halide compounds and examination of their phosphate dealkylation activity. This study could help identify optimized systems for understanding the phosphate dealkylation pathway and also for practical applications like organophosphate nerve agent and pesticide decontamination.

Chapter 2 will describe the synthesis and characterization of a series of mononuclear boron Schiff base halides based on various N-salicylidineimine Schiff base ligands. The application of these compounds for phosphate dealkylation will be examined in Chapter 3. Chapter 4 will discuss a series of five-coordinate aluminum bromide compounds based on Salen ligands and the cationinc compounds derived from them. The dealkylation of organophosphates with the Salen aluminum bromide compounds will be studied in Chapter 5. The directions this research may lead in continued research efforts will be described in Chapter 6.

Table 1.1. % Dealkylation of various phosphates with Salen boron halide compounds, $L[BX_2]_2$ (L = Salen(^{t}Bu) ligands)

L	**Salen(^{t}Bu)**		**Salpen(^{t}Bu)**		**Salben**		**Salhen**	
Carbons in "backbone" of the ligand	2		3		4		6	
X	Cl	Br	Cl	Br	Cl	Br	Cl	Br
Phosphate								
$(MeO)_3P(O)$	14	76	20	89	11	90	7	81
$(^nBuO)_3P(O)$		42		99		77		69
$(^nPentO)_3P(O)$				98				
$(MeO)_2P(O)H$				85				
$(MeO)_2P(O)Me$		61		98		87		47
$(^iPrO)_2P(O)H$				63				
$(PhO)_2((2\text{-Et})HexO)P(O)$		48		71		64		88
$(Me_3SiO)_3P(O)$		88		98		90		79
$(PhO)_3P(O)$		0		0		0		0

NOTE: Reaction time: 30 minutes.

SOURCE: Adapted from References 33 and 34.

Table 1.2. % Dealkylation of various phosphates with Salen phenyl boron bromide compounds, L[(^{p}tolyl)BBr]$_2$ (L = Salen(^{t}Bu) ligands)

L	**Salen(^{t}Bu)**	**Salpen(^{t}Bu)**	**Salben(^{t}Bu)**	**Salhen(^{t}Bu)**
Carbons in "backbone"	2	3	4	6
Phosphate				
$(MeO)_3P(O)$	45	52	92	80
$(EtO)_3P(O)$	40	50	71	56
$(^{n}BuO)_3P(O)$	31	58	70	47
$(MeO)_2P(O)H$	59	67	50	50
$(MeO)_2P(O)Me$	47	50	50	50
$(^{i}PrO)_2P(O)H$	42	32	37	26
$(PhO)_2$((2-Et)HexO)P(O)	12	46	52	42
$(Me_3SiO)_3P(O)$	43	48	69	89
$(PhO)_3P(O)$	0	0	0	0

NOTE: Reaction time: 30 minutes.

SOURCE: Adapted from Reference 33.

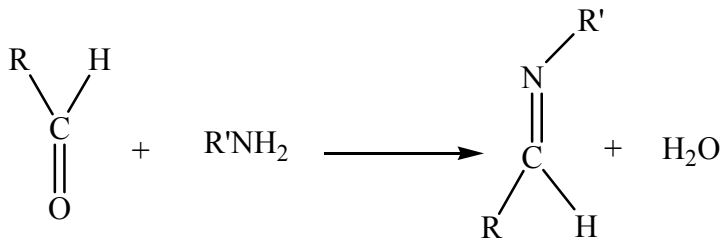

Figure 1.1. Formation of a Schiff base.

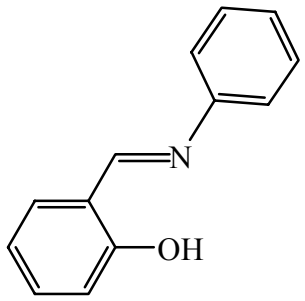

(a)

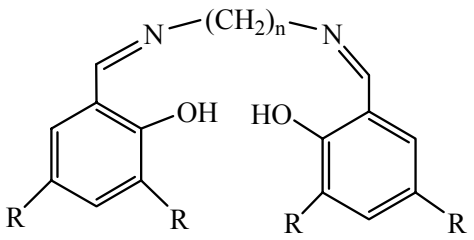

R=H		R = ^{t}Bu	
n=2	$salenH_2$	n=2	$salen(^{t}Bu)H_2$
n=3	$salpenH_2$	n=3	$salpen(^{t}Bu)H_2$
n=4	$salbenH_2$	n=4	$salben(^{t}Bu)H_2$
n=5	$salptenH_2$	n=5	$salpten(^{t}Bu)H_2$
n=6	$salhenH_2$	n=6	$salhen(^{t}Bu)H_2$

(b)

Figure 1.2. (a) N-phenylsalicylaldimine and (b) Salen ligands.

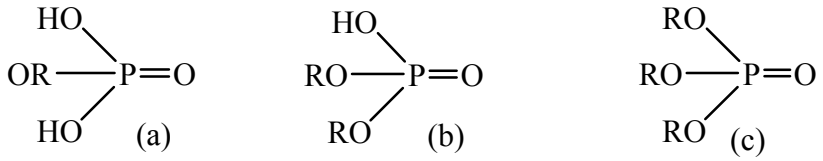

Figure 1.3. Phosphate esters: (a) monoester, (b) diester and (c) triester.

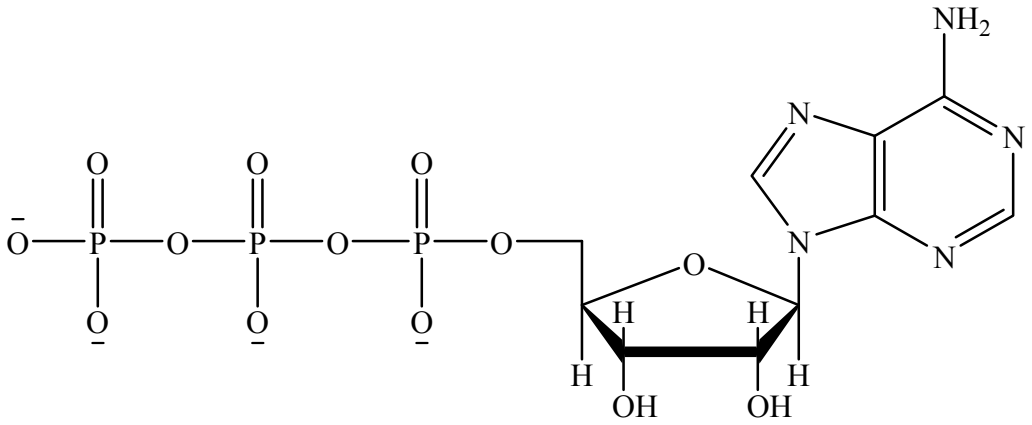

Figure 1.4. Phosphate ester bonds in ATP.

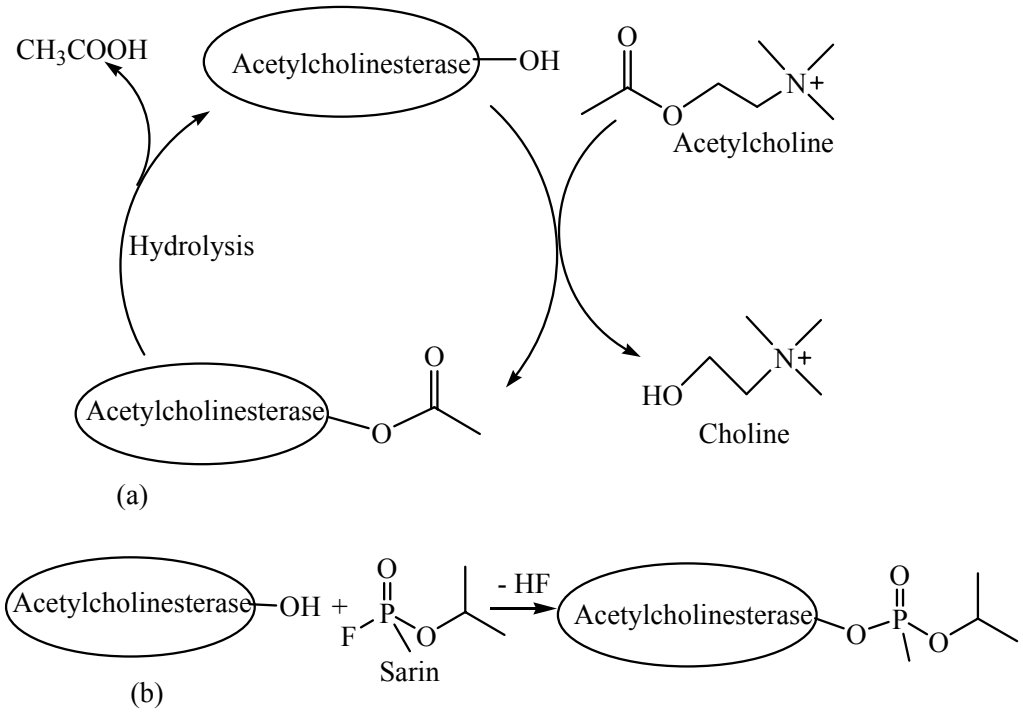

Figure 1.5. (a) Mode of action of the enzyme acetyl cholinesterase (b) Deactivation of acetylcholinesterase by nerve gas agent sarin.

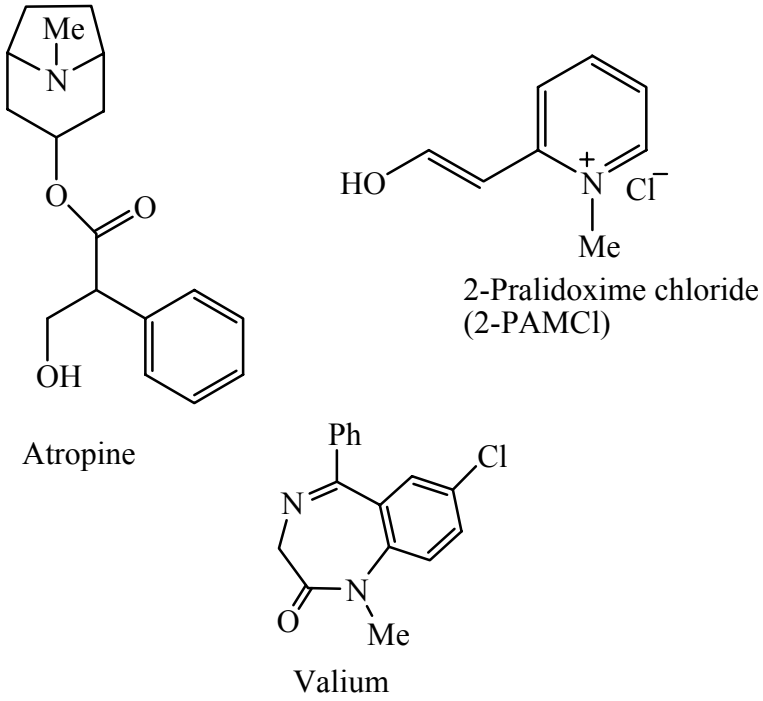

Figure 1.6. Some antidotes for nerve gas exposure.

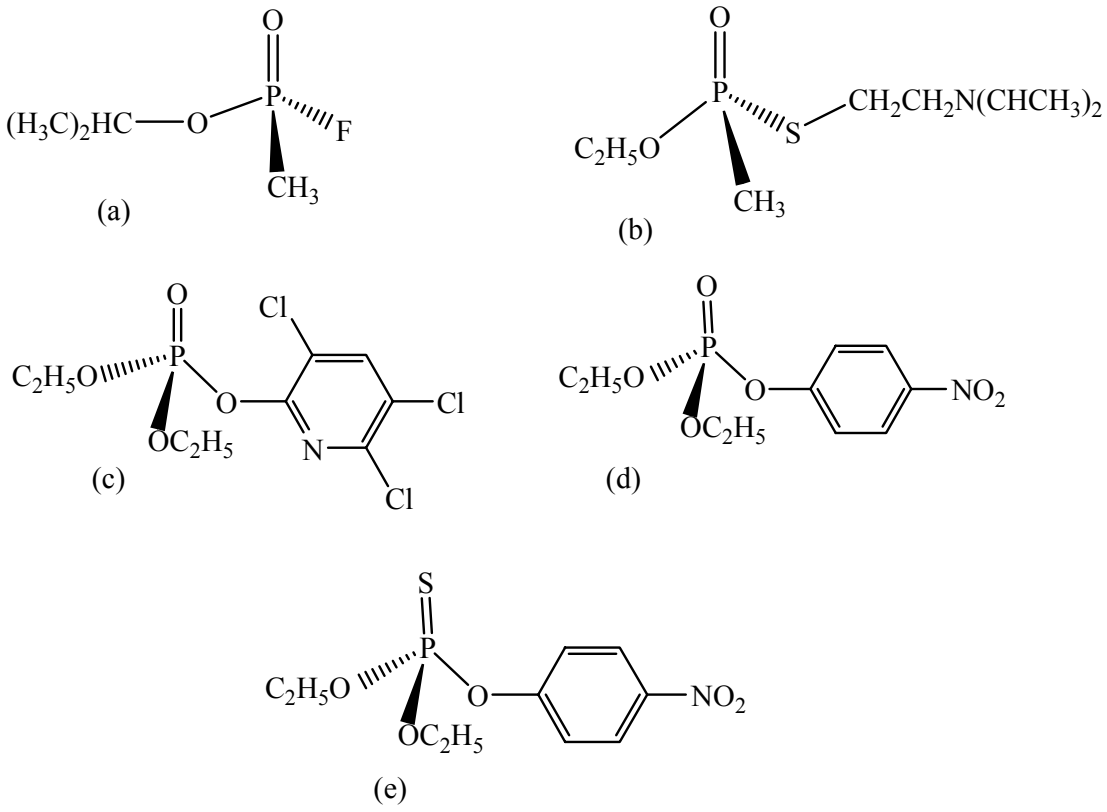

Figure 1.7. Structures of some organophosphate nerve gases and pesticides: (a) Sarin Gas, (b) VX gas, (c) Chloropyrifos, (d) Paraoxon and (e) Parathion.

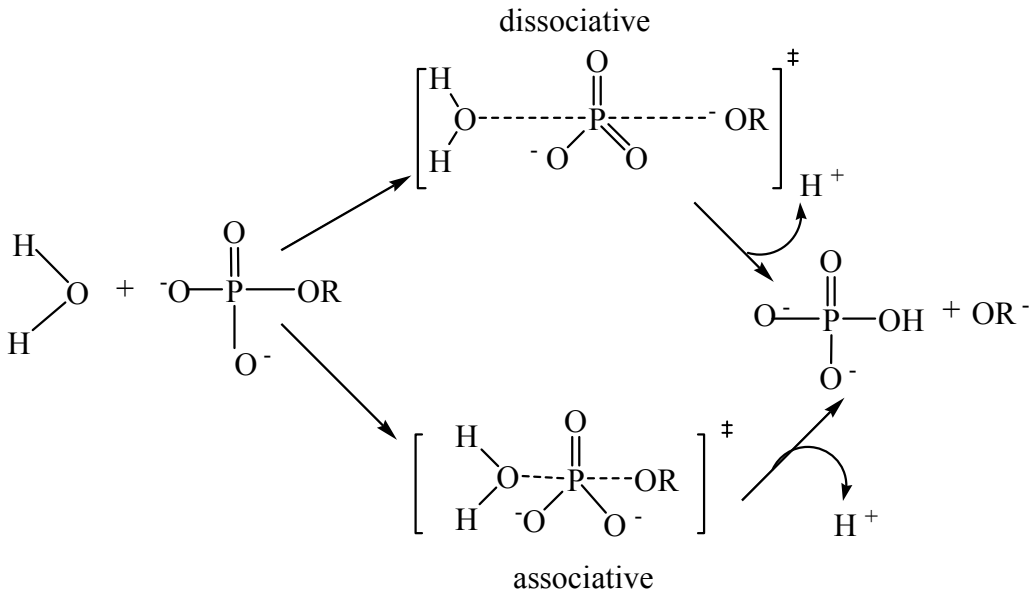

Figure 1.8. Associative vs. dissociative mechanism for phosphate hydrolysis.

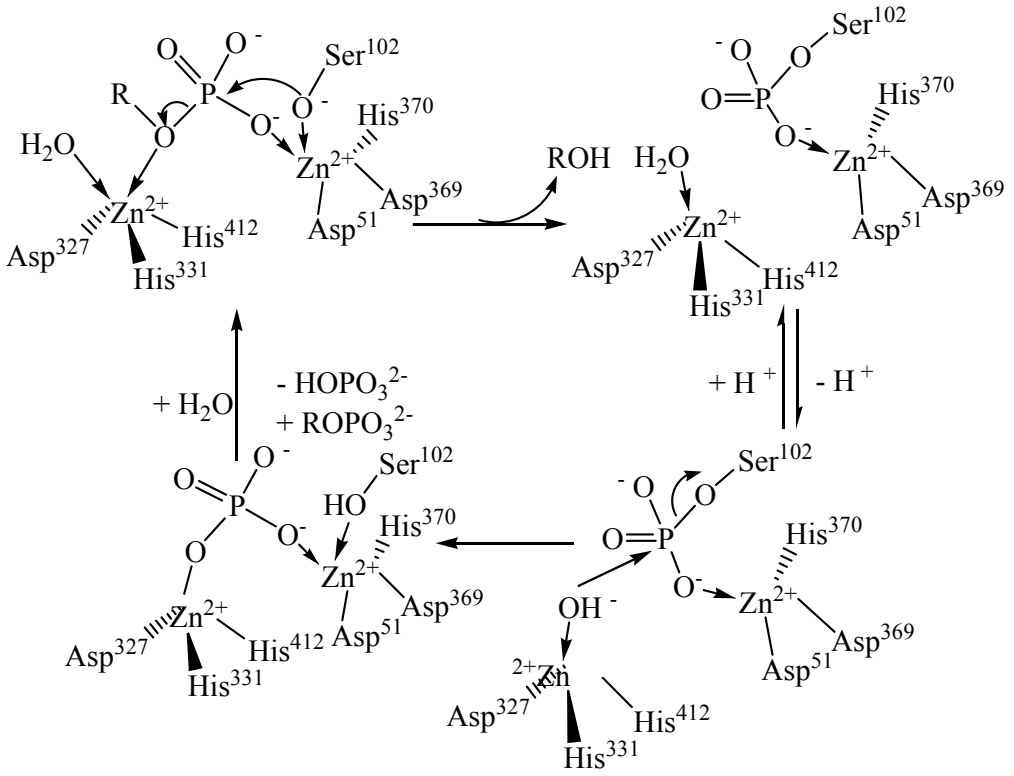

Figure 1.9. Proposed mechanism for phosphate ester cleavage by the active site of enzyme Alkaline Phosphatase (redrawn from reference [71]).

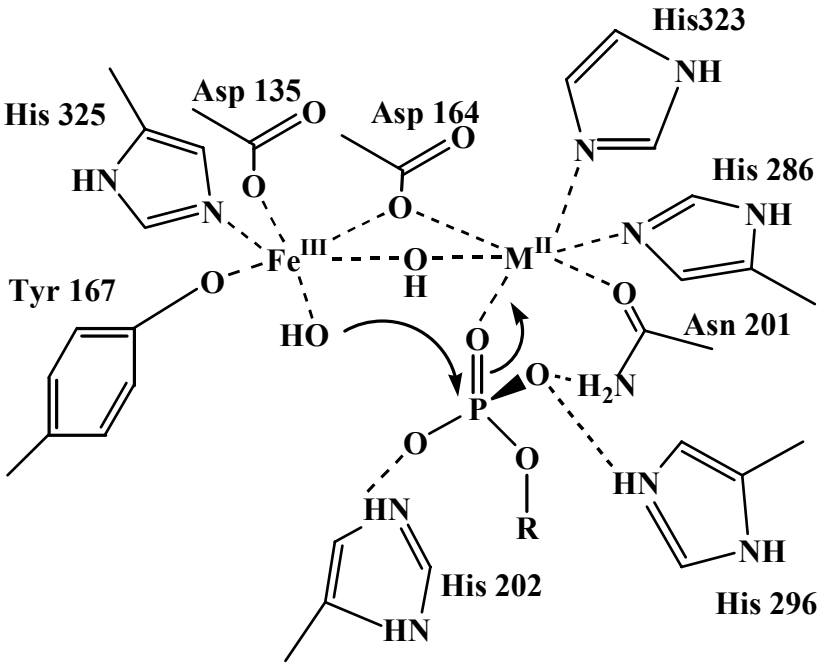

Figure 1.10. Binding mode and attack of Fe^{III} bound nucleophile for proposed mechanism of phosphate ester hydrolysis by PAP [163-166](redrawn from reference 64).

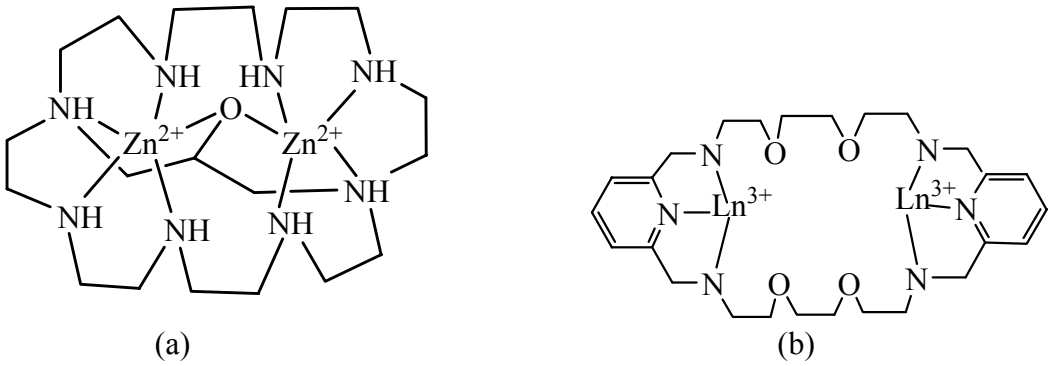

Figure 1.11. Examples of binuclear zinc (a) and lanthanide (b) model compounds.

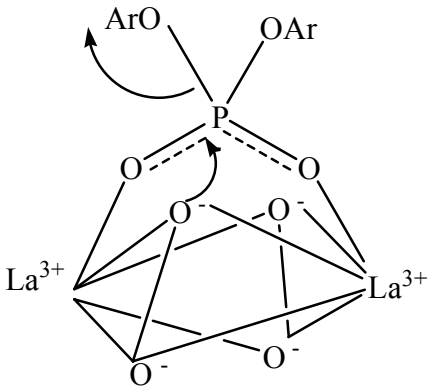

Ar = various aryl groups

Figure 1.12. Proposed mechanism for phosphate ester cleavage by a peroxide bridged binuclear lanthanide compound. [114, 115]

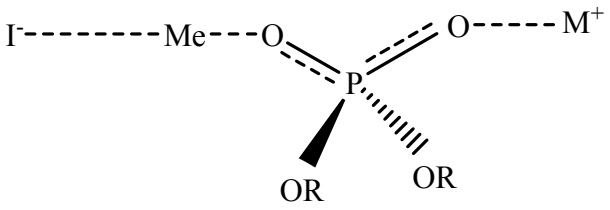

R = various alkyl groups

Figure 1.13. Proposed model for phosphate ester cleavage with metal iodide.

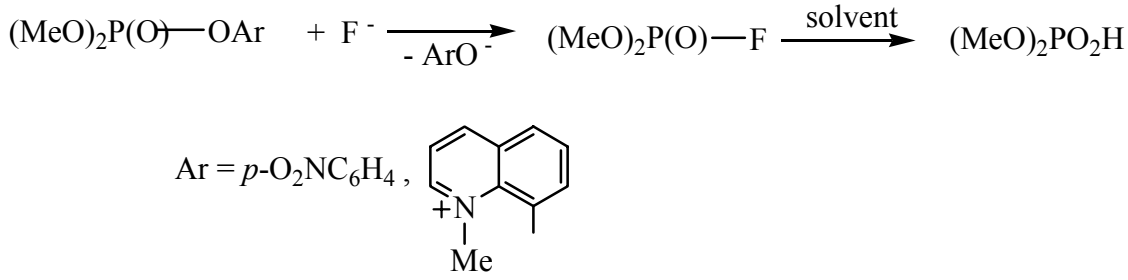

Figure 1.14. Cleavage of phosphate ester with fluoride ion.

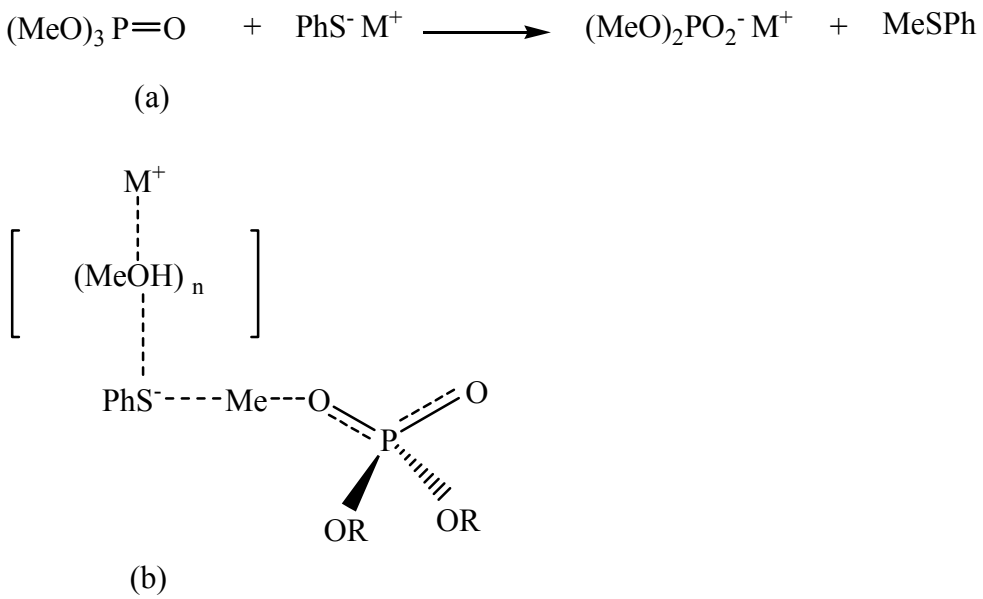

Figure 1.15. (a) Phosphate ester cleavage with thiophenoxide salts and (b) proposed transition state.

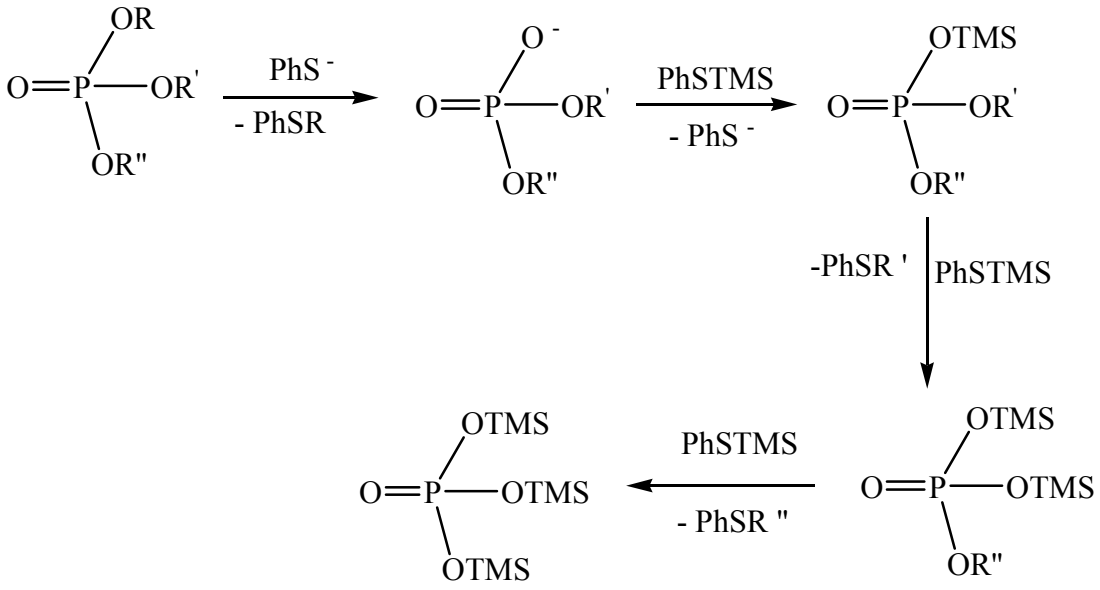

R, R', R" = various combinations of alkyl groups
TMS = trimethylsilyl group

Figure 1.16. Phosphate ester cleavage with phenylthiotrimethylsilane (PhSTMS).

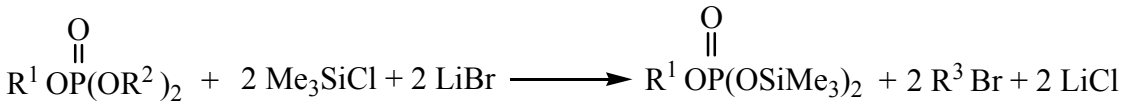

R^1	R^2
$H_2C=CMe$	Et
$Me_2C=CPh$	Et
$Cl_2C=CH$	Me

Figure 1.17. Dealkylation of phosphate ester with chlorotrimethylsilane and metal halide.

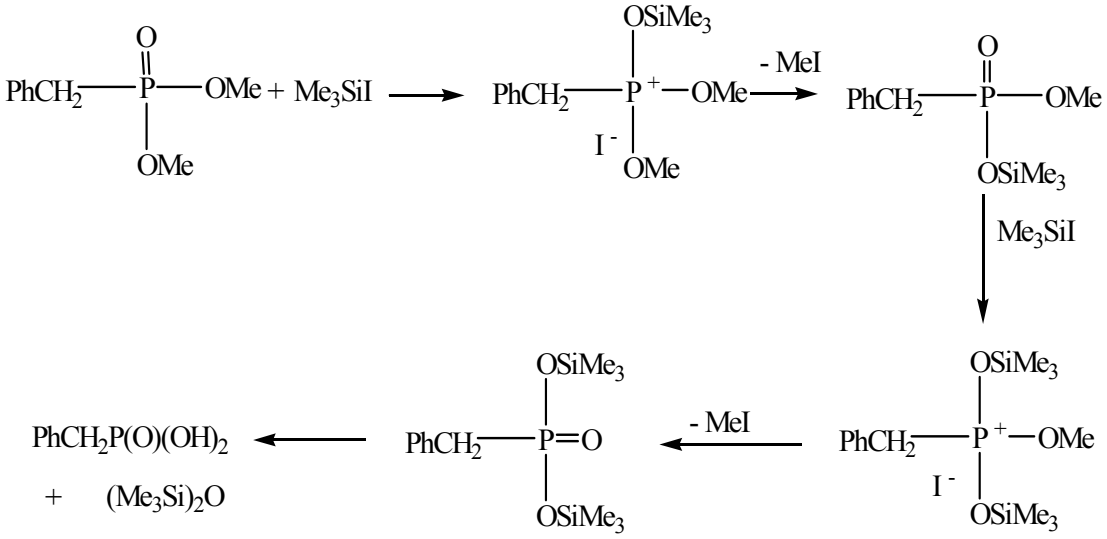

Figure 1.18. Dealkylation with iodotrimethylsilane.

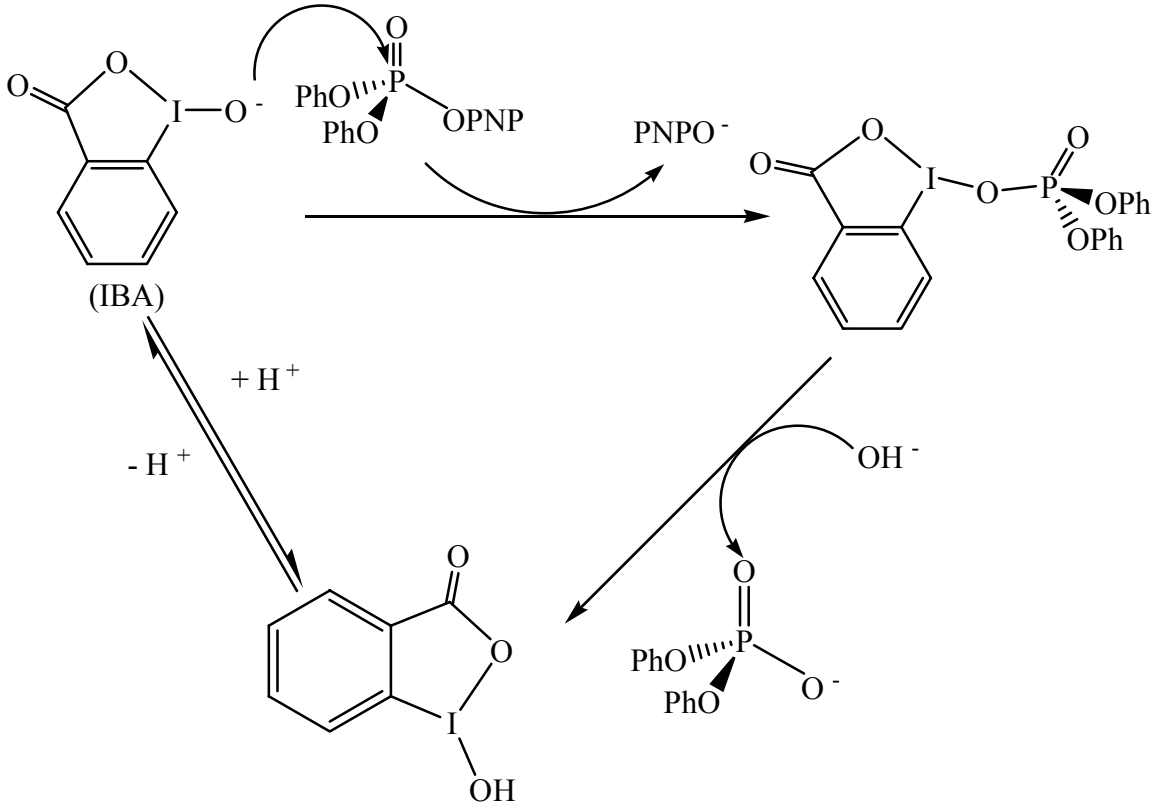

Figure 1.19. Cleavage of phosphate ester with *o*-iodosylbenzoate (IBA).

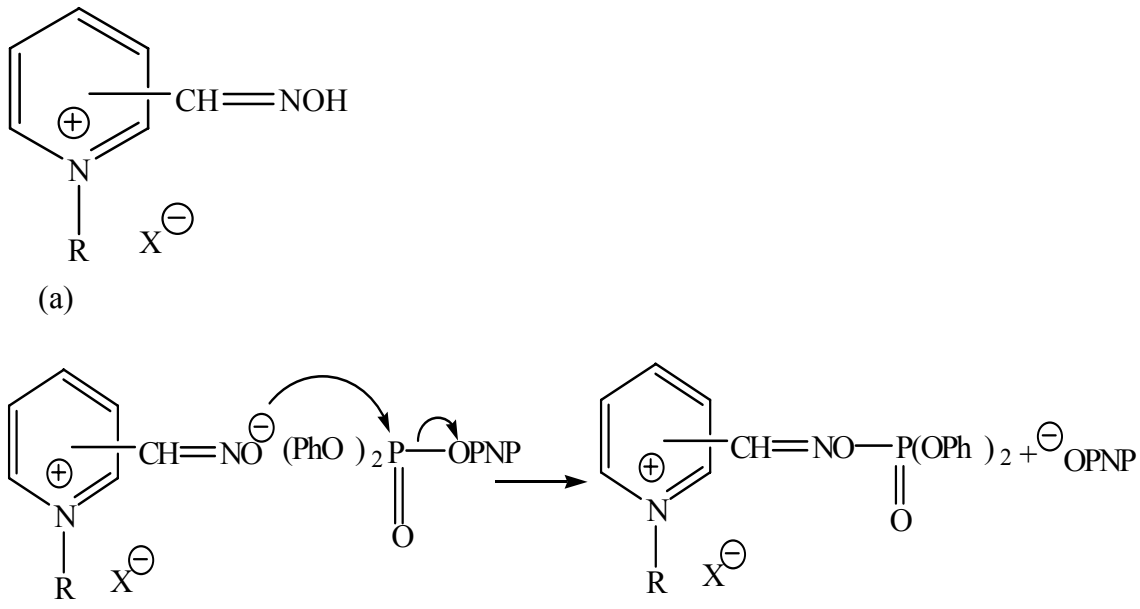

Figure 1.20. (a) Quaternary pyridinium aldoxime (b) Phosphate ester cleavage with aldoxime.

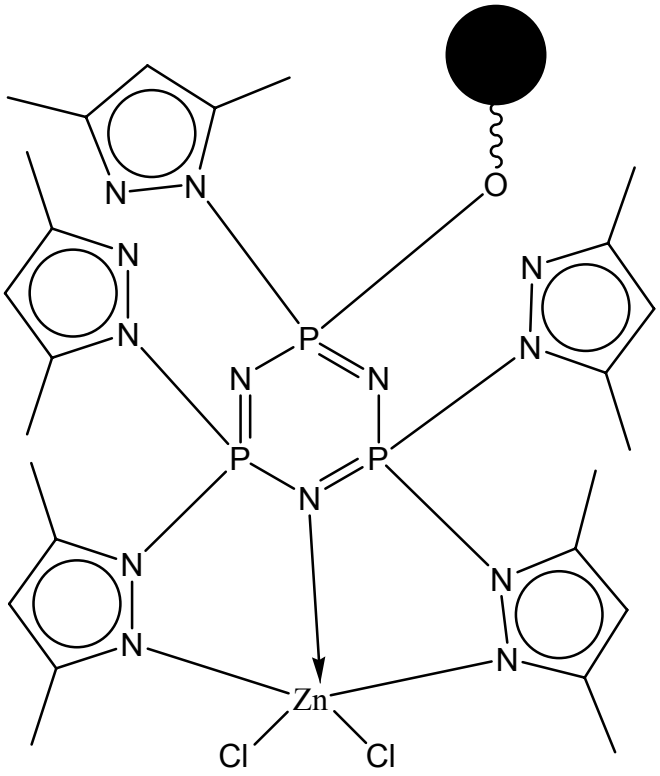

The dark cricle represents the polymer- support

Figure 1.21. Metallated polymer CPPL-Zn.

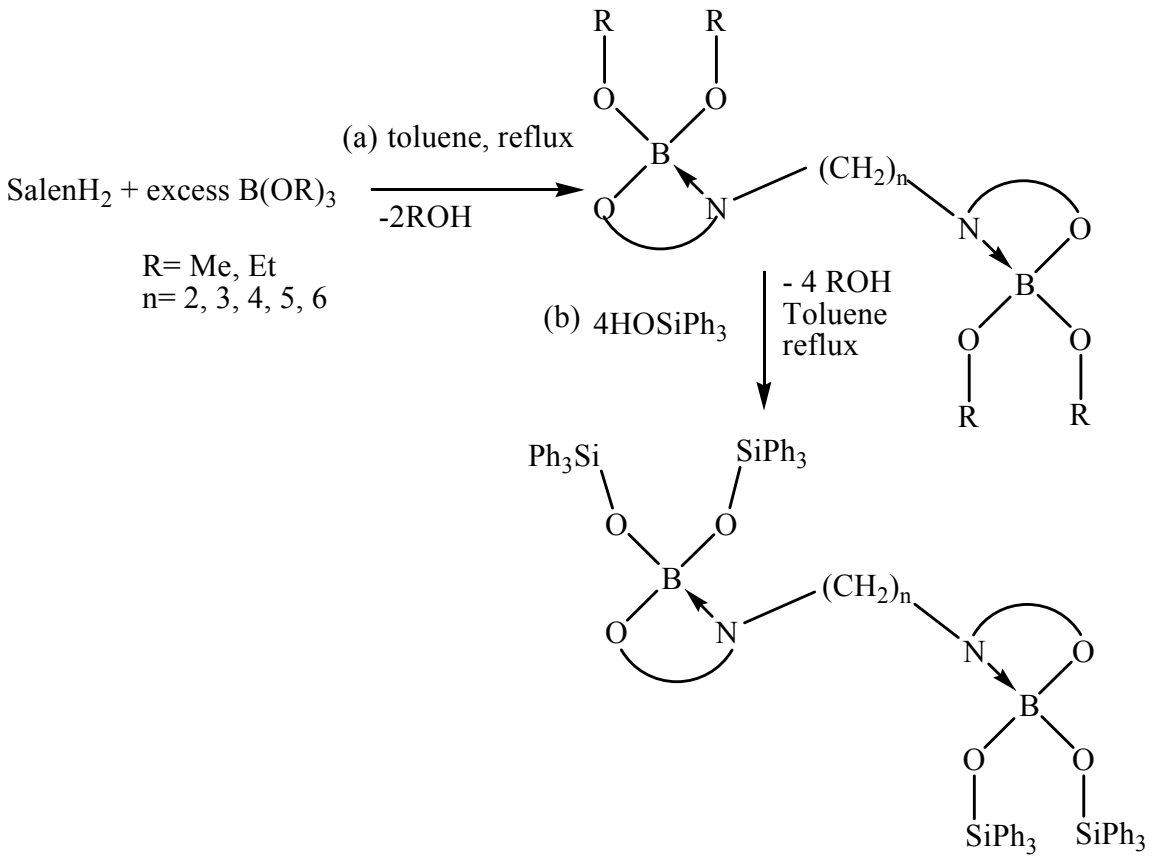

Figure 1.22. Synthesis of binuclear boron alkoxides (a) and siloxides (b).

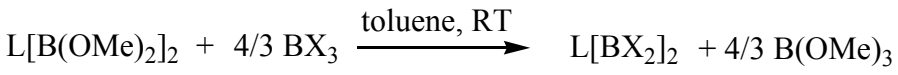

L= Salen(^{t}Bu) ligands
X= Cl, Br

Figure 1.23. Synthesis of binuclear boron halides.

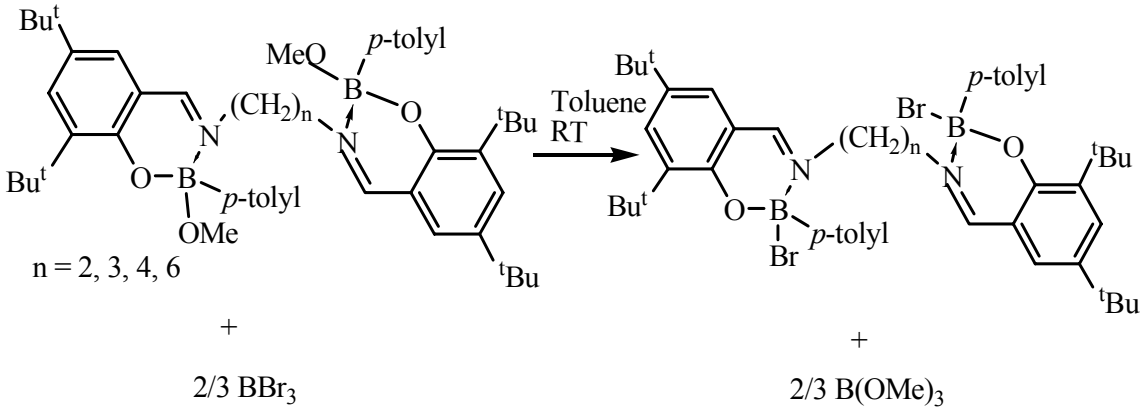

Figure 1.24. Synthesis of Salen[B(^{p}tolyl)Br]$_2$.

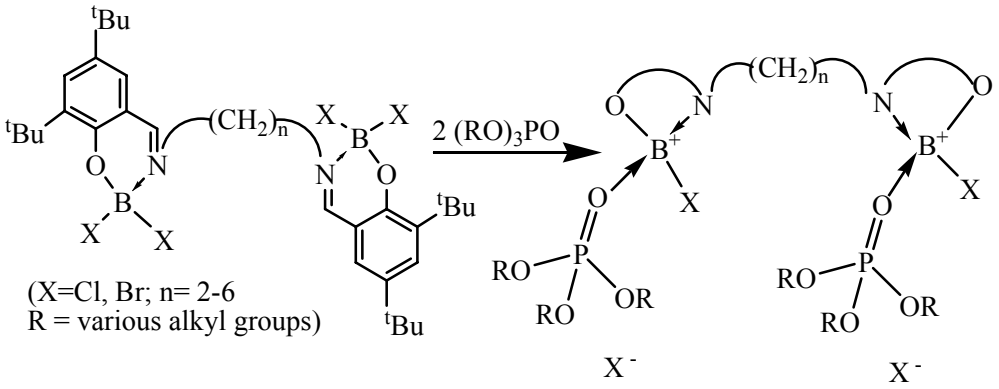

Figure 1.25. Formation of phosphate-coordinated boron cation.

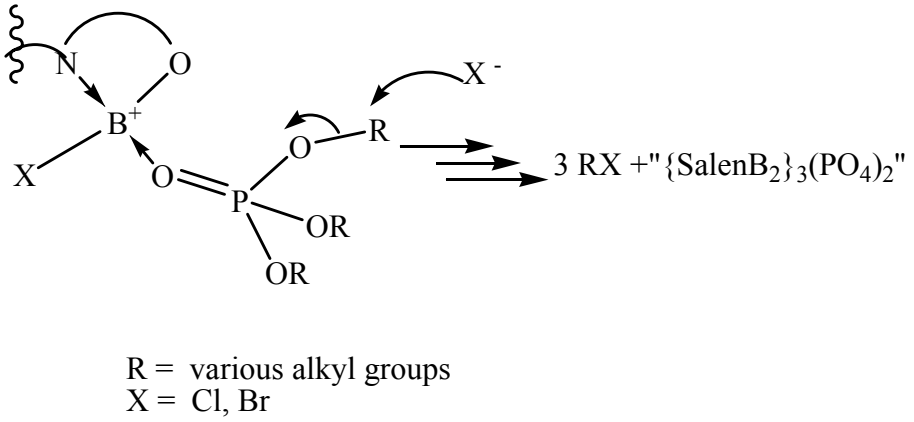

Figure 1.26. Attack of P-O-R bond by halide.

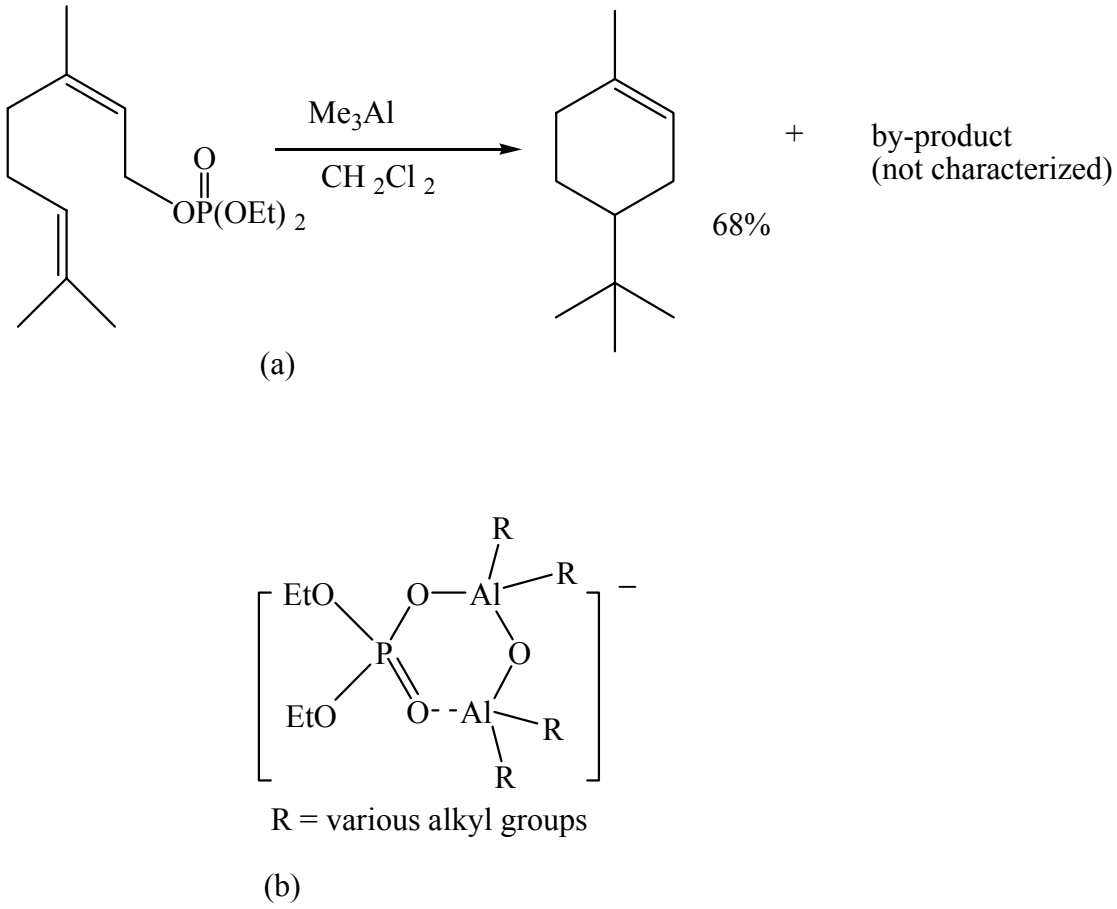

Figure 1.27. (a) Cleavage of allyl phosphate with organoaluminum reagents. (b) Intermediate for the reaction of dimeric aluminum reagent $R_2AlXAlR_2$ with allyl phosphate.

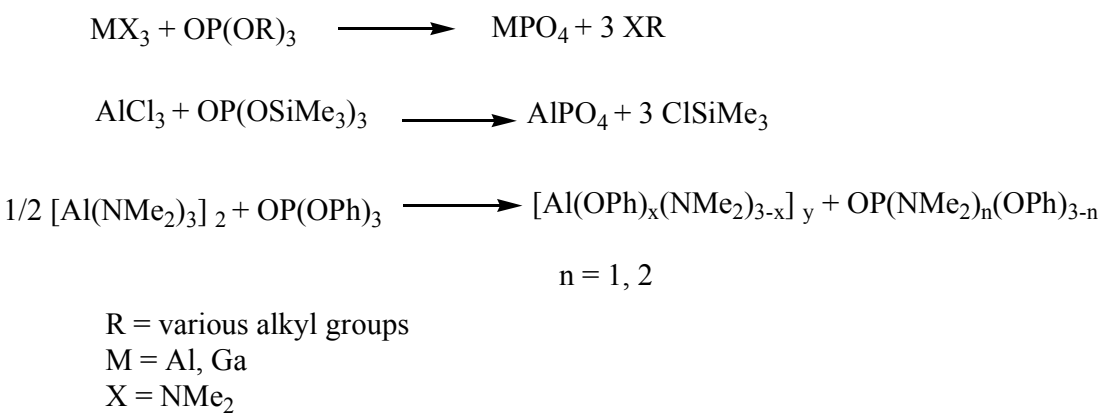

Figure 1.28. Reaction between organophosphate and aluminum or gallium amides.

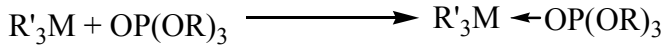

M = Al: R' = Me: R = Me, Et, Ph, $SiMe_3$
M = Al: R' = Et: R = $SiMe_3$
M = Ga: R' = Me: R = Me, $SiMe_3$

Figure 1.29. Reaction between trialkyl phosphates and aluminum and gallium alkyls.

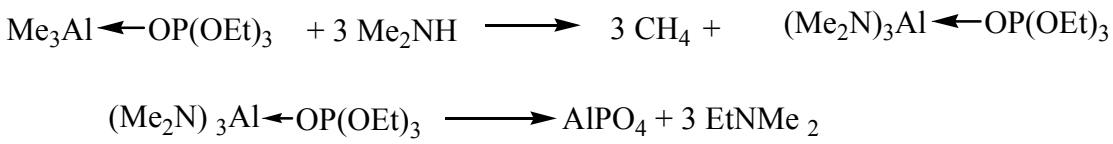

Figure 1.30. Reaction between phosphate adduct and dimethylamine.

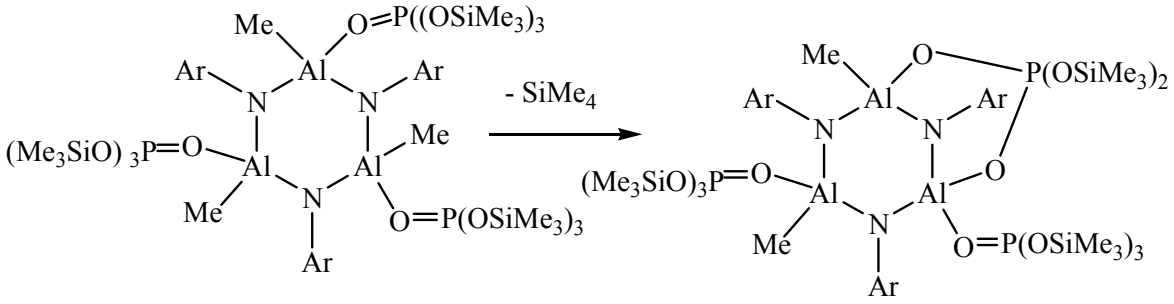

Ar = 2,6-diisopropylphenyl

Figure 1.31. Formation of bicyclic intermediate from phosphate adduct of alumazene.

Chapter 2

Synthesis of Mononuclear Boron Schiff Base Halides

2.1. Background

Boron halides have been used over the years in various organic syntheses, for example, ester ring closing [167] and Friedel-Crafts alkylations. [168] However, boron trihalides are very reactive and difficult to handle. The use of chelated boron compounds could help overcome this problem. Also, chelated boron compounds provide the option of tuning their properties by changing the size of the chelate rings and substituents on them. Schiff base boron compounds have been studied recently for their possible applications in catalysis. For example, binuclear Schiff base boron halides have been shown to be effective for dealkylation of organophosphates.[33-35] Unlike Schiff base aluminum compounds the boron chelates, e.g., chelated boron alkyls, cannot be prepared by an alcohol elimination reaction between the ligand LH_2 and BR_3 because of the low polarity of the B-C bond. The common methods for creating boron-ligand compounds are water elimination using a boronic acid and alcohol elimination using a borate (represented in the equations below).[169]

$$LH_2 + RB(OH)_2 \longrightarrow LBR + 2\ H_2O$$
$$LH_2 + B(OR)_3 \longrightarrow LBOR + 2\ ROH$$

The boron alkyls arising from the boronic acid reaction are generally stable whereas the boron alkoxides formed from the reaction using a borate could be further derivatized, for example, to boron siloxides.[148]

Binuclear boron halides of the type $LB[BX_2]_2$ (X = Cl, Br) (L = Salen ligands) can be prepared by the exchange reaction of the binuclear alkoxides $LB[B(OMe)_2]_2$ with BX_3.[33-35] In this chapter the synthesis and full characterization of a series of mononuclear boron halides of the type LBX and LBX_2 (L = various Schiff base N,O and N,O,O ligands; X = Cl, Br) made in this way will be described. The halides were prepared from their borate precursors LBOMe and $LB(OMe)_2$. The compounds will be shown to be of utility in the dealkylation of organophosphates in the following chapter.

2.2. Synthesis

The Schiff base boron halide compounds were prepared from their borate precursors. The borate precursors were prepared in good yield by alcohol elimination reaction between the Schiff base salicylidenimine ligand and excess trimethylborate under reflux. The byproduct MeOH could be removed under vacuum to drive the reaction to completion. The salicylidenimine ligands could be easily prepared by the condensation reaction between 3,5-di-*t*-butylsalicylaldehyde and the corresponding amines according to the literature procedures.[170] The synthetic route used for the preparation of compounds **1**-**12** is depicted in Figure 2.1. Thus the halides **2**, **3** and **7**-**12** were prepared from the corresponding borate precursors **1** and **4**-**6**. The borate precursors, in turn, were prepared by refluxing Schiff base ligands and excess trimethyl borate in toluene. The borates were converted to the boron halides by reaction with BCl_3 or BBr_3 at room temperature. All the compounds were isolated by removing the solvent under vacuum or by precipitation after concentration and cooling to -30 ºC. The by-product $B(OMe)_3$ was removed under vacuum. The compounds were pale white to orange in color.

2.3. Spectroscopy

Compounds **1-12** were characterized by ^{1}H, ^{13}C and ^{11}B NMR, MP, MS and EA. The ^{1}H NMR data for all the compounds showed two singlets for the ^{t}Bu-Ph groups in the range δ 1.24-1.54 ppm. The imine peaks appeared at δ 8.63, 8.52, 8.30 and 7.99 ppm for the borates **1**, **4**, **5** and **6**, δ 8.29, 8.58, 8.11 and 7.93 ppm for the chlorides **2**, **7**, **9** and **11** and δ 9.38, 8.81, 8.25 and 8.97 ppm for the bromides **3**, **8**, **10** and **12**, respectively. The imine peaks for the bromides appeared at higher chemical shift compared to the chlorides. The presence of only one set of ^{t}Bu peaks and one imine peak for each compound suggested a symmetric solution-state structure.

The ^{11}B NMR spectra showed single peaks at δ 2.33, 5.09, 2.38 and 2.00 ppm for the borates **1**, **4**, **5** and **6**, δ 2.48, 7.28, 2.05 and 3.30 ppm for the chlorides **2**, **7**, **9** and **11**, and δ 2.38, 6.47, 2.00 and 9.70 ppm for the bromides **3**, **8**, **10** and **12**, respectively. These shifts indicate the presence of four-coordinate boron [33] in all of the compounds. The IR spectra have a $\nu_{B\text{-}N}$ stretch in the region 1000-1042 cm^{-1} for all of the compounds. The mass spectra (EI) of the borates **1**, **4**, **5** and **6** showed peaks corresponding to molecular ion minus methoxy group and for **4**, **5** and **6** this was the most abundant peak. Compounds **4**, **5** and **6** showed molecular ions in low abundance. The chloride compounds **2**, **7**, **9** and **11** showed molecular ions minus the chloride in high abundance. Compounds **2**, **9** and **11** also showed molecular ion in low abundance. The bromide compounds **8**, **10** and **12** had molecular ion as well as molecular ion minus bromide in their spectra. However, **3** showed molecular ion minus the BBr_2 group (33 %) and also molecular ion minus BBr_2 and CH_3 (100 %). This indicated that the EI ionization process was sufficiently strong to break apart the compound. This was a rare occurrence for

Schiff base-group 13 compounds, which are usually not observed to release the group 13 element from the ligand.

2.4. Structures

The borate compounds **1** and **6** and the halide compounds **11** and **12** were structurally characterized by single-crystal X-ray diffraction studies. The X-ray crystal structures confirm the presence of four-coordinate boron atoms in these compounds (Figures 2.2, 2.3, 2.4 and 2.5). The crystal data collection parameters are shown in Tables 2.1 and 2.3 and selected bond lengths and angles are shown in Tables 2.2 and 2.4. The B─O bond lengths are in the range 1.414(4) - 1.485(4) Å for the borates **1** and **6** and 1.391(2)-1.437(2) Å for the halides **11** and **12**. These distances are slightly shorter than the B-N distances (1.537(2)-1.628(4)) Å, which is a reflection of the smaller covalent radius of oxygen. The B-Br bond length (2.201(2) Å in **12** is longer than the B-Cl bond length (1.965(2) Å) in **11**, which is a reflection of the greater covalent radius of Br compared to Cl. These distances are slightly larger compared to the binuclear boron halides reported previously. For example, in the binuclear Schiff base boron bromide salben(^{t}Bu)[BBr_2]$_2$ [35] the B-Br lengths are 2.023(8) and 2.077(9) Å and in the binuclear Schiff base boron chloride salpen(^{t}Bu)[BCl_2]$_2$ [34] the B-Cl bond lengths are 1.849(5) and 1.855(5) Å.

The geometry around the boron atom is slightly distorted tetrahedral in all four compounds. For compound **1** the largest deviations are shown by the angles O1-B1-N1 (106.8(3) °), O1-B1-O2 (112.1(3) °) and O1-B1-O3 (112.1(3) °) whereas for **6** the largest deviation is shown by the angle O2-B1-O3 (115.3(2) °). The angle O1-B1-N1 is slightly larger for **6** (109.4(2) °) compared to **1.** This could be due to the steric restriction arising from the boron being part of a second six-membered ring in **6**.

For the halide compounds **11** and **12** the largest deviation from the ideal tetrahedral angle is observed for the angle O2A-B1A-N1A, which is 113.18(16) ° for **11** and 114.92(14) ° for **12**. The angles O1A-B1A-Cl1A (108.04(13)) °, O2A-B1A-Cl1A (111.22(14) °) and N1A-B1A-Cl1A (103.83(13) °) in **11** are larger than the corresponding angles O1A-B1A-Br1A (106.87(11) °), O2A-B1A-Br1A (109.00(12) °) and N1A-B1A-Br1A (101.97(11) °) in **12**. This is contrary to what would be expected from Bent's Rule[171] considering the higher electronegativity of chlorine compared to bromine and thus less *s*-character in the B-Cl bond. The angle O1A-B1A-N1A (111.22(15)) for **11** and 112.33(14) for **12**) is close to that found in the bimetallic boron halides, salpen(^{t}Bu)[BCl_2]$_2$ (110.1(4)) [34] and salben(^{t}Bu)[BBr_2]$_2$ (112.8(6)). [35] A quantitative correlation called the THC value (Figure 2.6; THC = tetrahedral character) has been proposed to determine the deviation of the geometry around boron in compounds containing N→B bonds. [172] A THC value of 100 % refers to a perfectly tetrahedral and a value of 0 % refers to a trigonal planar geometry around the boron. Compounds **1**, **6**, **11** and **12** have THC values of 88, 83, 84 and 77 %, respectively. According to the previous observation the THC values should increase with increased N-B interaction, i.e., decrease in N→B bond length. [172] However, the N→B bond lengths in **1**, **6**, **11** and **12** (1.628(4), 1.585(4), 1.552(2) and 1.537(2) Å respectively) do not agree with this observation, possibly due to the restriction imposed by the ligand.

Interestingly, the mononuclear borates **1** and **6** do not show any hydrogen bonding as was observed for binuclear Salen[$(BOMe)_2$]$_2$ compounds.[146]

2.5. Hydrolysis of the boron halide compounds

The boron halide compounds are moisture sensitive. They are hydrolyzed by trace amounts of moisture present in the reaction medium. Binuclear compound **13** containing a B-O-B linkage was obtained during the preparation of the halide **7** by adventitious exposure to moisture (Figure 2.7). Similar Schiff base compounds with B-O-B bridges can be prepared intentionally from the combination of various Salen ligands with phenylboronic acid (Figure 2.8). [150, 173]

The ^{1}H NMR of **13** contained four ^{t}Bu peaks that indicated a non-symmetric solution state structure. The ^{11}B NMR showed two boron peaks at δ 3.19 and δ 7.33 ppm corresponding to four-coordinate boron atoms. The non-symmetry could arise from the non-planarity of the two BOBNCCO rings although this could not explain the presence of only one singlet for the imine protons. The IR shows a peak at 1620 cm^{-1} attributed to $\nu_{C=N}$ stretching. The mass spectra (EI) showed molecular ion peak in 5 % relative abundance.

An X-ray structure (shown in Figure 2.9) confirmed the presence of two four-coordinate boron atoms in **13**. The crystal data collection parameters are shown in Table 2.5, and selected bond distances and angles are contained in Table 2.6. The boron atoms are part of two seven-membered BOBNCCO heterocycles. There is a B-O-B bridge between the two boron atoms. The bridging B-O bond lengths are 1.406(6) and 1.390(6) Å whereas B-O(Ph) bond lengths range from 1.459(6) to 1.481(6) Å. The bridging B-O lengths are close to those observed in some previously reported binuclear Schiff base boron compounds containing B-O-B bridges although the B-O(Ph) lengths are slightly shorter. For example, in the compounds L[PhB)$_2$(μ-O)] (L = salen(^{t}Bu), salpen(^{t}Bu) and

acpen) the bridging B-O bond length ranges from 1.416(5) to 1.419(3) Å and B-O(Ph) length ranges from 1.493(3) to 1.511(4) Å.[173] The B-N bond lengths for **13** are 1.606(6) and 1.610(5) Å.[173] Each boron atom is in a distorted tetrahedral environment. The THC values for B1A and B2A are 75 % and 76 % respectively. The most acute angle for B1A is O2AB1AN1A (101.3(3)) and for B2A is O3A-B2A-N2A (101.9(3) °). The most obtuse angle is O2A-B1A-O5A (115.1(4) °) for B1A and O5A-B2A-O3A (115.2(4) °) for B2A. The B-O-B angle is 117.2(3) °. This angle is significantly smaller compared to the B-O-B bridged compounds L[PhB)$_2$(μ-O) (L = Salen(^{t}Bu) (131.4(3) °), salpen(^{t}Bu) (137.5(3) ° and acpen (128.6 °).[173]

2.6. Conclusion

A series of mononuclear Schiff base borates based on N,O and N,O,O ligands have been prepared. The borates were further derivatized to mononuclear Schiff base boron halides. The boron halides are moisture sensitive and one of them, on reaction with trace water present in the reaction medium, gave a binuclear compound containing a B-O-B linkage and BOBNCCO heterocycles. The boron halides could be further derivatized and used for phosphate dealkylation since the halides could potentially be replaced by a donor molecule to form cationic compounds.

2.7. Experimental

General remarks. All air-sensitive manipulations were conducted using standard bench-top Schlenk line techniques in conjunction with an inert atmosphere glove box. All solvents were rigorously dried prior to use. All glassware was cleaned with a base and an

acid wash and dried in an oven at 130 ºC overnight. The Schiff base ligands N-phenyl-3,5-di-*t*-butylsalicylaldimine, N-(2-hydroxyphenyl)-3,5-di-*t*-butylsalicylaldimine, N-(2-hydroxyethyl)-3,5-di-*t*-butylsalicylaldimine) and N-(3-hydroxpropyl)-3,5-di-*t*-butylsalicylaldimine) were synthesized according to the literature procedure. [170] NMR data were obtained on Varian Gemini-200 and Varian VXR-400 instruments. Chemical shifts were reported relative to $SiMe_4$ for ^1H and ^{13}C and $BF_3.Et_2O$ for ^{11}B and are reported in ppm. Infrared transmission spectra were recorded at room temperature in a potassium bromide pellet on a Fourier-transform Magna-IR ESP 560 spectrometer. Elemental analyses were performed on either a Perkin Elmer 2400 CHN Analyzer or a LECO CHN-2000 Analyzer.

X-ray data were collected on a either a Nonius Kappa-CCD (compounds **1**, **6**, **11** and **12**; Mo-K_α radiation) or a Bruker-Nonius X8 Proteum (compounds **13**; Cu-K_α radiation) diffractometer. All calculations were performed using the software package SHELXTL-Plus.[174-177] The structures were solved by direct methods and successive interpretation of difference Fourier maps followed by least-squares refinement. All non-hydrogen atoms were refined anisotropically. The hydrogen atoms were included using a riding model with isotropic parameters tied to the parent atom.

Synthesis of $LB(OMe)_2$ (LH = N-phenyl-3,5-di-*t*-butylsalicylaldimine) (1). To a rapidly stirred solution of N-phenyl-3,5-di-*t*-butylsalicylaldimine (3.00 g, 9.71 mmol) in toluene, $B(OMe)_3$(6.00 g, 57.7 mmol) was added and refluxed for 16 hours. The volatiles were removed under vacuum and a yellow solid was obtained which was washed with 20 mL of hexane and dried under vacuum. Yield: (3.4 g (92 %). X-ray quality crystals were grown from a concentrated toluene solution after slow cooling to -30 °C. Mp: 98 ºC

(dec.). ^{1}H NMR ($CDCl_3$): δ 1.33 (s, 9H, C(C*H*$_3$)$_3$), 1.48 (s, 9H, C(C*H*$_3$)$_3$), 3.22 (s, 6H, OC*H*$_3$),7.25 (m, 1H, Ph-*H*), 7.27 (m, 2H, Ph-*H*), 7.44 (m, 3H, Ph-*H*), 7.62 (m, 1H, Ph-*H*), 7.78 (m, 1H, Ph-*H*), 8.63 (s, 1H, N=C*H*); ^{13}C NMR ($CDCl_3$): δ 29.7 (C(*C*H$_3$)$_3$), 31.7 (C(*C*H$_3$)$_3$), 34.4 (*C*(CH$_3$)$_3$), 35.3 (*C*(CH$_3$)$_3$), 49.9 (O*C*H$_3$) 118.5 (Ph), 121.4 (Ph), 123.9 (Ph), 126.1 (Ph), 126.7 (Ph), 128.5 (Ph), 129.5 (Ph), 133.5(Ph), 137.2 (Ph), 140.8 (Ph), 148.9 (Ph), 158.5 (Ph), 164.0 (N*C*H). ^{11}B NMR ($CDCl_3$): δ 2.33 ($W_{1/2}$ = 58 Hz). IR (KBr) ν/ cm^{-1}: 3064w, 2962s, 2903m, 2860m, 1614s, 1575s, 1555w, 1478m, 1464m, 1437m, 1390w, 1360m, 1319w, 1273w, 1248m, 1196m, 1171s, 1130w, 1074w, 1025w, 973w, 903w, 878m, 865s, 823w, 801w, 759s, 728w, 688m. MS (EI, positive): 321 (M^+, 5%), 350 (M^+ - OCH_3, 45), 319 (M^+ -2 OCH_3, 10), 264 (M^+ - OCH_3 - ^{t}Bu, 100%). Anal. Calcd. for $C_{23}H_{32}O_3NB$: C 72.44, H 8.46, N 3.67. found: C 73.61, H 8.72, N 3.51.

Synthesis of $LBCl_2$ (LH = N-phenyl-3,5-di-*t*-butylsalicylaldimine) (2). To a rapidly stirred solution of **1** (0.71 g, 1.9 mmol) in toluene, 1 M BCl_3 in heptane (0.68 mL, 0.68 mmol) was added. The yellow cloudy mixture was stirred for 13 hours. The volatiles were removed under vacuum. The yellow solid was washed with hexane and dried under vacuum. Yield: 0.45 g (62 %). Mp: 255-257 ºC (dec.). ^{1}H NMR ($CDCl_3$): δ 1.32 (s, 9H, C(C*H*$_3$)$_3$), 1.48 (s, 9H, C(C*H*$_3$)$_3$), 7.27 (m, 1H, Ph-*H*), 7.36 (m, 1H, Ph-*H*), 7.47 (m, 2H, Ph-*H*), 7.66 (m, 2H, Ph-*H*), 7.78 (m, 1H, Ph-*H*), 8.29 (s, 1H, N=C*H*); ^{13}C NMR ($CDCl_3$): δ 29.6 (C(*C*H$_3$)$_3$), 31.3 (C(*C*H$_3$)$_3$), 34.6 (*C*(CH$_3$)$_3$), 35.4 (*C*(CH$_3$)$_3$), 125.2 (Ph),.126.5 (Ph), 129.5 (Ph), 129.7 (Ph), 136.0 (Ph), 144.2 (Ph), 164.2 (N*C*H). ^{11}B NMR ($CDCl_3$): δ 2.48 ($W_{1/2}$ = 57 Hz). IR (KBr) ν/ cm^{-1}: 2961s, 2905w, 2869w, 1619s, 1566s, 1555m, 1492w, 1468w, 1392w, 1380w, 1363w, 1254m, 1200m, 1132w, 1015m, 1005m, 918w, 904w, 849m, 762w, 720w, 692m. MS (EI, positive): 390 (M^+, 0.5%), 355 (M^+ - Cl, 2%),

320 (M^+- 2 Cl, 5%), 309 (M^+- BCl_2, 45%), 294 (M^+- BCl_2 – CH_3, 100%). Anal. Calcd. for $C_{21}H_{26}ONBCl_2$: C 64.65, H 6.72, N 3.59. found: C 66.11, H 8.44, N 3.51.

Synthesis of $LBBr_2$ (LH = N-phenyl-3,5-di-*t*-butylsalicylaldimine) (3). To a rapidly stirred solution of **1** (0.48 g, 1.3 mmol) in toluene, 1 M BBr_3 in heptane (0.42 mL, 0.42 mmol) was added with a syringe. The yellow reaction mixture was stirred for 20 hours. The volatiles were removed under vacuum and the yellow residue was washed with hexane and dried under vacuum. Yield: 0.45 g (75 %). Mp: 284-288 ºC (dec.). ^{1}H NMR ($CDCl_3$): δ 1.30 (s, 9H, C(C*H*$_3$)$_3$), 1.38 (s, 9H, C(C*H*$_3$)$_3$), 6.95 (d, 2H, Ph-*H*), 7.17-7.30 (m, 3H, Ph-*H*), 7.85 (d, 1H, Ph-*H*), 7.98 (d, 1H, Ph-*H*), 9.38 (s, 1H, N=C*H*); ^{13}C NMR ($CDCl_3$): δ 29.7 (C(*C*H$_3$)$_3$), 31.4 (C(*C*H$_3$)$_3$), 34.9 (*C*(CH$_3$)$_3$), 35.3 (*C*(CH$_3$)$_3$), 123.4 (Ph),.125.5 (Ph), 128.4 (Ph), 129.3 (Ph), 129.8 (Ph), 130.2 (Ph), 132.8 (Ph), 137.0 (Ph), 138.9 (Ph), 141.6 (Ph), 145.0 (Ph), 153.6 (Ph), 167.7 (N*C*H). ^{11}B NMR ($CDCl_3$): δ 2.38 ($W_{1/2}$ = 60 Hz). IR (KBr) ν/ cm^{-1}: 2959s, 2901w, 2870w, 1625m, 1594w, 1563s, 1493w, 1469m, 1442w, 1414w, 1381m, 1363w, 1255m, 1203m, 1134w, 1067w, 1030m, 774w, 757w, 690w. MS (EI, positive): 309 (M^+ - BBr_2, 33%), 294 (M^+- BBr_2 – CH_3, 100%). Anal. Calcd. for $C_{21}H_{26}ONBBr_2$: C 52.65, H 5.47, N 2.92. found: C 53.00, H 5.15, N 2.85.

Synthesis of L[B(OMe)] (LH_2 = N-(2-hydroxyphenyl)-3,5-di-*t*-butylsalicylaldimine) (4). To a rapidly stirred solution of N-(2-hydroxyphenyl)-3,5-di-*t*-butylsalicylaldimine) (3.31g, 10.2 mmol) in toluene, excess $B(OMe)_3$(6.50 g, 62.5 mmol) was added and refluxed for 8 hours. The volatiles were removed under vacuum to yield an orange solid. Yield: 3.1 g (82 %). Mp: 210 ºC (dec.). ^{1}H NMR ($CDCl_3$): δ 1.30 (s,9H, C(C*H*$_3$)$_3$), 1.49 (s,9H, C(C*H*$_3$)$_3$), 3.15 (s, 3H, OC*H*$_3$), 6.86-7.66 (m, 6H, Ph-*H*), 8.52 (s,

1H, N=C*H*); ^{13}C NMR ($CDCl_3$): δ 29.5 (C(*C*H_3)$_3$), 31.2 (C(*C*H_3)$_3$), 34.2 (*C*(CH_3)$_3$), 35.4 (*C*(CH_3)$_3$), 49.7 (O*C*H_3), 114.3 (Ph), 114.7 (Ph), 119.1 (Ph),125.3 (Ph), 128.2 (Ph), 129.0 (Ph), 131.3 (Ph),133.0(Ph),139.8 (Ph),142.2 (Ph), 150.5 (Ph), 154.6 (Ph),157.3 (N*C*H). ^{11}B NMR ($CDCl_3$): δ 5.09. IR (KBr) ν/ cm^{-1}: 2959s, 2905w, 2868w, 1628s, 1556m, 1545m, 1480s, 1419m, 1390m, 1380m, 1362m, 1324s, 1259m, 1202m, 1181s, 1108s, 1039w, 1018m, 1007m, 987m, 886w, 752s. MS (EI, positive): MS (EI, positive): 365 (M^+, 11 %), 334 (M^+ - OCH_3, 100%). Anal. Calcd. for $C_{22}H_{28}O_3NB$: C 72.34, H 7.73, N 3.83. found: C 73.20, H 8.33, N 3.60.

Synthesis of L[B(OMe)] (LH_2 = N-(2-hydroxyethyl)-3,5-di-*t*-butylsalicylaldimine) (5). To a rapidly stirred solution of N-(2-hydroxyethyl)-3,5-di-*t*-butylsalicylaldimine (3.50 g, 12.6 mmol) in toluene, $B(OMe)_3$(4.20 g, 40.8 mmol) was added and refluxed for 18 hours. The volatiles were removed under vacuum and the yellow residue was washed with hexane. Yield: 3.2 g (81 %). Mp: 302-306 ºC (dec.). ^{1}H NMR ($CDCl_3$): δ 1.27 (s, 9H, C(C*H*$_3$)$_3$), 1.42 (s, 9H, C(C*H*$_3$)$_3$), 3.17 (s, 3H, OC*H*$_3$), 3.30-3.48 (m, 2H, NC*H*$_2$), 3.63-3.86 (m, 2H, OC*H*$_2$);7.04 (d,1H, Ph-*H*), 7.52 (d, 1H, Ph-*H*), 8.30 (s, 1H, N=C*H*). ^{13}C NMR ($CDCl_3$): δ 29.3 (C(*C*H_3)$_3$), 31.2 (C(*C*H_3)$_3$), 34.1 (*C*(CH_3)$_3$), 35.0 (*C*(CH_3)$_3$), 49.5 (O*C*H_3), 58.9 (N*C*H_2), 59.8 (O*C*H_2) 114.7 (Ph), 125.3 (Ph), 131.9 (Ph), 138.2 (Ph), 140.4, (Ph),157.8(Ph), 166.8 (N*C*H). ^{11}B NMR ($CDCl_3$): δ 2.38. IR (KBr) ν/ cm^{-1}: 2954s, 2905w, 2863w, 1644s, 1567w, 1479w, 1462w, 1444w, 1384w, 1360w, 1309w, 1254m, 1210m, 1149s, 1132m, 1017s, 989m, 805w, 774w. MS (EI, positive): 286 (M^+ - OCH_3, 100%). Anal. Calcd. for $C_{18}H_{28}O_3NB$: C 68.15, H 8.90, N 4.42. found: C 68.25, H 9.18, N 4.23.

Synthesis of L[B(OMe)] (LH_2 = N-(3-hydroxypropyl)-3,5-di-*t*-butylsalicylaldimine) (6). To a rapidly stirred solution of N-(3-hydroxypropyl)-3,5-di-*t*-butylsalicylaldimine (4.28 g, 14.7 mmol) in toluene, $B(OMe)_3$ (2.00 g, 19.2 mmol) was added and refluxed for 16 hours. The volatiles were removed under vacuum and a pale yellow solid was obtained which was dried under vacuum. Yield: 4.5 g (92%). Mp: 190-192 ºC (dec.). ^{1}H NMR ($CDCl_3$): δ 1.26 (s, 9H, C(C*H*$_3$)$_3$), 1.43 (s, 9H, C(C*H*$_3$)$_3$), 1.68-1.86 (m, 1H, C*H*$_2$), 2.00-2.24 (m, 1H, C*H*$_2$), 3.23 (s, 3H, OC*H*$_3$), 3.56-3.66 (m, 1H, NC*H*$_2$), 3.92-3.99 (m, 1H, NC*H*$_2$), 4.09- 4.31 (m, 2H, OC*H*$_2$);7.03 (d, 1H, Ph-*H*), 7.53 (d, 1H, Ph-*H*), 7.99 (s, 1H, N=C*H*). ^{13}C NMR ($CDCl_3$): δ 29.4 (C(*C*H$_3$)$_3$), 30.4 (*C*H$_2$), 31.2 (C(*C*H$_3$)$_3$), 34.0 (*C*(CH$_3$)$_3$), 35.1 (*C*(CH$_3$)$_3$), 49.7 (O*C*H$_3$), 54.5 (N*C*H$_2$), 61.2 (O*C*H$_2$) 114.8 (Ph), 125.0 (Ph), 132.1 (Ph), 138.7 (Ph), 140.5, (Ph),157.2(Ph), 160.7 (N*C*H). ^{11}B NMR ($CDCl_3$): δ 2.00 ($W_{1/2}$ = 140 Hz). IR (KBR) ν/ cm^{-1}: 2955s, 2901m, 2867m, 1661s, 1567m, 1478m, 1448m, 1452m, 1429m, 1392w, 1361m, 1344m, 1307m, 1283w, 1265m, 1244m, 1202m, 1186m, 1153m, 1105s, 1082m, 1039m, 989m, 970m, 923m, 884m, 776w.MS (EI, positive): 331 (M^+, 1%), 300 (M^+ - OCH_3, 100)%. Anal. Calcd. for $C_{19}H_{30}O_3NB$: C 68.89, H 9.13, N 4.23. found:C 69.55, H 9.28, N 4.31.

Synthesis of L[BCl] (LH_2 = N-(2-hydroxyphenyl)-3,5-di-*t*-butylsalicylaldimine) (7). To a rapidly stirred solution of **4** (1.00g, 2.74 mmol) in toluene, excess 1 M BCl_3 in heptane (2.75 mL, 2.75 mmol) was added. The reaction mixture was stirred for 13 hours. The golden yellow solution was cannula filtered and the volatiles were removed from the filtrate under vacuum to give a yellow solid. Yield: 0.96 g (95 %). Mp: 298 ºC (dec.). ^{1}H NMR ($CDCl_3$): δ 1.36 (s, 9H, C(C*H*$_3$)$_3$), 1.54 (s, 9H, C(C*H*$_3$)$_3$), 6.97-7.81 (m, 6H, Ph-*H*), 8.58 (s, 1H, N=C*H*); ^{13}C NMR ($CDCl_3$): δ 29.6 (C(*C*H$_3$)$_3$), 31.2 (C(*C*H$_3$)$_3$), 34.4

($C(CH_3)_3$), 35.4 ($C(CH_3)_3$), 115.0 (Ph), 115.3 (Ph), 120.6 (Ph),125.8 (Ph), 128.2 (Ph), 129.0 (Ph), 132.0 (Ph),134.1(Ph),140.6 (Ph),144.1 (Ph), 150.3 (Ph), 153.2 (Ph),156.3 (N*C*H). ^{11}B NMR ($CDCl_3$): δ 7.28. IR (KBr) ν/ cm^{-1}: 2960s, 2901w, 2869w, 1631s, 1563m, 1549w, 1479s, 1467m, 1424m, 1392m, 1382m, 1363m, 1327m, 1254m, 1202m, 1190s, 1111w, 1031w, 747m. MS (EI, positive): 286 (M^+-Cl, 100%, 319 (M^+- Cl - O, 15%). Anal. Calcd. for $C_{21}H_{25}O_2NBCl$: C 68.23, H 6.82, N 3.79. found: C 68.75, H 7.65, N 4.04.

Synthesis of L[BBr] (LH_2 = N-(2-hydroxyphenyl)-3,5-di-*t*-butylsalicylaldimine) (8). To a rapidly stirred solution of **4** (1.00 g, 2.74 mmol) in toluene, excess 1 M BBr_3 in heptane (2.78 mL, 2.78 mmol) was added. The reaction mixture was stirred for 13 hours. The solution was concentrated to about one third of its volume. The yellow precipitate was cannula filtered and dried under vacuum. Yield: 0.73 g (65 %). Mp: 234-238 ºC (dec.). ^{1}H NMR ($CDCl_3$): δ 1.34 (s, 9H, C(CH_3)$_3$), 1.52 (s, 9H, C(CH_3)$_3$), 7.00-7.83 (m, 6H, Ph-*H*), 8.81 (s, 1H, N=C*H*); ^{13}C NMR ($CDCl_3$): δ 29.6 (C(CH_3)$_3$), 31.2 (C(CH_3)$_3$), 34.4 ($C(CH_3)_3$), 35.4 ($C(CH_3)_3$), 115.3 (Ph), 118.3 (Ph), 121.3 (Ph),.126.3 (Ph), 128.6 (Ph), 129.0 (Ph), 132.1 (Ph), 134.8(Ph),140.7 (Ph), 144.9 (Ph), 150.9 (Ph), 152.8 (Ph),155.4 (N*C*H). ^{11}B NMR ($CDCl_3$): δ 6.47 (4-coordinate boron). IR (KBr) ν/ cm^{-1}: 2960s, 2905w, 2869w, 1629s, 1564m, 1549m, 1479s, 1424m, 1392m, 1380m, 1363m, 1328s, 1253m, 1203w, 1189w, 1103w, 1014w, 864w, 769w, 747m, 694w, 664w. MS (EI, positive): 414 (M^+, 3%) 334 (M^+ - Br, 100%, 318 (M^+- Br - O, 20%). Anal. Calcd. for $C_{21}H_{25}O_2NBBr$: C 60.90, H 6.08, N 3.38. found: C 61.58, H 6.07, N 3.16.

Synthesis of L[BCl] (LH_2 = N-(2-hydroxyethyl)-3,5-di-*t*-butylsalicylaldimine) (9).

To a rapidly stirred solution of **5** (0.97g, 3.1 mmol) in toluene, 1 M BCl_3 in heptane (1.1 mL, 1.1 mmol) was added. The reaction mixture was stirred for 24 hours. Then it was cannula filtered and the pale yellow residue was dried under vacuum. Yield: 0.78 g (80 %). Mp: > 320 ºC (dec.). ^{1}H NMR ($CDCl_3$): δ 1.24 (s, 9H, C(C*H*$_3$)$_3$), 1.42 (s, 9H, C(C*H*$_3$)$_3$), 3.44-3.55 (m, 2H, NC*H*$_2$), 3.33-3.44 (m, 2H, OC*H*$_2$); 7.07 (d, 1H, Ph-*H*), 7.56 (d, 1H, Ph-*H*), 8.11 (s, 1H, N=C*H*). ^{13}C NMR ($CDCl_3$): δ 29.86 (C(*C*H$_3$)$_3$), 31.4 (C(*C*H$_3$)$_3$), 34.3 (*C*(CH$_3$)$_3$), 35.2 (*C*(CH$_3$)$_3$), 60.5 (N*C*H$_2$) 61.2 (O*C*H$_2$), 115.0 (Ph), 125.8 (Ph), 133.7 (Ph), 139.0 (Ph), 141.4, (Ph),157.2(Ph), 164.9 (N*C*H). ^{11}B NMR ($CDCl_3$): δ 2.05 ($W_{1/2}$ = 360 Hz). IR (KBr) ν/ cm^{-1}: 2960s, 2905w, 2870w, 1640s, 1573m, 1479s, 1444s, 1395m, 1378s, 1363s, 1334m, 1302m, 1283m, 1261m, 1243m, 1214m, 1202m, 1190m, 1138m, 1085m, 1027m, 913w, 879w, 851w, 818w, 802w, 774w.MS (EI, positive): 322 (M^+, 1 %), (M^+ - Cl, 90%). Anal. Calcd. for $C_{17}H_{25}O_2NBCl$: C 63.48, H 7.83, N 4.36. found: C 63.37, H 8.78, N 4.15.

Synthesis of L[BBr] (LH_2 = N-(2-hydroxyethyl)-3,5-di-*t*-butylsalicylaldimine) (10). To a rapidly stirred solution of **5** (0.54 g, 1.7 mmol) in toluene, 1 M BBr_3 in heptane (0.60 mL, 0.60 mmol) was added with a syringe. The clear yellow solution was stirred for 17 hours. The volatiles were removed under vacuum and the off white residue was washed with hexane and dried under vacuum. Yield: 0.47 g (75 %). Mp: 228-232 °C (dec.). ^{1}H NMR ($CDCl_3$): δ 1.32 (s, 9H, C(C*H*$_3$)$_3$), 1.47 (s, 9H, C(C*H*$_3$)$_3$), 3.94 (m, 4H, NC*H*$_2$ and OC*H*$_2$); 7.17 (d, 1H, Ph-*H*), 7.59 (d, 1H, Ph-*H*), 8.25 (s, 1H, N=C*H*). ^{13}C NMR ($CDCl_3$): δ 29.4 (C(*C*H$_3$)$_3$), 31.2 (C(*C*H$_3$)$_3$), 33.2 (*C*(CH$_3$)$_3$), 35.0 (*C*(CH$_3$)$_3$), 50.8 (N*C*H$_2$), 55.0 (O*C*H$_2$), 115.4 (Ph), 125.6 (Ph), 132.2 (Ph), 138.3 (Ph), 140.6, (Ph),157.8(Ph), 164.9 (N*C*H). ^{11}B NMR ($CDCl_3$): δ 2.00 ($W_{1/2}$ = 122 Hz). IR (KBr) ν/

cm^{-1}: 2958s, 2901w, 2869w, 1644s, 1566m, 1479m, 1469m, 1441m, 1391m, 1378s, 1360m, 1336m, 1304m, 1259m, 1240w, 1203w, 1188m, 1135s, 1042m, 975m, 931w, 877w, 827w, 811w, 775w, 762w. MS (EI, positive): 366 (M^+, 30%), 286 (M^+ - Br, 55%, 270 (M^+- Br-O, 45%). Anal. Calcd. for $C_{17}H_{25}O_2NBBr$: C 55.77, H 6.88, N 3.83. found: C 54.98, H 7.36, N 3.96.

Synthesis of L[BCl] (LH_2 = N-(3-hydroxypropyl)-3,5-di-*t*-butylsalicylaldimine) (11). To a rapidly stirred solution of **6** (1.1 g, 3.2 mmol) in toluene, 1 M BBr_3 in heptane (1.1 mL, 1.1 mmol) was added. The clear golden yellow solution was stirred for 14 hours. The volatiles were removed under vacuum and the yellow residue was washed with hexane and dried under vacuum Yield: 0.88 g (81 %). X-ray quality crystals were isolated after cooling a concentrated toluene solution to -30 °C. Mp: 192-194 ºC (dec.). ^{1}H NMR ($CDCl_3$): δ 1.29 (s, 9H, C(C*H*$_3$)$_3$), 1.45 (s, 9H, C(C*H*$_3$)$_3$), 2.02 (q, 2H, C*H*$_2$), 4.06 (t, 2H, NC*H*$_2$), 4.24 (t, 2H, OC*H*$_2$) 7.13 (d, 1H, Ph-*H*), 7.66 (d, 1H, Ph-*H*), 7.93 (s, 1H, N=C*H*). ^{13}C NMR ($CDCl_3$): δ 28.8 (*C*H$_2$), 29.4 (C(*C*H$_3$)$_3$), 31.2 (C(*C*H$_3$)$_3$), 34.1 (*C*(CH$_3$)$_3$), 35.1 (*C*(CH$_3$)$_3$), 53.8 (N*C*H$_2$), 61.3 (O*C*H$_2$) 115.4 (Ph), 125.4 (Ph), 133.1 (Ph), 139.2 (Ph), 142.0 (Ph),155.9 (Ph), 161.3 (N*C*H). ^{11}B NMR ($CDCl_3$): δ 3.3 ($W_{1/2}$ = 166 Hz). IR (KBr) ν/ cm^{-1}: 2960s, 2866w, 1649s, 1572m, 1479m, 1461m, 1441m, 1432w, 1384m, 1365m, 1345m, 1285w, 1265m, 1246w, 1193m, 1164m, 1125w, 1093w, 1024w, 959w, 930w, 872w, 831w, 773w, 758w. MS (EI, positive): 336 (M^+, 1%), 300 (M^+ - Cl, 100%). Anal. Calcd. for $C_{18}H_{27}O_2NBCl$: C 64.41, H 8.11, N 4.17. found: C 65.72, H 6.86, N 4.06.

Synthesis of L[BBr] (LH_2 = N-(3-hydroxypropyl)-3,5-di-*t*-butylsalicylaldimine) (12). To a rapidly stirred solution of **6** (0.69 g, 2.1 mmol) in toluene, 1 M BBr_3 in heptane (0.75 mL, 0.75 mmol) was added. The clear yellow solution was stirred for 6 hours. Then

it was concentrated to about one-third of its volume and yellow crystals were obtained after cooling at -30ºC overnight. The crystals were isolated by cannula filtration and dried under vacuum. Yield: (0.50 g (63 %). Mp: softens at 174 ºC and melts at 178-181 ºC (dec.). ^{1}H NMR ($CDCl_3$): δ 1.27 (s, 9H, C(C*H*$_3$)$_3$), 1.42 (s, 9H, C(C*H*$_3$)$_3$), 2.11 (m, 2H, C*H*$_2$), 4.31 (s, br, 4H, NC*H*$_2$ and OC*H*$_2$), 7.48 (d, 1H, Ph-*H*), 7.78 (s, br, 1H, Ph-*H*), 8.97 (s, 1H, N=C*H*). ^{13}C NMR ($CDCl_3$): δ 26.3 (*C*H$_2$), 29.8 (C(*C*H$_3$)$_3$), 31.4 (C(*C*H$_3$)$_3$), 34.8 (*C*(CH$_3$)$_3$), 35.4 (*C*(CH$_3$)$_3$), 52.3 (N*C*H$_2$), 63.0 (O*C*H$_2$) 116.9 (Ph), 127.2 (Ph), 135.9 (Ph), 140.0 (Ph), 145.5 (Ph),154.5 (Ph), 166.6 (N*C*H). ^{11}B NMR ($CDCl_3$): δ 9.7 ($W_{1/2}$ = 383 Hz). IR (KBr) ν/ cm^{-1}: 2962s, 2869w, 1638s, 1573s, 1471m, 1459m, 1452m, 1437w, 1386w, 1365m, 1347m, 1285m, 1265m, 1247s, 1196s, 1180m, 1135m, 1097m, 1084m, 1046w, 1000w, 961w, 931w, 874w, 831m, 772m, 755w, 661m, 623m, 607m, 545m. MS (EI, positive): 380 (M^+, 5%), 300 (M^+ - Br, 100). Anal. Calcd. for $C_{18}H_{27}O_2NBBr$: C 56.87, H 7.16, N 3.69. found: C 56.04, H 5.91, 3.36.

Hydrolyzed product (13): To a rapidly stirred solution of **4** (1.00 g, 2.74 mmol) in toluene 1 M BCl_3 in heptane (1.00 mL, 1.00 mmol) was added. The deep brown solution was stirred for 18 hours. The volatiles were removed under vacuum to obtain a yellow solid. The solid was recrystallized from dichloromethane to give yellow X-ray quality crystals of **13**. Yield: 0.61 g (33 %). Mp: 303 - 305 ºC (dec.). ^{1}H NMR ($CDCl_3$): δ 1.24 (s, 9H, C(C*H*$_3$)$_3$), 1.29 (s, 9H, C(C*H*$_3$)$_3$), 1.31 (s, 9H, C(C*H*$_3$)$_3$), 1.45 (s, 9H, C(C*H*$_3$)$_3$), 6.52-7.73 (m, 12H, Ph-*H*), 8.51 (s, 2H, N=C*H*); ^{13}C NMR ($CDCl_3$): δ 29.5 (C(*C*H$_3$)$_3$),29.8 (C(*C*H$_3$)$_3$), 31.2 (C(*C*H$_3$)$_3$), 31.3 (C(*C*H$_3$)$_3$), 34.3 (*C*(CH$_3$)$_3$), 35.2 (*C*(CH$_3$)$_3$), 38.1 (*C*(CH$_3$)$_3$), 114.9 (Ph), 120.6 (Ph), 121.8 (Ph), 122.0 (Ph), 125.6 (Ph), 126.2 (Ph), 129.6 (Ph), 132.0 (Ph), 133.0 (Ph), 134.2 (Ph), 139.4 (Ph), 141.3 (Ph),144.9

(Ph), 151.6 (Ph), 159.4 (N*C*H). ^{11}B NMR ($CDCl_3$): δ 3.19 ($W_{1/2}$ = 720 Hz), 7.33 (W1/2 = 320 Hz). IR (KBr) ν/ cm^{-1}: 2959s, 2909w, 2869w, 1620m, 1586m, 1563m, 1548m, 1486m, 1468m, 1441m, 1414m, 1391m, 1378w, 1362m, 1324w, 1293m, 1263s, 1255s, 1204s, 1187m, 1155m, 1110w, 1016w, 944m, 905m, 749m. MS (EI, positive): 684 (M^+, 5 %), 334 (M^+ - $C_{21}H_{25}O_3NB$, 100%). Anal. Calcd. for $C_{42}H_{50}O_5NB_2$: C 73.70, H 7.36, N 4.09. found: C 73.77, H 7.11, N 3.62.

Table 2.1. Crystallographic data and refinement details for compounds **1** and **6**

	1	**6**
Empirical formula	$C_{23}H_{32}BNO_3$	$C_{19}H_{30}BNO_3$
M/ g mol^{-1}	381.31	331.25
Color	Yellow	Yellow
Crystal size/mm	0.90 x 0.15 x 0.03	0.20 x 0.10 x 0.08
Crystal system, space group	Monoclinic	Monoclinic
Space group	C c	P 2_1/c
a/ Å	11.5730(4)	16.2045(3)
b/ Å	26.0370(11)	11.2564(3)
c/ Å	c = 8.5110(3)	10.4662(5)
α/ °	90.00	90.00
β/ °	120.9071(19)	94.7290(11)
γ/ °	90.00	90.00
V/ $Å^3$	2200.42(14)	1902.58(11)
ρ_{calc}/ g cm^{-3}	1.151	1.156
Z	4	4
F(000)	824	720
Radiation used	Mo-K_α	Mo-K_α
μ /mm^{-1}	0.074	0.076
T/ K	90.0(2)	90.0(2) K
hkl range	$-13 \le h \le 13$, $-30 \le k \le 30$, $-10 \le l \le 10$	$-19 \le h \le 19$, $-13 \le k \le 13$, $-12 \le l \le 12$
Θ range/ °	1.56 - 25.00	1.26 - 25.00
Reflections measured	3820	6477
Unique reflections (R_{int})	3808 (0.0241)	3359 (0.0748)
Obsd reflections, n [$I \ge 2\sigma$	2648	1647

(I)]

Refinement method	Full-matrix least-squares on F^2	Full-matrix least-squares on F^2
Refined parameters/restraints	261/2	224/0
R1 [$I > 2\sigma$]	R1 = 0.0512, wR2 = 0.0950	0.0556, wR2 = 0.1277
R1 (all data)	R1 = 0.0980, wR2 = 0.1108	0.1418, wR2 = 0.1583
Goodness-of-fit on F^2	1.134	0.924
Largest diff. peak and hole/ e. $Å^{-3}$	0.238 and -0.177	0.190 and -0.234

Table 2.2. Selected bond distances (Å) and angles (º) for the borate compounds **1** and **6**.

1			
B1-O1	1.485(4)	O3-C23	1.412(4)
B1-O2	1.414(4)	N1-C15	1.302(4)
B1-O3	1.426(4)	N1-C16	1.442(4)
B1-N1	1.628(4)		
O1-B1-N1	106.8(3)	O1-B1-O2	112.1(3)
O2-B1-N1	108.5(3)	O1-B1-O3	112.1(3)
O3-B1-N1	108.9(3)	O2-B1-O3	108.4(3)
6			
B1-O1	1.473(3)	O3-C19	1.428(3)
B1-O2	1.431(3)	N1-C15	1.286(3)
B1-O3	1.444(3)	N1-C16	1.466(3)
B1-N1	1.585(4)		
O1-B1-N1	109.4(2)	O1-B1-O2	107.6(2)
O2-B1-N1	108.2(2)	O1-B1-O3	111.2(2)
O3-B1-N1	105.0(2)	O2-B1-O3	115.3(2)

Table 2.3. Crystallographic data and refinement details for compounds **11** and **12**

	11	**12**
Empirical formula	$C_{18.15}H_{27.46}BCl_{0.85}NO_{2.15}$	$C_{18}H_{27}BBrNO_2$
M/ g mol^{-1}	335.00	380.13
Color		Pale yellow
Crystal size/mm	0.45 x 0.35 x 0.25	0.30 x 0.20 x 0.08
Crystal system	Triclinic	Triclinic
Space group	P -1	P -1
a/ Å	11.63150(10)	11.5811(1)
b/ Å	11.82500(10)	11.9058(1)
c/ Å	16.5808(2)	16.5674(1)
α/ °	100.1133(4)	101.1731(3)
β/ °	102.1617(5)	101.3603(4)
γ/ °	115.9115(5)	115.8035(3)
V/ Å^3	1910.10(3)	1912.52(3)
ρ_{calc}/ g cm^{-3}	1.165	1.320
Z	4	4
F(000)	720	792
Radiation used	Mo-K_α	Mo-K_α
μ /mm $^{-1}$	0.188	2.157
T/ K	90.0(2)	90.0(2)
hkl range	-15≤ h ≤ 15, -15≤ k ≤ 15, -21≤ l ≤ 21	-15 ≤ h ≤ 15, -15≤ k ≤ 15, -21≤ l ≤ 21
Θ range/ °	1.32 - 27.49	1.32 - 27.50
Reflections measured	17406	47040
Unique reflections (R_{int})	8762 (0.0334)	8775 (0.0410)
Obsd reflections, n [I ≥ 2σ	6064	7220

(I)]

Refinement method	Full-matrix least-squares on F^2	Full-matrix least-squares on F^2
Refined parameters/restraints	453/85	261/2
R1 [$I > 2\sigma$]	0.0523, wR2 = 0.1419	0.0267, wR2 = 0.0598
R1 (all data)	0.0834, wR2 = 0.1599	0.0388, wR2 = 0.0641
Goodness-of-fit on F^2	1.076	1.017
Largest diff. peak and hole/ e. $Å^{-3}$	0.496 and -0.367	0.408 and -0.409

Table 2.4. Selected bond distances (Å) and angles (º) for the boron halide compounds **11** and **12**

11			
B1A-O1A	1.437(2)	B1A-N1A	1.552(2)
B1A-O2A	1.400(2)	B1A-Cl1A	1.965(2)
O1A-B1A-N1A	111.22(15)	O1A-B1A-Cl1A	108.04(13)
O1A-B1A-O2A	109.16(16)	O2A-B1A-Cl1A	111.22(14)
O2A-B1A-N1A	113.18(16)	N1A-B1A-Cl1A	103.83(13)
12			
B1A-O1A	1.426(2)	B1A-N1A	1.537(2)
B1A-O2A	1.391(2)	B1A-Br1A	2.201(2)
O1A-B1A-N1A	112.33(14)	O1A-B1A-Br1A	106.87(11)
O1A-B1A-O2A	111.01(15)	O2A-B1A-Br1A	109.00(12)
O2A-B1A-N1A	114.92(14)	N1A-B1A-Br1A	101.97(11)

Table 2.5. Crystallographic data and refinement details for compound **13**

	13
Empirical formula	$C_{44}H_{54}B_2Cl_4N_2O_5$
M/ g mol^{-1}	854.31
Color	Yellow
Crystal size/mm	0.12 x 0.08 x 0.05
Crystal system	Orthorhombic
Space group	$P2_12_12_1$
a/ Å	12.9606(2)
b/ Å	19.6141(3)
c/ Å	51.9064(7)
α/ °	90.00
β/ °	90.00
γ/ °	90.00
V/ Å^3	13195.2(3)
ρ_{calc}/ g cm^{-3}	1.290
Z	12
F(000)	5400
Radiation used	Cu-K_α
μ /mm $^{-1}$	2.810
T/ K	90.0(2)
hkl range	$-9 \leq h \leq 15$, $-22 \leq k \leq 23$, $-46 \leq l \leq 62$
Θ range/ °	2.41 to 67.99
Reflections measured	93693
Unique reflections (R_{int})	23333 (0.0767)
Obsd reflections, n [$I \geq 2\sigma$ (I)]	16374

Refinement method	Full-matrix least-squares on F^2
Refined parameters/restraints	1658/ 1678
R1 [$I > 2\sigma$]	0.0686, wR2 = 0.1648
R1 (all data)	0.1032, wR2 = 0.1867
Goodness-of-fit on F^2	1.026
Largest diff. peak and hole/ e. $Å^{-3}$	0.609 and -2.022

Table 2.6. Selected bond distances (Å) and angles (º) for compound **13**

B1A-O1A	1.459(6)	B2A-O3A	1.481(6)
B1A-O2A	1.480(5)	B2A-O4A	1.463(5)
B1A-O5A	1.406(6)	B2A-O5A	1.390(6)
B1A-N1A	1.606(6)	B2A-N2A	1.610(5)
O1A-B1A-N1A	106.2(3)	O5A-B2A-N2A	112.1(3)
O1A-B1A-O2A	111.3(3)	O5A-B2A-O3A	115.2(4)
O1A-B1A-O5A	109.4(4)	O5A-B2A-O4A	110.1(4)
O2A-B1A-N1A	101.3(3)	O3A-B2A-N2A	101.9(3)
O2A-B1A-O5A	115.1(4)	O3A-B2A-O4A	110.9(3)
O5A-B1A-N1A	113.0(3)	O4A-B2A-N2A	106.1(3)
B1A-O5A-B2A	117.2(3)		

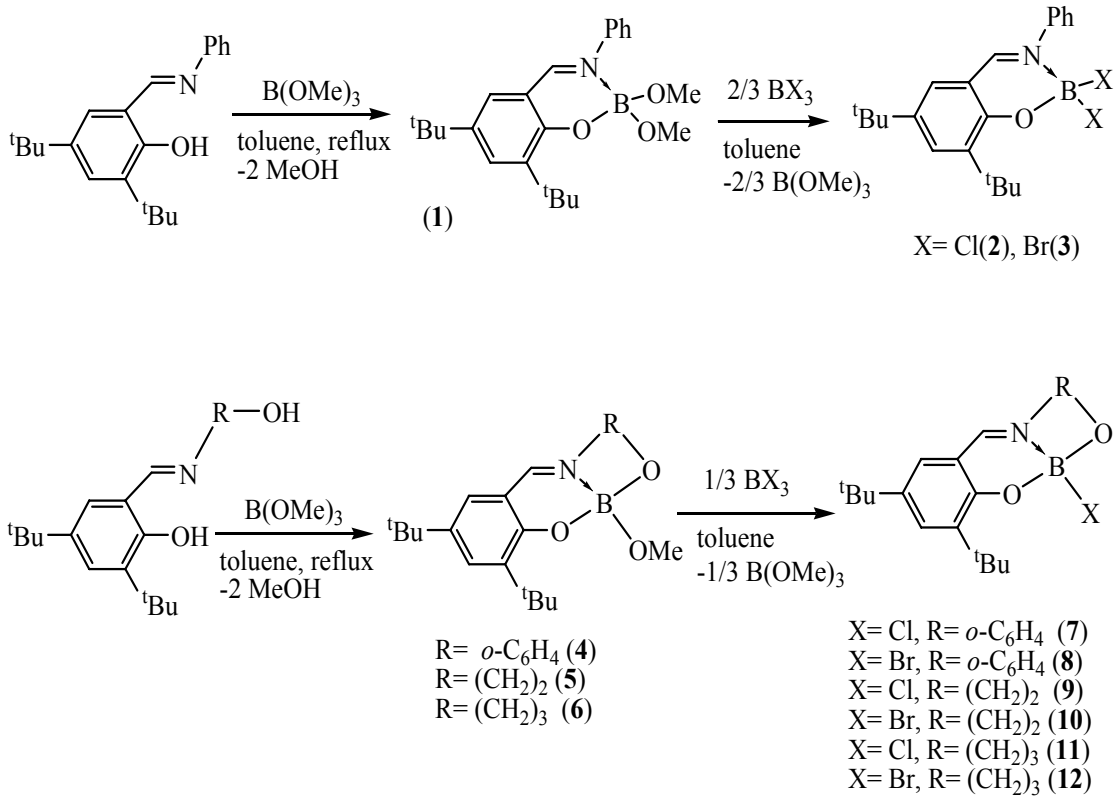

Figure 2.1. Preparation of compounds **1**-**12**.

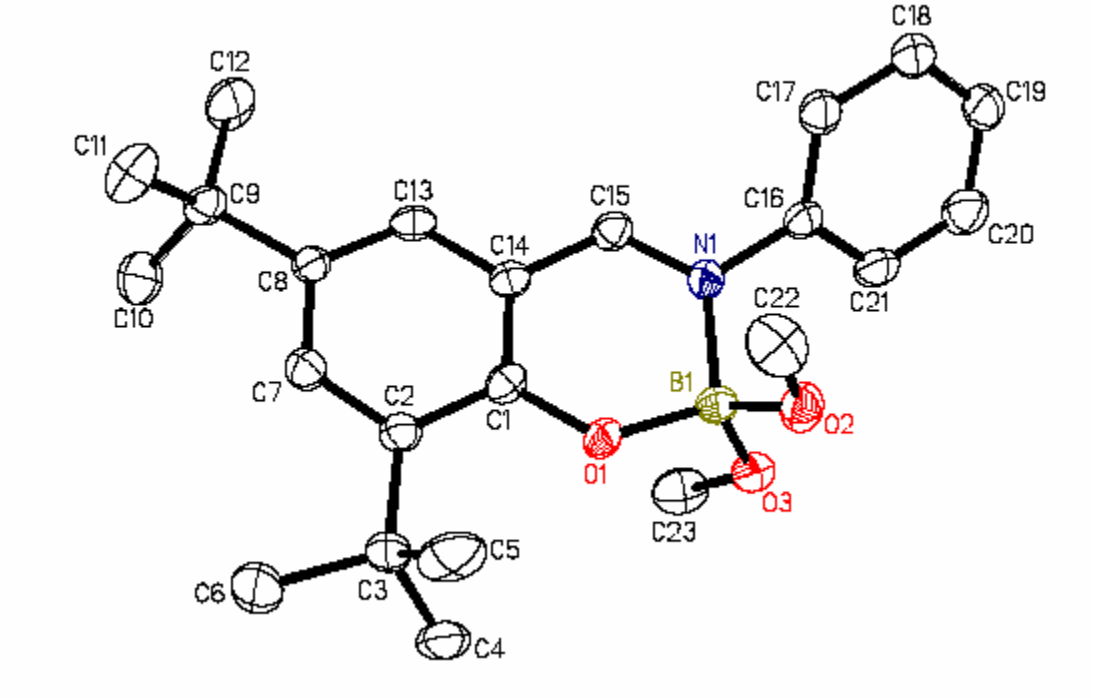

Figure 2.2. Structure of **1**.

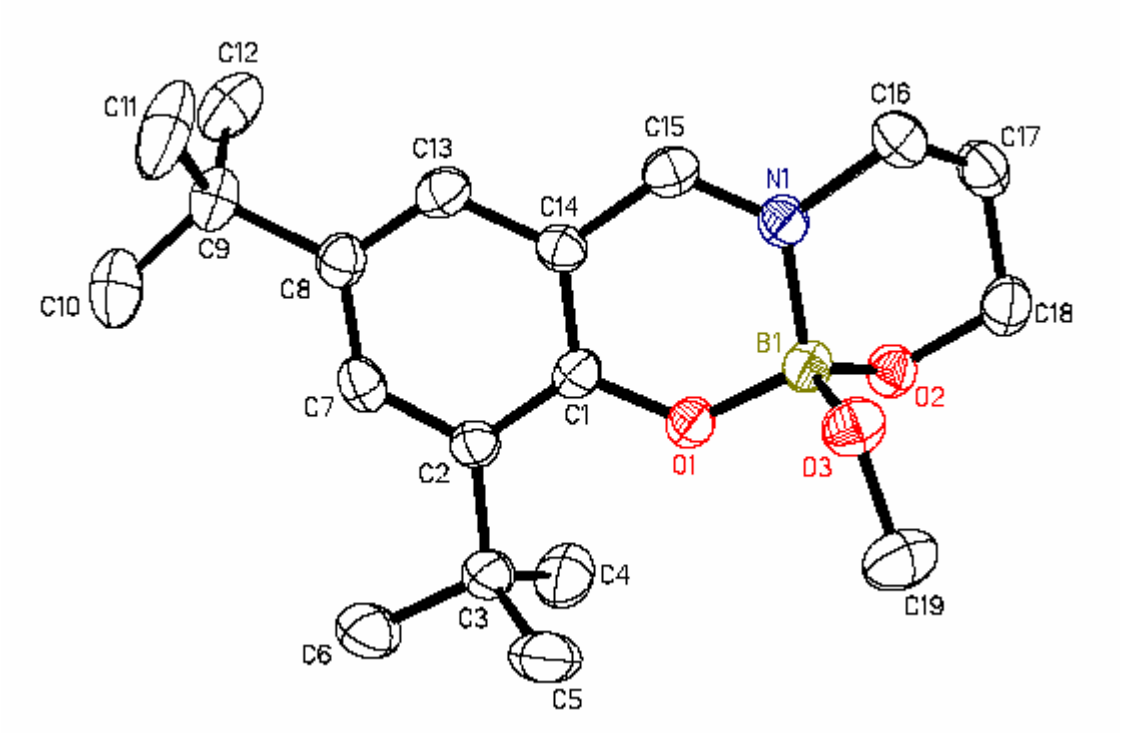

F**igure 2.3**. Structure of **6**.

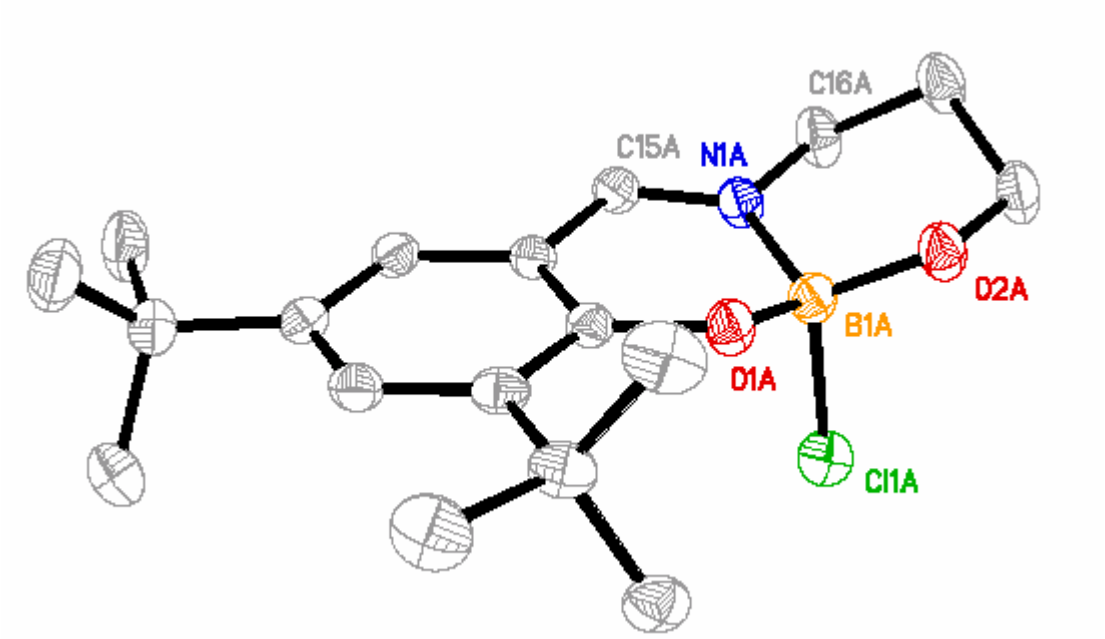

Figure 2.4. Structure of **11**.

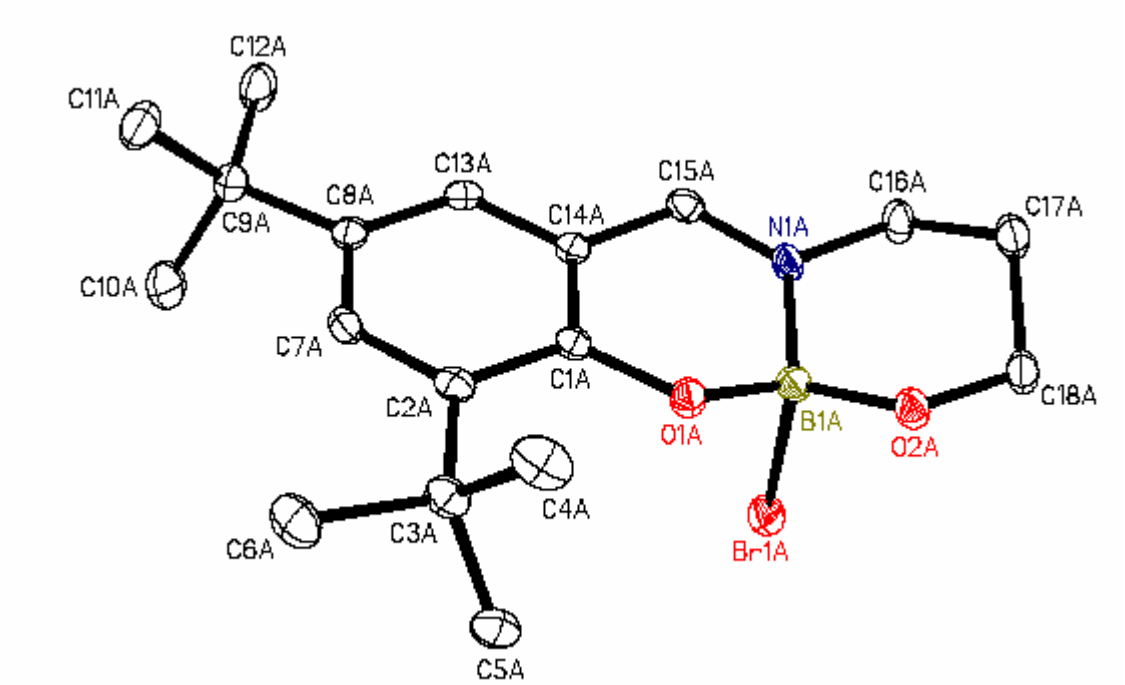

Figure 2.5. Structure of **12**.

$$\text{THC \%} = \left[1 - \frac{\sum_{n=1-6} \left| 109.5 - \theta_n \right|^{\circ}}{90^{\circ}} \right] \times 100$$

(a)

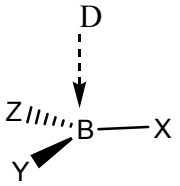

THC = 0 %

(b)weak interaction of donor with boron

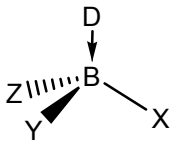

THC = 100 %

(c) strong interaction of donor with boron

Figure 2.6. THC diagram. (a) Equation for calculating THC % (θ_n (n = 1-6) are the angles around the boron atom). (b) Weak interaction between boron and the donor leading to three-coordinate trigonal boron. (c) Strong interaction between boron and the donor leading to tetrahedral four-coordinate boron.

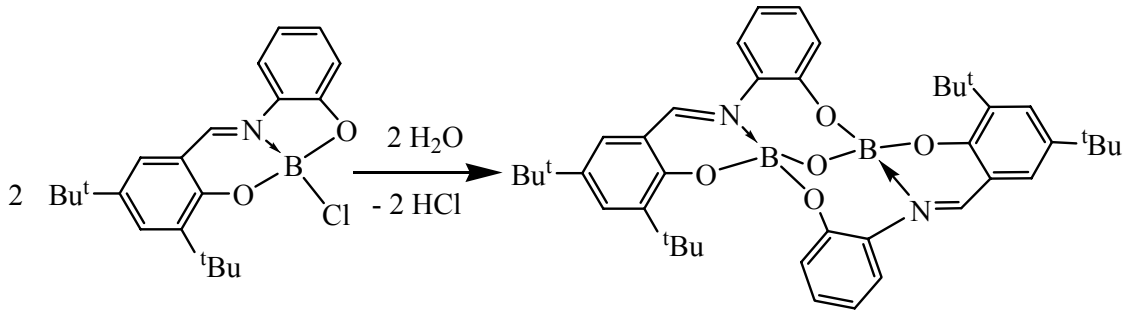

(**7**) (**13**)

Figure 2.7. Formation of hydrolyzed product **13** from the halide compound **7**.

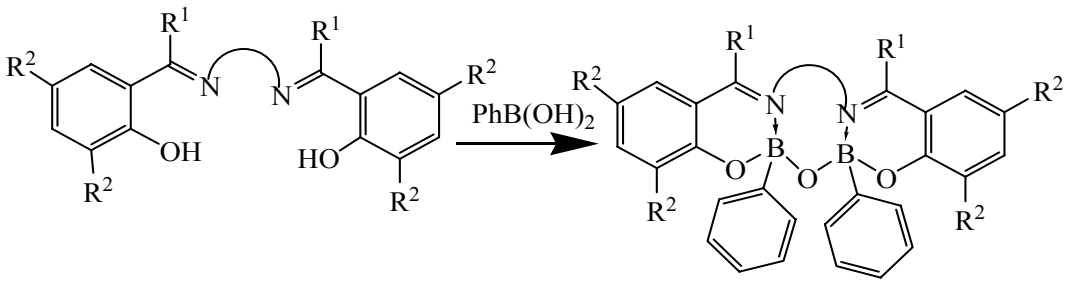

R^1, R^2 = various combinations of H and alkyl groups

Figure 2.8. Formation of binuclear oxo-bridged boron compounds from Salen ligands.

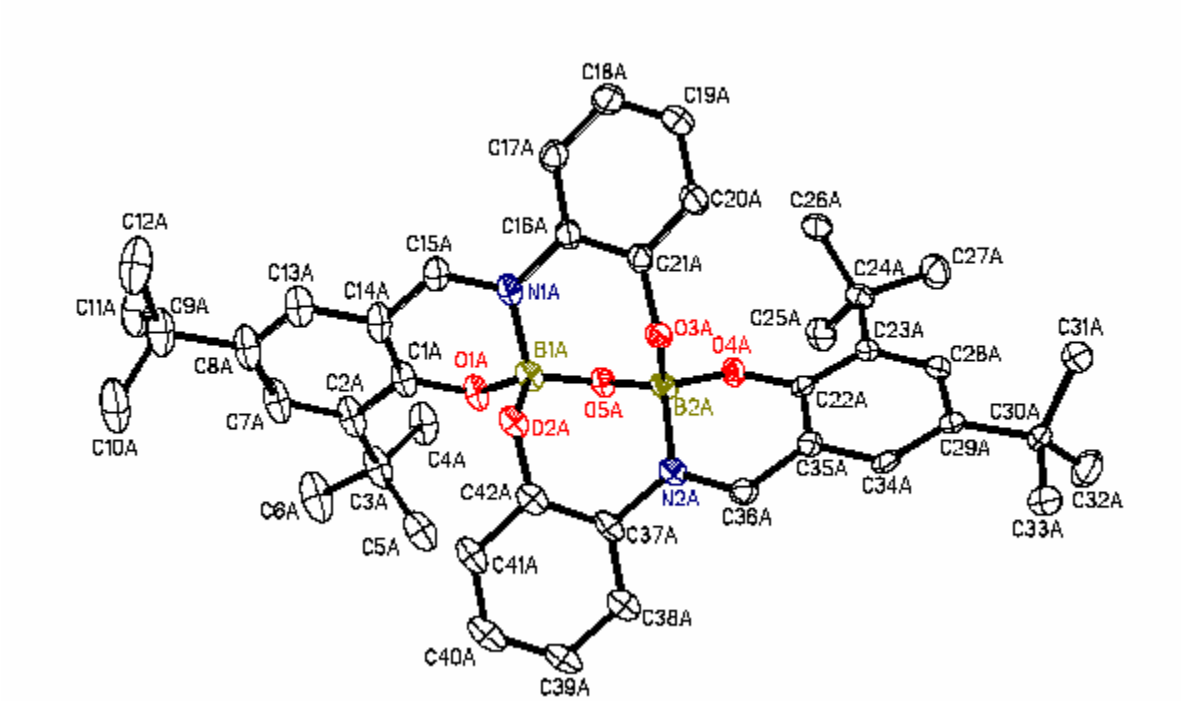

Figure 2.9. Structure of the hydrolyzed product **13.**

Chapter 3

Dealkylation of Organophosphates with Mononuclear Boron Chelates

3.1. Background

In Chapter 1 the effectiveness of binuclear boron halides for the dealkylation of a series of organophosphates under mild conditions was discussed.[33-35] For example, salpen(^{t}Bu)[BBr_2]$_2$ dealkylates trimethyl phosphate up to 89 % conversion in 30 minutes.[33] The binuclear compounds catalyzed the reactions between phosphate esters and boron tribromide. To determine the full utility of the chelated boron compounds it is necessary to try similar mononuclear boron compounds for phosphate dealkylation. This would allow a comparison with the binuclear system to both understand how the reaction proceeds and to determine the optimal system. Although a mononuclear boron compound ^{t}BuSal(^{t}Bu)[BBr_2]$_2$ was previously found to dealkylate trimethylphosphate at 92% conversion in 30 minutes a systematic study was not conducted. A series of mononuclear Schiff base boron halides for the dealkylation of trimethyl phosphate will be presented in this chapter. The mononuclear boron mono- and dihalide compounds of the type LBX and LBX_2 reported in chapter 2 will be used for this study.

3.2. Dealkylation of trimethylphosphate with various mononuclear compounds

The mononuclear Schiff base boron halide compounds **2**, **3**, **7**-**12** (see Figure 2.1) dealkylated trimethyl phosphate at room temperature in stoichiometric reaction to produce methyl bromide and an unidentified phosphate material which remained in solution (Figure 3.1 and Table 3.1). The dealkylation reaction was conducted in NMR tubes in $CDCl_3$ and the percent conversion was determined from the integration of the ^{1}H

NMR peaks for the methyl bromide produced and the unchanged methoxy groups of the phosphate. The reaction mixture stayed clear throughout. The possible dealkylation pathway for the LBX compounds is shown in Figure 3.2. The best results were obtained from the monobromide compounds **8** (90 % after 30 min) and **12** (64 % after 30 min, 74 % after 2 h and 100 % after 24 h). These results are comparable to the binuclear boron halides studied before. In compounds **8** and **12** with an ONO environment either an *o*-phenylene or a propylene backbone connects the N and O atoms. These compounds were far more active than the chloride analogues, **7** and **11**. This could be expected from the lower B-Br bond strength (396 kJ mol^{-1}) compared to B-Cl bond strength (511 kJ mol^{-1}) and the consequent ease of formation of the phosphate coordinated cations. Interestingly, the LBX (X = Cl, Br) compounds, **9** and **10**, with an ethylene backbone between the N and O atoms, were almost inactive towards phosphate dealkylation. Compound **3,** the dibromide $LBBr_2$, also showed negligible activity. However, the dichloride compound (**2**) showed moderate activity (17 % in 30 minutes, 61 % in 2 h and 85 % in 24 h). The higher activity of chloride compared to bromide for LBX_2 could not be explained by the B-X bond strength. Thus, a correlation of higher reactivity vs. B-X bond strength occurs only for the monohalide compounds. That the $LBCl_2$ compounds are more reactive can be explained by the fact that the inductive effect of the second halide makes the formation of $LBCl^+$ easier to achieve.

3.3. Preparation of a chelated monomeric boron phosphinate through dealkylation

Although it was not possible to get the structure of the fully dealkylated phosphate triester, the dealkylated product, **14** (Figure 3.4), produced from *tert*-butyl-diphenylphosphinate, $Ph_2P(O)O^tBu$ and the boron bromide compound **8** was fully

characterized. Molecular phosphates and phosphonates have been of interest due to their possible use as precursors to solid-state materials. [178-181] Monomeric main group or transition metal chelate compounds with terminal phosphinates are rare. Previously reported metal phosphinate compounds of Ti, [182, 183] Zr [184], Ta, [183] Sn, [185, 186] Pb [185] Al, [187, 188] Ga,[189, 190] and In [189] contained bridging phosphinate groups and almost all of the compounds were di- or polynuclear. A unique example of a mononuclear metal chelate phosphinate compound is $Sn(CH_2Ph)_2[O_2P(C_6H_{11})_2]_2[HO_2P(C_6H_{11})_2]_2$ (Figure 3.3). [186] In this compound the phosphinate groups participate in intramolecular hydrogen bonding. The aluminum phosphinate Salen chelate compounds contained six-coordinate aluminum and some of them showed unique coupling reactions with THF.[188] Compound **14** is a rare example of a monomeric chelated compound with a terminal phosphinate group.

Compound **14** was prepared by refluxing **8** and $Ph_2P(O)O^tBu$ in toluene (Figure 3.4). The byproduct ^{t}BuBr was removed under vacuum. Compound **14** is soluble in organic solvents. The ^{1}H NMR showed ^{t}Bu peaks at δ 1.31 and δ 1.50 ppm, and an imine peak at δ 8.57 ppm. The ^{11}B NMR showed a single peak at δ 3.57 ppm which is in the appropriate region for a four-coordinate boron atom. Interestingly, the ^{31}P NMR showed two peaks at δ 28.90 and δ 33.97 ppm in the intensity ratio of 4:3. The presence of two peaks suggests that there might be some type of rearrangement in the solution state. Alternatively, the peak at 28.90 ppm could be due to the presence of some diphenylphosphinic acid (for which the literature value of ^{31}P shift is 25.50 ppm [191]) produced from the hydrolysis of the starting phosphinate material by the adventitious HCl present in the NMR solvent $CDCl_3$. The ^{31}P chemical shift in **14** is close to some other

phosphinate compounds, for example, in $[(\eta^5\text{-Cp})TiCl_2(\mu\text{-}Ph_2PO_2)\}_2]$ the ^{31}P shift is 34.5 ppm.[183]

The IR showed strong $\nu_{B\text{-}N}$ absorption at 1014 cm^{-1}, $\nu_{C=N}$ at 1640 cm^{-1} and $\nu_{P=O}$ at 1212 cm^{-1}. The mass spectrum (EI, positive) showed a molecular ion peak in 15 % abundance and a M^+-$PhPO_2$ peak in 45 % abundance. The base peak (100 %) was due to $M^+ - PhPO_2 - H$.

3.3.1. Structure of 14

The crystal structure of the boron phosphinate, compound **14**, was determined by single-crystal X-ray diffraction. The crystal data collection parameters are shown in Table 3.2 and selected bond lengths and angles are contained in Table 3.3. The compound contains a four-coordinate boron and a four-coordinate phosphorus atom. The B-O bond lengths (1.432(2), 1.463(2) and 1.476(2) Å) are shorter than the B-N bond length (1.568(3) Å). The P1-O3 bond length (1.5633(13) Å) is in a single bond range (1.59-1.60 Å) and the P1-O4 bond (1.4811(13) Å) is close to the double bond range (1.45-1.46 Å).[192] It may be mentioned that in a previously reported molecular borophosphonate cage compound $[^tBuPO_3BEt]_4$ the average P-O bond length was 1.50 Å, intermediate between P-O and P=O.[193]

The geometry around the boron is distorted tetrahedral. The THC value (defined in chapter 2) [172] for **14** is 81 %. The largest deviation from a perfect tetrahedral angle is shown by O2-B1-N1 (102.22(15) °), and is caused by the constraints imposed by the chelate.

The phosphorus atom is in a distorted tetrahedral environment. The angle O3-P1-O4 (116.50(7)) °) is the most obtuse angle whereas the angle C22-P1-C28 (106.26(9) °) is

the most acute. The angle P1-O3-B1 is 132.43(12) ° is significantly smaller than the Al-O-P angle (138.8(3) °) in the dimeric aluminum phosphinate compound [salophen(thf)(^{t}Bu)$AlO_2P(H)Ph]_2$.[188]

3.4. Conclusion

Compounds **2**, **3**, **7**-**12** dealkylated trimethyl phosphate to various extents at room temperature. The monobromide compounds **8** and **12** were the most effective and their activity was comparable to the results obtained from binuclear Salen boron bromide compounds. However, mononuclear compounds are less stable to air and moisture compared to their binuclear counterparts. For any useful application this problem has to be addressed. Although the structure of the fully dealkylated product could not be determined, a monodealkylated product (compound **14)** was fully characterized. Compound **14** is the first example of a chelated boron phosphinate. Interestingly the compound has a terminal phosphinate group in contrast to bridging phosphinate groups found in many other metal chelates. The dealkylation reaction has the potential to produce novel structures when used with phosphate di- and triesters, i.e., phosphonates and phosphates.

3.5. Experimental

General remarks. All air-sensitive manipulations were conducted using standard bench-top Schlenk line technique in conjunction with an inert atmosphere glove box. All solvents were rigorously dried prior to use. All glassware was cleaned with a base and an acid wash and dried in an oven at 130 ºC overnight. NMR data were obtained on Varian Gemini-200 and Varian VXR-400 instruments. Chemical shifts were reported relative to

$SiMe_4$ for ^{1}H and ^{13}C, $BF_3 \cdot Et_2O$ for ^{11}B and 85 % H_3PO4 for ^{31}P and are reported in ppm. Infrared transmission spectra were recorded at room temperature in a potassium bromide pellet on a Fourier-transform Magna-IR ESP 560 spectrometer. Elemental analyses were performed on either a Perkin Elmer 2400 CHN Analyzer or a LECO CHN-2000 Analyzer.

X-ray data for compound **14** were collected on a Nonius Kappa-CCD diffractometer using Mo-K_α radiation. All calculations were performed using the software package SHELXTL-Plus.[174-177] The structures were solved by direct methods and successive interpretation of difference Fourier maps followed by least-squares refinement. All non-hydrogen atoms were refined anisotropically. The hydrogen atoms were included using a riding model with isotropic parameters tied to the parent atom.

Dealkylation of phosphates. In a typical experiment the chelate compound (for **8,** 30 mg, 0.070 mmol) was dissolved in 1 mL $CDCl_3$ in a glass vial. The solution was transferred to an NMR tube and trimethylphosphate (2.8 μL, 0.024 mmol, density 1.197 g/mL) was added with a syringe. The mixture was shaken and monitored by ^{1}H NMR. The % dealkylation was calculated from the peak integrations of methyl halide produced and unchanged phosphate.

Synthesis of LBOP(O)Ph_2 (LH_2 = N-(2-hydroxyphenyl)-3,5-di-*t*-butylsalicylaldimine) (14). To a rapidly stirred solution of **8** (0.57 g, 1.6 mmol) in toluene *tert*-butyl-diphenylphosphinate (0.41 g, 1.6 mmol) was added. The golden yellow reaction mixture was refluxed for 7 hours. The volatiles were removed under vacuum and a yellow solid was obtained, which was dried under vacuum and washed with hexane. Yield: 0.59 g (68 %). Mp: 239-240 ºC (dec.). δ 1.31 (s, 9H, $C(CH_3)_3$), 1.50 (s, 9H,

C(CH_3)$_3$), 6.64 (m, 1H, Ph-*H*), 6.86 (m, 1H, Ph-*H*), 7.14-7.23 (m, 4H, Ph-*H*), 7.25-7.39 (m, 4H, Ph-*H*), 7.44-7.54 (m, 4H, Ph-*H*), 7.66-7.79 (m, 2H, Ph-*H*), 8.57 (s, 1H, N=C*H*); ^{13}C NMR ($CDCl_3$): δ 29.7 (C(CH_3)$_3$), 31.5 (C(CH_3)$_3$), 35.7 (C(CH_3)$_3$), 38.0 (C(CH_3)$_3$), 120.2 (Ph), 128.0 (Ph), 128.2 (Ph), 129.2 (Ph), 131.4 (Ph), 132.8 (Ph), 143.3 (Ph), 157.6 (N*C*H) ^{11}B NMR ($CDCl_3$): δ 3.57 ($W_{1/2}$ = 47 Hz). ^{31}P{H} NMR ($CDCl_3$): δ 28.90 (s), δ 33.97 (s). IR (KBR) ν/ cm^{-1}: 2959m, 2909w, 2867w, 1640s, 1564w, 1548w, 1482m, 1440m, 1391m, 1384m, 1365w, 1327m, 1259m, 1212s, 1184m, 1127m, 1082m, 1014s, 994s, 966m, 888w, 750m, 725m, 694m, 544m. MS (EI, positive): 331 (M^+, 15 %), 334 (M^+ - Ph_2PO_2, 45)%), 333 (M^+ - Ph_2PO_2 - H, 100 %). Anal. Calcd. for $C_{33}H_{35}O_4NBP$: C 71.88, H 6.40, N: 2.54. found: C 70.78, H 6.73, N 1.84.

Table 3.1. Percent dealkylation [a] of trimethylphosphate with Schiff base boron halides

Compound	**2**	**3**	**7**	**8**	**9**	**10**	**11**	**12**
30 min	17	10	9	90	2	4	3	64
2 h	61	13	24	90	6	4	8	74
4 h			40	92	7			
6 h			52	94	7			
8 h			62	94	9			
10 h			68	94	11			
12 h			73	94	11			
24 h	85	18	84	94	13	4	57	100

[a] Calculated from the integration of ^{1}H NMR spectra of methyl halide produced and unchanged trimethyl phosphate at room temperature in $CDCl_3$.

Table 3.2. Crystallographic data and refinement details for compound **14**.

	14
Empirical formula	$C_{36.50}H_{39}BNO_4P$
M/ g mol^{-1}	597.47
Color	Yellow
Crystal size/mm	0.15 x 0.15 x 0.05
Crystal system	Triclinic
Space group	P -1
a/ Å	12.1241(2)
b/ Å	12.3740(2)
c/ Å	12.4470(2)
α/ °	73.7525(6)
β/ °	89.0625(7)
γ/ °	62.5102(6)
V/ Å^3	1576.34(4)
ρ_{calc}/ g cm^{-3}	1.259
Z	2
F(000)	634
Radiation used	Mo-K_α
μ /mm $^{-1}$	0.128
T/ K	90.0(2)
hkl range	$-15 \leq h \leq 15$, $-16 \leq k \leq 15$, $-16 \leq l \leq 16$
Θ range/ °	1.72 – 27.45
Reflections measured	13929
Unique reflections (R_{int})	7183 (0.0532)
Obsd reflections, n [$I \geq 2\sigma$ (I)]	4399

Refinement method	Full-matrix least-squares on F^2
Refined parameters/restraints	431/0
R1 [$I > 2\sigma$]	R1 = 0.0501, wR2 = 0.1109
R1 (all data)	R1 = 0.1036, wR2 = 0.1318
Goodness-of-fit on F^2	1.005
Largest diff. peak and hole/ e. $Å^{-3}$	.326 and -0.416

Table 3.3. Selected bond distances (Å) and angles (º) for the borate compound **14**.

B1-O1	1.432(2)	P1-O3	1.5633(13)
B1-O2	1.463(2)	P1-O4	1.4811(13)
B1-O3	1.476(2)	P1-C22	1.799(2)
B1-N1	1.568(3)	P1-C28	1.8004(19)
N1-C15	1.293(2)		
N1-C16	1.413(2)		
O1-B1-N1	109.97(16)	O3-P1-O4	116.50(7)
O2-B1-N1	102.22(15)	O3-P1-C22	107.33(8)
O3-B1-N1	110.45(16)	O3-P1-C28	112.93(8)
O1-B1-O2	114.49(16)	O4-P1-C22	111.30(8)
O1-B1-O3	107.91(15)	O4-P1-C28	112.93(8)
O2-B1-O3	111.71(16)	C22-P1-C28	106.26(9)
		P1-O3-B1	132.43(12)

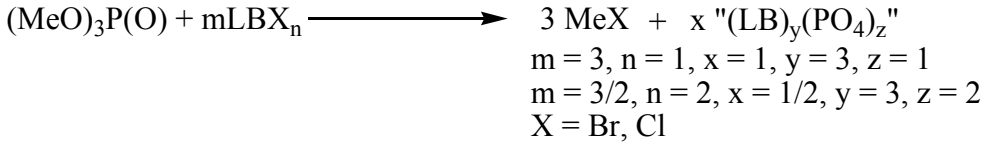

Figure 3.1. Reaction between trimethylphosphate and mononuclear Schiff base boron halides.

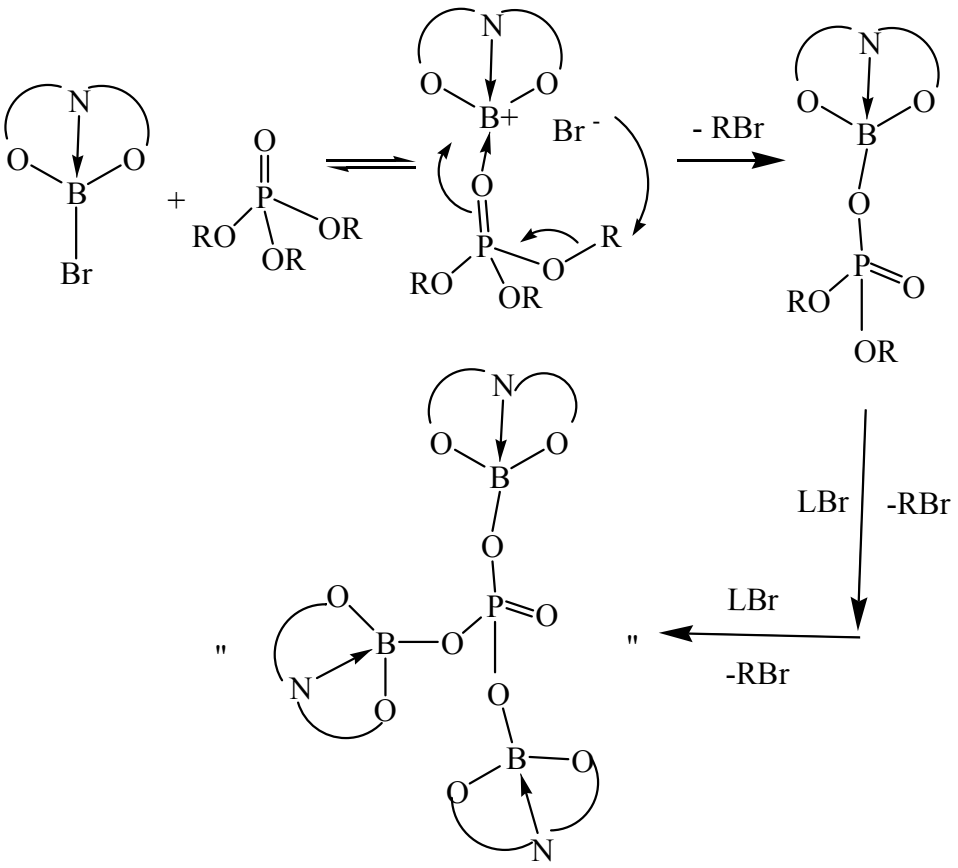

Figure 3.2. Possible dealkylation pathway for the boron compound LBX.

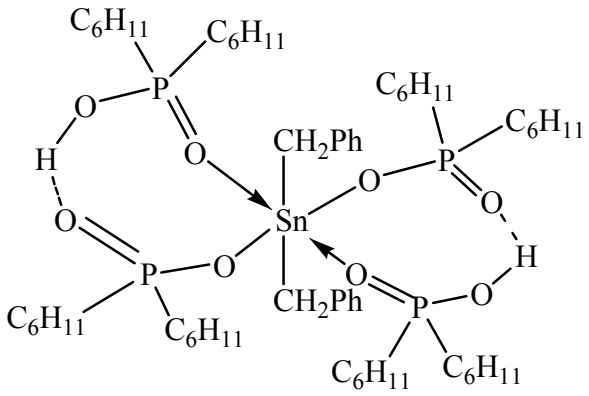

Figure 3.3. Monomeric tin phosphinate.

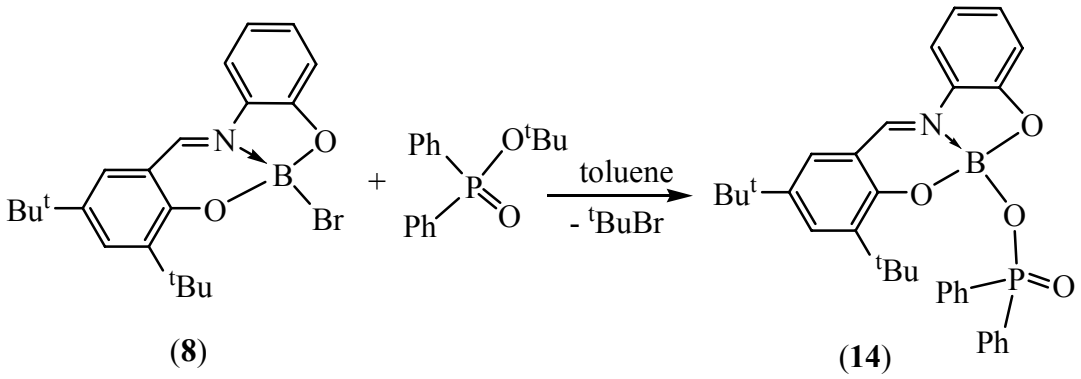

Figure 3.4. Synthesis of **14**.

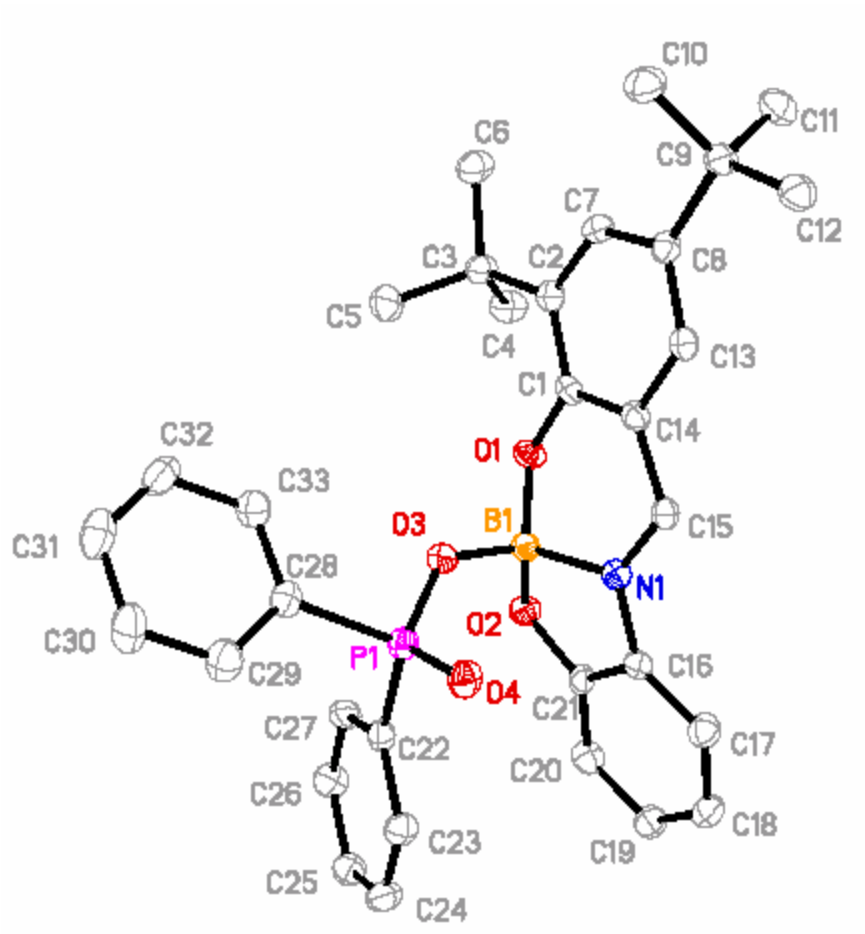

Figure 3.5. Crystal structure of compound **14**.

Chapter 4

Salen Aluminum Bromides: Synthesis, Structure and Cation Formation

4.1. Introduction

Examples of five-coordinate group 13 bromide compounds reported so far have been limited to indium. [194] This is despite the fact that the chloride compounds have been quite popular for synthetic and catalytic applications. [17, 195-198] Specifically, Salen aluminum chloride (Salen = *N,N′*- alkylene(or arylene)bis(salicylideneimine)) compounds have been the subject of interest recently for their ease of synthesis and cation formation, and subsequent use in catalysis. The compounds contain five-coordinate aluminum with a single ^{27}Al NMR peak in the range δ 43-57 ppm. The coordination environment around the central aluminum is either trigonal bipyramidal (tbp) or square pyramidal (sqp) depending on the "backbone" (the connection between the nitrogens) of the ligand. With three or more methylene units in the backbone (e.g., salpen) a tbp geometry is obtained whereas for two methylene units (e.g., salen) or 1,2 arylene (e.g., salophen) a sqp geometry is observed.[199]

SalenAlCl compounds have been used in oxirane polymerization,[17] phospho-transfer reactions (Figure 4.1),[195] conjugate addition of nucleophiles to unsaturated imides[196-198] and an inverse electron demand Diels-Alder reaction.[200] The chloride group in Salen(^{t}Bu)AlCl can be displaced by strong donors, such as, H_2O, MeOH, THF, or HMPA to give cationic aluminum compounds (Figure 4.2).[19, 20, 201] Also, solvent-free cations can be achieved by removing the chloride of SalenAlCl with $GaCl_3$ (Figure 4.2).[202] In general, the utility of the SalenAlCl compounds has relied on their ability to produce the

cation $[SalenAl(base)_2]^+$. It is likely that the bromide derivatives will have greater utility based upon the weaker Al─Br bond strength. Thus it is anticipated that cation formation may occur for the bromide derivatives with less strong Lewis bases, thereby broadening the potential applicability of the compounds.

This chapter will detail the synthesis of five-coordinate Salen aluminum bromides and the formation of six-coordinate aluminum cations on combination with a Lewis base. [203]

4.2. Synthesis

Salen(^{t}Bu)H_2 ligands were prepared by the condensation reaction between 3,5-di-*t*-butylsalicylaldehyde and appropriate diamine following the literature procedure (Figure 4.3) .[204] The Salen aluminum bromide compounds **15-18** were prepared by alkane elimination between diethylaluminum bromide (prepared *in situ* by the redistribution of triethylaluminum and aluminum(III) bromide) and Salen(^{t}Bu)H_2 under reflux (Figure 4.4). The compounds were isolated by removing the solvent under vacuum or by precipitation after concentration and cooling to -30 ºC**.** The compounds were yellow and soluble in chloroform.

4.3. Characterization

4.3.1. Spectroscopy

Compounds **15-18** were characterized by NMR, IR and MS. The ^{1}H NMR data were very close to the corresponding chloride analogues reported in the literature.[17, 205] For example, the ^{1}H NMR data for all four compounds show two singlets for the ^{t}Bu-Ph groups in the range δ 1.30-1.63 ppm. For **15**, **16** and **17** there are multiple CH_2 peaks corresponding to the alkylene backbone protons from the ligand ranging from δ 1.80 to

3.97 ppm. There is only one imine singlet for each compound at δ 8.40, 8.29, 8.23 and 8.94 ppm, respectively. Like their chloride analogues, these values decrease slightly with increasing backbone length from **15** to **17**, and increases in **18** because of the greater electronegativity and deshielding effect of the aryl backbone compared to an alkyl backbone. The presence of only one set of ^{t}Bu peaks and one imine peak for each compound suggests a symmetric solution-state structure.

The ^{27}Al NMR showed broad single peaks centered at δ 38, 36, 36 and 32 ppm, respectively, for **15-18** which indicate the presence of five-coordinate aluminum. However, these are shifted upfield from the related chloride analogues salen(^{t}Bu)AlCl (δ 57 ppm), salpen(^{t}Bu)AlCl (δ 43 ppm and salophen(^{t}Bu)AlCl (δ 52 ppm).[205] This is in accordance with the lower electronegativity of Br compared to Cl and hence more shielding of the Al center.

The IR spectra showed strong absorptions due to $\nu_{C=N}$ at 1648, 1642, 1643 and 1621 cm^{-1} for **15-18**, respectively. The mass spectra (EI) of **15** and **17** contained molecular ion peaks in low abundance. All four compounds had a peak corresponding to the molecular ion minus bromide, and for **15**, **16** and **17** this was the most abundant peak. Compounds **15** and **18** also had peaks corresponding to molecular ion minus bromide and one oxygen, and for **18** this was the most abundant peak. It was interesting to note that the loss of bromide occurred and not the loss of ^{t}Bu from the ligand. This might provide some indication of the relative weakness of the Al—Br bond in the compounds.

4.3.2. Structures

The solid-state structures of compounds **15-18** were determined by single-crystal X-ray diffraction. Compounds **15** and **17** crystallized in orthorhombic space group Pbca

while **16** and **18** crystallized in triclinic space group $P\bar{1}$. The X-ray crystal structures confirmed the presence of five-coordinate aluminum atoms in **15-18** (Figures 4.5, 4.6, 4.7 and 4.8). The crystal data collection parameters are listed in Table 4.1 and selected bond lengths and angles in Table 4.2. The Al─Br bond lengths fall in the range 2.35-2.38 Å which are longer than the Al─Cl bond length (~ 2.18 Å) in Salen(^{t}Bu)AlCl compounds.[199] The Al─N bond lengths (~ 1.96-2.02 Å) are marginally longer than the Al─O bond length (~1.75-1.81 Å). The geometries of these compounds are close to either square pyramidal (sqp) or trigonal bipyramidal (tbp) depending on the ligand backbone. Salen and salophen have rigid backbones and favor square pyramidal geometry while salpen and salben with longer, flexible, propylene and butylene backbones, respectively, favor tbp geometry around the aluminum. A similar trend was observed previously in the case of salen aluminum alkyl, chloride and siloxide compounds. [199, 206, 207]

A quantitative measure, expressed as the "τ value", can be used to describe the distortion from perfectly sqp or tbp geometry in these compounds (Figure 4.9). [208] A perfectly sqp geometry has a τ value equal to zero whereas a perfectly tbp geometry has a τ value equal to 1. In Table 4.3 the calculated τ values for compounds **15- 18,** along with some previously described five-coordinate Salen aluminum chloride compounds, are listed. Compounds **15** and **18** have τ values close to 0 indicative of a distorted sqp geometry whereas **16** and **17** have τ values close to 1 indicating a distorted tbp geometry. This value may be important in determining the accessibility of a sixth coordination site on aluminum. [209] Attempts have been made to relate the τ value to the hyperfine splitting in the EPR spectra for five-coordinate copper (II) complexes.[210] The hyperfine splitting constant A_{II} is sensitive to the type of ligand coordinating to the metal center. This

constant for a series of five-coordinate copper complexes of pyridine-2,6-dicarboxamide ligands were determined and a linear correlation was found between τ and A_{II} values. However, for some of the complexes this correlation breaks down due to structural features such as out-of-plane distortions and ligand strain.

4.4. Six-coordinate aluminum cations

4.4.1 Synthesis

Four cationic compounds, [salen(^{t}Bu)Al($Ph_3PO)_2$]Br (**19**), [salpen(^{t}Bu)Al($Ph_3PO)_2$]Br (**20**), [salophen(^{t}Bu)Al($Ph_3PO)_2$]Br (**21**) and [salophen(^{t}Bu)Al{$(PhO)_3PO)$}$_2$]Br (**22**) were formed by displacement of the bromide from compounds **15, 16** and **18** with either triphenylphosphine oxide or triphenyl phosphate (Figure 4.10). Similar cationic compounds were formed previously from Salen(^{t}Bu)AlCl with H_2O, THF or MeOH.[17, 18] Salen aluminum chlorides do not form cations with triphenylphosphine oxide, which confirms the value of the SalenAlBr compounds in making new cations. Triphenylphosphine oxide was also found to form [$Me_2Al(OPPh_3)_2$]Br from Me_2AlBr.[211] However, it was not a strong enough base to displace chloride from Me_2AlCl even under reflux. Instead, the adduct Me_2AlCl•$OPPh_3$ formed (Figure 4.11).

4.4.2. Spectroscopy

The ^{1}H NMR spectra of **19**, **21** and **22** show two peaks for the ^{t}Bu groups of the ligand with each peak corresponding to 18 protons. Interestingly, for **20**, there is only one ^{t}Bu peak with 36 protons. This could be attributed to the shielding of the *ortho*- ^{t}Bu group of the ligand due to the ring current of the phenyl groups of triphenylphosphine oxide. This shielding causes an upfield shift of the ^{t}Bu group thus superimposing it on the peak of the

other. [212] In the aromatic regions there are overlapping peaks due to the phenyl groups from both the ligands and triphenylphosphine oxide or triphenylphosphate. The ^{27}Al NMR shows very broad peaks at δ -6, 0, and 12 ppm for **19**, **20**, and **22**, respectively. These correspond to the presence of six-coordinate aluminum.[188] However, for **21** this value is δ 42 ppm which is more likely to be the shift of a five-coordinate aluminum atom.[205] Thus the solution product for **21** appears to be different from the solid-state structure found in the X-ray crystal studies where the aluminum atom is six-coordinate (see next paragraph). One possible explanation could be that one of the two loosely bound triphenylphosphine oxide ligands dissociates in the polar NMR solvent ($CDCl_3$) making the aluminum five-coordinate. The ^{31}P NMR spectra of **19**, **20** and **21** show peaks at δ 34, 35 and 33 ppm, respectively. These are downfield from the NMR shift of δ 29 ppm of free triphenylphosphine oxide [213] because of the deshielding of the phosphorus due to coordination to aluminum. However, for **22** this shift is δ -21 ppm which is slightly upfield from the shift of -18 ppm of free triphenylphosphate.[213] The IR spectrum shows strong P═O absorption at 1173, 1162, 1172 and 1278 cm^{-1} for **19**, **20**, **21**, and **22**, respectively. For **22**, the stretching of the P─O bond of the P─O─C linkage of the phosphate gives rise to a strong band at 1029 cm^{-1}. In the mass spectra (EI) of the six-coordinate aluminum compounds no parent ion or parent ion minus bromide ion was observed. However, all the compounds show peaks corresponding to parent ion minus the bromide and two triphenylphosphine oxide or triphenylphosphate moieties in high abundance. This indicates the weak coordination between the Lewis base and the aluminum.

4.4.3. Structure

Compounds **20**, **21** and **22** were structurally characterized by single crystal X-ray diffraction. The data collection parameters are contained in Table 4.4 while Table 4.5 lists selected bond lengths and angles. Compounds **20** and **21** crystallize in orthorhombic space group Pbca whereas **22** crystallizes in monoclinic space group $P2_1/n$. Their structures consist of a central six-coordinate aluminum atom in a distorted octahedral geometry (Figures 4.12, 4.13 and 4.14). The ligand occupies four equatorial positions and two phosphine oxide or the phosphate molecules occupy the two axial positions. The equatorial bond angle is larger for O-Al-O (~89.38 - 96.1º) compared to N-Al-N (~80.7 - 90.85 º). This is a reflection of the steric restrictions of the ligand creating a more "open" front for the compound. The axial O-Al-O bond angles are distorted (~ 169.1 - 174.6º) from ideal linearity. The amount of distortion is more for the phosphine oxide compounds **20** and **21** compared to the phosphate compound **22.** This is probably due to the fact that the P-O-Ar linkage in **22** allows the bulky phenyl group to move away from the equatorial ligand atoms and thus avoid steric congestion. The axial Al-O distances (~ 1.92 – 1.97 Å) are longer than the equatorial Al-O distances (~1.79 – 1.84 Å) due to the greater steric requirements of the axial groups. Interesting observations were made in terms of Al-O-P bond angles in the three cationic compounds. The two Al-O-P angles were widely different in each of the phosphineoxide compound **20** (~170 and ~153 º) and the phosphate compound **22** (~157 and 166 º). But in the phosphineoxide compound **21** these angles are much closer (~164 and 161 º). These variations in bond angles could arise from different degrees of interactions involving the phenyl rings and the ^{t}Bu groups. These values also show that all the three compounds are characterized by rather linear Al-

O-P linkages. A similarly large Al-O-P angle (~166 º) was observed in the compound $(Me_2N)_3Al{\cdot}OPPh_3$.[157]

4.5. Conclusion

Four new five-coordinate aluminum bromides salen(^{t}Bu)AlBr (**15**), salpen(^{t}Bu)AlBr (**16**), salben(^{t}Bu)AlBr (**17**) and salophen(^{t}Bu)AlBr (**18**) have been synthesized and fully characterized. The compounds have distorted trigonal bipyramidal or square pyramidal geometries. Compounds **15** and **18** are closer to sqp whereas **16** and **17** are closer to tbp. These compounds readily formed six coordinate aluminum cations when combined with triphenylphosphine oxide or triphenyl phosphate. The six-coordinate cations have distorted octahedral geometries. The ready cation formation with Salen aluminum bromide compounds could be useful for their application in organic synthesis and catalysis.

4.6. Experimental

General remarks. All air-sensitive manipulations were conducted using standard bench-top Schlenk line techniques in conjunction with an inert atmosphere glove box. All solvents were rigorously dried prior to use. All glassware was cleaned with a base and an acid wash and dried in an oven at 130 ºC overnight. The ligands salen(^{t}Bu)H_2, salpen(^{t}Bu)H_2, salben(^{t}Bu)H_2 and salophen(^{t}Bu)H_2 were synthesized according to the literature procedure.[204] NMR data were obtained on Varian Gemini-200 and Varian VXR-400 instruments. Chemical shifts were reported relative to $SiMe_4$ for ^{1}H and ^{13}C, $AlCl_3$ in D_2O for ^{27}Al and 85 % H_3PO_4 for ^{31}P, and are reported in ppm. Infrared transmission spectra were recorded at room temperature in a potassium bromide pellet on

a Fourier-transform Magna-IR ESP 560 spectrometer. Elemental analyses were performed on a Perkin Elmer 2400 CHN Analyzer.

X-ray data were collected on a either a Nonius Kappa-CCD (compounds **16**, **17**, **20**, **21** and **22**; Mo-K_α radiation) or a Bruker-Nonius X8 Proteum (compounds **15** and **18**; Cu-K_α radiation) diffractometer. All calculations were performed using the software package SHELXTL-Plus.[174-177] The structures were solved by direct methods and successive interpretation of difference Fourier maps followed by least-squares refinement. All non-hydrogen atoms were refined anisotropically. The hydrogen atoms were included using a riding model with isotropic parameters tied to the parent atom.

Synthesis of salen(^{t}Bu)AlBr (15). A rapidly stirred solution of Et_2AlBr in toluene, prepared *in situ* by the redistribution of triethylaluminum (0.42 g, 3.6 mmol) and aluminum(III) bromide (1 M solution in dibromomethane, 1.8 mL, 1.8 mmol), was combined with a solution of salen(^{t}Bu)H_2 (2.69 g, 5.46 mmol) in toluene by cannula. The reaction mixture was refluxed for 8 hours and filtered. The volatiles were removed under vacuum from the clear yellow filtrate to give a yellow microcrystalline solid which was purified by recrystallization from toluene. Single crystals suitable for X-ray analysis were grown from slow diffusion of hexane vapor into a concentrated CH_2Cl_2 solution. Yield: 2.7 g (74%). Mp: 330-332ºC (dec.).^{1}H NMR ($CDCl_3$): δ 1.33 (s, 18H, C(CH_3)$_3$), 1.57 (s, 18H, C(CH_3)$_3$), 3.97 (m, 4H, NCH_2), 7.08 (d, 2H, Ph*H*), 7.60 (d, 2H, Ph*H*), 8.40 (s, 2H, N=C*H*); ^{13}C NMR ($CDCl_3$): δ 29.7 (C(*C*H$_3$)$_3$), 31.3 (C(*C*H$_3$)$_3$), 34.0 (*C*CH$_3$)$_3$), 35.5 (*C*CH$_3$)$_3$), 54.5 (N*C*H$_2$), 118.2 (Ph), 127.3 (Ph), 131.6 (Ph), 139.1 (Ph), 141.3 (Ph), 162.7 (Ph), 170.4 (NCH); ^{27}Al NMR ($CDCl_3$): δ 38 ($W_{1/2}$ = 5183 Hz). IR (KBr) ν in cm^{-1}: 2962m, 2905w, 2866w, 1648s, 1628s, 1544m, 1475m, 1444m, 1421w, 1390w, 1361w,

1310w, 1257w, 1180w, 867w, 845m, 816w, 786w, 756w, 608m, 586w. MS (EI, positive): 597 (M^+, 8%), 517 (M^+ - Br, 100%), 501 (M^+ - Br - O, 44%). Anal. Calcd. for $C_{32}H_{46}O_2N_2AlBr$: C 64.31, H 7.76, N 4.69. found: C 62.13, H 7.93, N 4.43.

Synthesis of salpen(^{t}Bu)AlBr (16). A rapidly stirred solution of Et_2AlBr in toluene, prepared *in situ* by the redistribution of triethylaluminum (0.24 g, 2.1 mmol) and aluminum(III) bromide (1 M solution in dibromomethane, 1.0 mL, 1.0 mmol), was combined with a solution of salpen(^{t}Bu)H_2 (1.57 g, 3.10 mmol) in toluene by cannula. The reaction mixture was refluxed for 17 hours. The cloudy yellow solution was concentrated under vacuum to about one third of its volume. The yellow precipitate was isolated by cannula filtration, washed with ~15 mL of hexane, dried under vacuum and recrystallized from toluene. X-ray quality crystals were grown from slow diffusion of hexane vapor into a concentrated CH_2Cl_2 solution. Yield: 1.0 g (55%). Mp: 333-334ºC (dec.). ^{1}H NMR ($CDCl_3$): δ 1.30 (s, 18H, C(C*H*$_3$)$_3$), 1.50 (s, 18H, C(C*H*$_3$)$_3$), 2.23 (m, 2H, $CH_2CH_2CH_2$), 3.85 (m, 4H, NC*H*$_2$), 7.07 (d, 2H, Ph-*H*), 7.56 (d, 2H, Ph-*H*), 8.29 (s, 2H, N=C*H*); ^{13}C NMR ($CDCl_3$): δ 27.2 (*C*H$_2$), 29.7 (C(*C*H$_3$)$_3$), 31.3 (C(*C*H$_3$)$_3$), 33.9 (*C*CH$_3$)$_3$), 35.4 (*C*CH$_3$)$_3$), 55.1 (N*C*H$_2$), 118.1 (Ph), 127.2 (Ph), 131.4 (Ph),138.9 (Ph), 141.0 (Ph), 162.5 (Ph), 172.0 (N=*C*H); ^{27}Al NMR ($CDCl_3$): δ 36 ($W_{1/2}$ = 3339 Hz). IR (KBr) ν in cm^{-1}: 2956m, 2906w, 2866w, 1642s, 1624s, 1548m, 1463s, 1418m, 1390w, 1361m,1312m,, 1259m, 1180m, 1097w, 863m, 847m, 784w,755w, 601m. MS (EI, positive): 531 (M^+ - Br, 100%). Anal. Calcd. for $C_{33}H_{48}O_2N_2AlBr$: C 64.80, H 7.91, N 4.58. found: C 62.12, H 7.78, N 4.36.

Synthesis of salben(^{t}Bu)AlBr (17). To a rapidly stirred solution of Et_2AlBr in toluene, prepared *in situ* by the redistribution of triethylaluminum (0.35 g, 3.1 mmol) and

aluminum(III) bromide (1 M solution in dibromomethane, 1.31 mL, 1.31 mmol), a solution of salben(^{t}Bu)H_2 (2.05 g, 3.93 mmol) in toluene was cannula transferred. The cloudy yellow reaction mixture was refluxed for 14 hours. The cloudy yellow solution was concentrated under vacuum to about one third of its volume. The yellow precipitate was isolated by cannula filtration, washed with two portions of 15 mL of hexane and dried under vacuum. X-ray quality crystals were grown from slow diffusion of hexane vapor into a concentrated CH_2Cl_2 solution of salben(^{t}Bu)AlBr. Yield: 1.8 g (73 %). Mp: 314-316ºC (dec.). ^{1}H NMR ($CDCl_3$): δ 1.30 (s,18H, C(C*H*$_3$)$_3$), 1.49 (s,18H, C(C*H*$_3$)$_3$), 1.80 (m, 4H, $CH_2C\mathit{H}_2C\mathit{H}_2CH_2$), 3.62 (m, 4H, NC*H*$_2$), 7.08 (d, 2H, Ph-*H*), 7.57 (d,2H, Ph-*H*), 8.23 (s, 2H, N=C*H*); ^{13}C NMR ($CDCl_3$): δ 27.7 (*C*H$_2$), 29.9 (C(*C*H$_3$)$_3$), 31.5 (C(*C*H$_3$)$_3$), 34.2 (*C*CH$_3$)$_3$), 35.6 (*C*CH$_3$)$_3$), 57.7 (N*C*H$_2$), 118.6 (Ph), 126.1 (Ph), 127.4 (Ph), 128.5 (Ph), 129.2 (Ph), 132.4 (Ph), 134.4 (Ph), 141.1 (Ph), 170.8 (N=*C*H); ^{27}Al NMR ($CDCl_3$): δ 36 ($W_{1/2}$ = 2485 Hz). IR (KBr) ν/ cm^{-1}: 2959 s, 2909 m, 2866 w, 1643 s, 1566 m, 1468 m, 1429 w, 1390 w, 1359 w,1309w, 1261 m, 1205 s, 1132 s, 1014 w, 986 m, 847 m,800 w. MS (EI, positive): 545 (M^+ - Br, 100%). Anal. Calcd. for $C_{34}H_{50}O_2N_2AlBr$: C 65.28, H 8.06, N 4.48. found: C 63.08, H 7.88, N 4.64.

Synthesis of salophen(^{t}Bu)AlBr (18). A rapidly stirred solution of Et_2AlBr in toluene, prepared *in situ* by the redistribution of triethylaluminum (0.21 g, 1.8 mmol) and aluminum(III) bromide (1 M solution in dibromomethane 0.90 mL, 0.90 mmol), was combined with a solution of salophen(^{t}Bu)H_2 (1.46 g, 2.70 mmol) in toluene by cannula. The golden yellow solution was refluxed for 15 hours. Then it was concentrated under vacuum to about one third of its volume. Yellow crystals precipitated after cooling at -30 ºC for 24 hours. The crystals were isolated by cannula filtration, washed with hexane and

dried under vacuum. Yield: 1.5 g (88 %). Mp: 320 ºC (dec.). ^{1}H NMR ($CDCl_3$): δ 1.37 (s, 18H, C(CH_3)$_3$), 1.63 (s, 18H, C(CH_3)$_3$), 7.24 (d, 2H, Ph-*H*), 7.35 (m, 2H, Ph-*H*), 7.66 (m, 2H, Ph-*H*), 7.71 (d, 2H, Ph-*H*), 8.94 (s, 2H, N=C*H*); ^{13}C NMR ($CDCl_3$): δ 29.8 (C(*C*H$_3$)$_3$), 31.2 (C(*C*H$_3$)$_3$), 34.1 (C(*C*H$_3$)$_3$), 35.6 (C(*C*H$_3$)$_3$), 115.4 (Ph), 115.7 (Ph), 118.5 (Ph), 126.7 (Ph), 127.5 (Ph), 128.2 (Ph), 129.1 (Ph), 133.2 (Ph), 137.5 (Ph), 139.8 (Ph), 141.6 (Ph), 161.2 (Ph), 162.4 (Ph), 164.1 (N=*C*H); ^{27}Al NMR ($CDCl_3$): δ 32 ($W_{1/2}$ = 5183 Hz). IR (KBR) ν in cm^{-1}: 2961s, 2905w, 2868w, 1621s, 1554m, 1542s, 1469s, 1474m, 1445m, 1420m, 1391m,, 1361s, 1311m, 1255m, 1202w, 1179w, 865w, 847m, 786w, 757w, 610m. MS (EI, positive): 646 (M^+, 13%), 565 (M^+ - Br, 95%), 549 (M^+ - Br- O, 100%). Anal. Calcd. for $C_{36}H_{46}O_2N_2AlBr$: C 66.97, H 7.18, N 4.34. found: C 67.23, H 7.35, N 4.14.

Synthesis of [salen(^{t}Bu)Al(Ph$_3$PO)$_2$]Br (19). A rapidly stirred solution of salen(^{t}Bu)AlBr (0.41 g, 0.69 mmol) in toluene was combined with triphenylphosphine oxide (0.38 g, 1.4 mmol). The cloudy yellow slurry became clear greenish yellow with heating. The solution was refluxed for 16 hours. A pale yellow precipitate formed after cooling to room temperature. The precipitate was isolated by cannula filtration and dried under vacuum. Yield: 0.77 g (97 %). Mp: 260 ºC. ^{1}H NMR ($CDCl_3$): δ 1.31 (s, 18H, C(CH_3)$_3$), 1.42 (s, 18H, C(CH_3)$_3$), 3.67 (s, br, 4H, NCH_2), 6.86 (d, 2H, Ph-*H*), 7.29-7.54 (m, 32H, Ph-*H*), 8.04 (s, 2H, N=C*H*); ^{13}C NMR ($CDCl_3$): δ 29.8 (C(*C*H$_3$)$_3$), 31.4 (C(*C*H$_3$)$_3$), 33.9 (C(*C*H$_3$)$_3$), 35.5 (C(*C*H$_3$)$_3$), 53.3 (N*C*H$_2$), 118.6 (Ph), 127.3 (Ph), 128.1 (Ph), 128.6 (Ph), 128.9 (Ph), 128.1 (Ph), 129.5 (Ph), 128.1 (Ph), 130.4 (Ph), 132.0 (Ph), 132.3 (Ph), 132.8 (Ph), 132.9 (Ph), 137.5 (Ph), 139.9 (Ph), 162.7 (Ph), 168.7 (NCH); ^{27}Al NMR ($CDCl_3$): δ -6 ($W_{1/2}$ = 7859 Hz). ^{31}P{^{1}H} NMR ($CDCl_3$): δ 34 (s) IR (KBr) ν in cm^{-}

[1]: 2951s, 2901w, 2862w, 1621s, 1547w, 1439m, 1422w, 1391w, 1358w, 1258w, 1173s ($\nu_{P=O}$), 1121m, 856w, 787w, 757w, 724s, 694m, 610m, 539s. MS (MALDI-TOF): 795 (M^+ - Br - Ph_3PO, 100%), 517 (M^+ - Br – 2 Ph_3PO, 36%). Anal. Calcd. for $C_{68}H_{76}O_4N_2P_2AlBr$: C 70.76, H 6.64, N 2.43. found: C 70.43, H 7.01, N 2.22.

Synthesis of [salpen(^{t}Bu)Al(Ph_3PO)$_2$]Br (20). A rapidly stirred solution of salpen(^{t}Bu)AlBr (0.32 g, 0.53 mmol) in toluene was combined with triphenylphosphine oxide (0.29 g, 1.1 mmol). The cloudy yellow slurry became clear yellow with heating. The solution was refluxed for 10 hours. A yellow precipitate formed after cooling down to room temperature and concentrating the solution. The precipitate was isolated by cannula filtration and dried under vacuum. Yield: 0.42g (69 %). Mp: 246 ºC. ^{1}H NMR ($CDCl_3$): δ 1.31 (s, 36H, C(C*H*$_3$)$_3$), 2.08 (m, 2H, $CH_2CH_2CH_2$), 3.56 (m, 4H, NC*H*$_2$),7.05 (d, 2H, Ph-*H*), 7.27-7.59 (m, 32H, Ph-*H*), 8.29 (s, 2H, N=C*H*); ^{13}C NMR ($CDCl_3$): δ 27.2 (*C*H$_2$), 29.9 (C(*C*H$_3$)$_3$), 31.6 (C(*C*H$_3$)$_3$), 34.2 (C(*C*H$_3$)$_3$), 35.5 (C(*C*H$_3$)$_3$), 56.6 (N*C*H$_2$), 118.8 (Ph), 128.1 (Ph), 128.4 (Ph), 129.0 (Ph), 129.2 (Ph), 130.3 (Ph), 131.3 (Ph), 132.4 (Ph), 132.6 (Ph), 133.1 (Ph), 133.2 (Ph), 139.2 (Ph), 140.2 (Ph), 162.6 (Ph), 172.8 (N=*C*H); ^{27}Al NMR ($CDCl_3$): δ 0 ($W_{1/2}$ = 4835 Hz). ^{31}P{^{1}H} NMR($CDCl_3$): δ 35 (s) IR (KBr) ν in cm^{-1}: 2950s, 2905w, 2866w, 1632s, 1620s, 1548m, 1478m 1461m, 1439s, 1426s, 1391w, 1358m, 1316m, 1279w, 1255m, 1200w, 1162s ($\nu_{P=O}$), 1120s, 1094w, 999w, 841m, 786w, 753m, 726s, 693s, 537s. MS (MALDI-TOF): 809, (M^+ - Br - Ph_3PO, 11%), 531 (M^+ - Br - 2 Ph_3PO, 100%). Anal. Calcd. for $C_{69}H_{78}O_4N_2P_2AlBr$: C 70.94, H 6.73, N 2.40. found: C 68.86, H 6.84, N 2.13.

Synthesis of [salophen(^{t}Bu)Al(Ph_3PO)$_2$]Br (21). A rapidly stirred solution of salophen(^{t}Bu)AlBr (0.51 g, 0.79 mmol) in toluene was combined with

triphenylphosphine oxide (0.44 g, 1.6 mmol). The yellow slurry was refluxed for 14 hours and then cooled down to room temperature and concentrated. Yellow crystals precipitated which were isolated by cannula filtration and dried under vacuum. Yield: 0.58 g (61 %). Mp: 304-305 ºC (dec.). ^{1}H NMR ($CDCl_3$): δ 1.34 (s, 18H, C(C*H*$_3$)$_3$), 1.50 (s, 18H, C(C*H*$_3$)$_3$), 6.92 (d, 2H, Ph-*H*), 7.06-7.40 (m, 34H, Ph-*H*), 7.62 (d, 2H, Ph-*H*), 8.11 (s, 2H, N=C*H*); ^{13}C NMR ($CDCl_3$): δ 30.1 (C(*C*H$_3$)$_3$), 31.6 (C(*C*H$_3$)$_3$), 34.3 (C(*C*H$_3$)$_3$), 35.9 (C(*C*H$_3$)$_3$), 116.2 (Ph), 119.1 (Ph), 125.6 (Ph), 126.7 (Ph), 128.5 (Ph), 128.6 (Ph), 128.8 (Ph), 128.9 (Ph), 129.3 (Ph), 129.8 (Ph), 132.2 (Ph), 132.4 (Ph), 133.0 (Ph), 133.1 (Ph), 137.6 (Ph), 138.2 (Ph), 140.8 (Ph), 159.9 (Ph), 164.9 (N=*C*H); ^{27}Al NMR ($CDCl_3$): δ 42 ($W_{1/2}$ = 5078 Hz); ^{31}P{^{1}H} NMR($CDCl_3$): δ 33 (s). IR (KBr) ν in cm^{-1}: 2954s, 2901w, 2862w, 1614s, 1586s, 1547m, 1536s, 1469m, 1440m, 1413 w, 1391m, 1357w, 1266w, 1199m, 1172s ($\nu_{P=O}$), 1121s, 847w, 787w, 757w, 756w, 726s, 693m, 602w, 538s. MS (MALDI-TOF): 843 (M^+ - Br - Ph_3PO, 100%). Anal. Calcd. for $C_{72}H_{76}O_4N_2P_2AlBr$: C 71.93, H 6.37, N 2.33. found: C 69.03, H 7.80, N 3.64.

Synthesis of [salophen(*t*Bu)Al{(PhO)$_3$PO)}$_2$]Br (22). To a rapidly stirred solution of salophen(*t*Bu)AlBr (0.68 g, 1.1 mmol) in toluene, triphenylphosphate (0.69 g, 2.1 mmol) was added. The clear golden yellow solution was stirred at room temperature for 17 hours. Concentration followed by slow evaporation at room temperature gave yellow crystals which were cannula filtered, washed with hexane and dried under vacuum. Yield: 1.1 g (79 %). Mp: 120-122 ºC (dec.). ^{1}H NMR ($CDCl_3$): δ 140 (s, 18H, C(C*H*$_3$)$_3$), 6.81-7.60 (m, 38H, Ph-*H*), 7.62 (d, 2H, Ph-*H*), 8.43 (s, 2H, N=C*H*); ^{13}C NMR ($CDCl_3$): δ 30.0 (C(*C*H$_3$)$_3$), 31.6 (C(*C*H$_3$)$_3$), 34.4 (C(*C*H$_3$)$_3$), 35.9 (C(*C*H$_3$)$_3$), 116.0 (Ph), 118.6 (Ph), 119.7 (Ph), 119.8 (Ph), 125.5 (Ph), 126.2 (Ph), 128.4 (Ph), 128.6 (Ph), 129.2 (Ph), 130.1 (Ph),

132.8 (Ph), 137.5 (Ph), 139.0 (Ph), 141.3 (Ph), 149.9 (Ph), 150.0 (Ph), 161.5 (Ph), 164.3 (N=*C*H); ^{27}Al NMR ($CDCl_3$): δ 12 ($W_{1/2}$ = 15053 Hz). $^{31}P\{^1H\}$ NMR($CDCl_3$): δ -21 (s) IR (KBR) ν in cm^{-1}: 2953m, 2901w, 2866w, 1614s, 1587s, 1547m, 1536m, 1487s, 1392w, 1359w, 1278s ($\nu_{P=O}$), 1266m, 1220w, 1184vs, 1163s, 1029s ((ν_{P-O}), 1078m, 983s, 848w, 783w, 753m, 726s, 686w, 610w, 523w. MS (MALDI-TOF): 843 (M^+ - Br - 2 $(PhO)_3PO$, 100%). Anal. Calcd. for $C_{72}H_{76}O_{10}N_2P_2AlBr$: C 66.61, H 5.90, N 2.16. found: C 66.90, H 6.17, N 2.02.

Table 4.1. Crystallographic data and refinement details for compounds **15-18**

	15	**16**	**17**	**18**
Empirical formula	$C_{32.25}H_{46}AlBrCl_{.50}N_2O_2$	$C_{33.50}H_{49}AlBrClN_2O_2$	$C_{34}H_{50}AlBrN_2O_2$	$C_{36}H_{46}AlBrN_2O_2$
M/ g mol^{-1}	618.33	654.09	625.65	645.64
Color	Yellow	Yellow	Pale yellow	Yellow
Crystal size/mm	0.32 x 0.25 x 0.03	0.30 x 0.30 x 0.10	0.20 x 0.15 x 0.15	0.30 x 0.30 x 0.01
Crystal system	Orthorhombic	Triclinic	Orthorhombic	Triclinic
Space group	Pbca	$P\bar{1}$	Pbca	$P\bar{1}$
a/ Å	18.9792(4	14.4180(2)	9.8704(3)	10.7690(3)
b/ Å	9.7445(2)	14.8094(2)	25.0262(7)	12.4573(5)
c/ Å	35.3217(7)	17.2404(3)	26.8713(9)	13.6139(5)
α/ °	90.00	76.0377(6)	90.00	92.427(2)
β/ °	90.00	69.8258(6)	90.00	95.630(2)
γ/ °	90.00	85.9439(6)	90.00	110.941(2)
V/ Å^3	6532.5(2)	3352.95(9)	6637.7(4)	1691.58(10)
ρ_{calc} /g cm^{-3}	1.257	1.296	1.252	1.268
Z	8	4	8	2
F(000)	2608	1380	2656	680
Radiation used	Cu-K$_\alpha$	Mo-K$_\alpha$	Mo-K$_\alpha$	Cu-K$_\alpha$
μ /mm $^{-1}$	2.575	1.363	1.296	2.157
T/ K	90.0(2)	90.0(2) K	90.0(2)	90.0(2)
hkl range	-22 ≤h ≤6, -9 ≤ k 11, -41 ≤ l ≤ 41	-16 ≤ h ≤ 17, -17 ≤ k ≤ 17, -20 ≤ l ≤ 20	-11 ≤ h ≤ 11, -29 ≤ k ≤ 29, -31 ≤ l ≤ 31	-11 ≤h ≤12, -13 ≤ k ≤ 4, -15 ≤l ≤15

Θ range/ °	2.50 -68.01	1.29-25.00	1.52 -25.00	3.27 -59.99
Reflections measured	31154	76859	10083	16067
Unique reflections (R_{int})	5672 (0.0617)	11822 (0.0000)	5695 (0.0531)	4987 (0.0730)
Obsd reflections, n [$I \geq 2\sigma(I)$]	4849	7985	3718	4157
Refinement method	Full-matrix least-squares on F^2	Full-matrix least-squares on F^2	Full-matrix least-squares on F^2	Full-matrix least-squares on F^2
Refined parameters /restraints	368/0	755/0	373/0	391/0
R1 [$I > 2\sigma$]	0.0631, wR2 = 0.1671	0.0706, wR2 = 0.1880	0.0481, wR2 = 0.0940	0.052, wR2 = 0.1470
R1 (all data)	0.0724, wR2 = 0.1725	0.1153, wR2 = 0.2193	0.0972, wR2 = 0.1094	0.0700, wR2 = 0.1553
Goodness-of-fit on F^2	1.134	1.020	1.026	1.037
Largest diff. peak and hole/ e. $Å^{-3}$	1.444 and -0.622	1.350 and -0.758	0.471 and -.512	1.934 and -0.609

Table 4.2. Selected bond distances (Å) and angles (º) for compounds **15-18**

Salen(^{t}Bu)AlBr (**15**)			
Al1-N1	2.002(4)	Al1-O2	1.777(3)
Al1-N2	2.001(4)	Al1-Br1	2.3580(14
Al-O1	1.794(3)		
O1-Al1-O2	92.18(15)	O1-Al1-Br1	102.80(12)
O1-Al1-N1	88.38(15)	O2-Al1-Br1	109.17(12)
O1-Al1-N2	158.47(17)	O2-Al1-N1	146.44(16)
O2-Al1-N2	88.84(15)	N1-Al1-Br1	103.37(12)
N1-Al1-N2	79.10(15)	N2-Al1-Br1	97.14(12)
Salpen(^{t}Bu)AlBr (**16**)			
Al1A-N1A	1.958(5)	Al1A-O2A	1.755(4)
Al1A-N2A	2.023(5)	Al1A-Br1A	2.3640(19)
AlA-O1A	1.814(4)		
O1A-Al1A-O2A	90.4(2)	O1A-Al1A-Br1A	94.13(15)
O1A-Al1A-N1A	89.6(2)	O2A-Al1A-Br1A	120.05(17)
O1A-Al1A-N2A	173.5(2)	O2A-Al1A-N1A	127.3(2)
O2A-Al1A-N2A	90.0(2)	N1A-Al1A-Br1A	112.51(16)
N1A-Al1A-N2A	85.0(2)	N2A-Al1A-Br1A	91.26(15)
Salben(^{t}Bu)AlBr (**17**)			
Al1-N1	1.963(3)	Al1-O2	1.754(2)
Al1-N2	2.001(3)	Al1-Br1	2.3804(11)

Al1-O1	1.808(2)		
O1-Al1-O2	91.70(11)	O1-Al1-Br1	92.90(8)
O1-Al1-N1	89.25(11)	O2-Al1-Br1	116.97(9)
O1-Al1-N2	176.32(12)	O2-Al1-N1	119.87(12)
O2-Al1-N2	91.16(11)	N1-Al1-Br1	123.01(9)
N1-Al1-N2	87.32(12)	N2-Al1-Br1	87.86(9)

Salophen(^{t}Bu)AlBr (**18**)

Al1-N1	1.998(4)	Al1-O2	1.783(3)
Al1-N2	1.992(4)	Al1-Br1	2.3508(12)
Al-O1	1.776(3)		
O1-Al1-O2	90.51(14)	O1-Al1-Br1	109.79(11)
O1-Al1-N1	88.53(15)	O2-Al1-Br1	101.01(11)
O1-Al1-N2	142.22(15)	O2-Al1-N1	161.65(15)
O2-Al1-N2	90.26(15)	N1-Al1-Br1	96.55(11)
N1-Al1-N2	79.44(15)	N2-Al1-Br1	107.11(11)

Table 4.3. "Tau" (τ) values of some Salen aluminum halide compounds.

Compound	τ value	Reference
Salpen(^{t}Bu)AlCl	0.77	[199]
Salomphen(^{t}Bu)AlCl	0.18	[199]
Salen(^{t}Bu)AlBr (**15**)	0.20	This work
Salpen(^{t}Bu)AlBr (**16**)	0.77	This work
Salben(^{t}Bu)AlBr (**17**)	0.89	This work
Salophen(^{t}Bu)AlBr (**18**)	0.32	This work

Table 4.4. Crystallographic data and refinement details for compounds **20-22**

	20	**21**	**22**
Empirical formula	$C_{76}H_{86}AlBrN_2O_4P_2$	$C_{76.99}H_{81.70}AlBrN_2O_4P_2$	$C_{75.50}H_{79}AlBrN_2O_{10}P_2$
M/ g mol^{-1}	1260.30	1267.84	1343.24
Color	pale yellow	Yellow	Yellow-brown
Crystal size/ mm	0.50 x 0.20 x 0.15	0.35 x 0.21 x 0.02	0.30 x 0.08 x 0.08
Crystal system	Orthorhombic	Orthorhombic	Monoclinic
Space group	Pbca	Pbca	$P2_1/n$
a/ Å	22.3928(2)	22.6120(3)	19.3380(4)
b/ Å	22.5503(2)	22.8580(3)	15.3855(3)
c/ Å	25.8204(3)	26.7850(4)	23.7586(6)
α/ °	90.00	90	90
β/ °	90.00	90	103.8434(9)
γ/ °	90.00	90	90
V/ Å^3	13038.4(2)	13844.2(3)	6863.4(3)
ρ_{calc}/g cm^{-3}	1.284	1.217	1.300
Z	8	8	4
F(000)	5328	5341	2816
μ (Mo-K_α) /mm^{-1}	0.745	0.702	0.719
T/ K	90.0(2)	90.0(2) K	90.0(2)
hkl range	$-28 \le h \le 28$, $-29 \le k \le 29$, $-33 \le l \le 33$	$-24 \le h \le 24$, $-24 \le k \le 24$, $-28 \le l \le 28$	$-20 \le h \le 20$, $-16 \le k \le 16$, $-25 \le l \le 25$
Θ range/ °	1.50 - 27.49	1.48 to 22.50	1.55 - 22.50
Reflections	28736	34655	17173

measured			
Unique reflections (R_{int})	14950 (0.0725)	9057 (0.1170)	8987 (0.1057)
Obsd reflections, n [I≥ 2σ (I)]	8931	5480	4508
Refinement method	Full-matrix least-squares on F^2	Full-matrix least-squares on F^2	Full-matrix least-squares on F^2
Refined parameters /restraints	795/75	897/ 513	840/ 691
R1 [I > 2σ]	0.0491, wR2 = 0.1011	0.0809, wR2 = 0.2129	0.0823, wR2 = 0.2024
R1 (all data)	0.1085, wR2 = 0.1172	0.1407, wR2 = 0.2431	0.1760, wR2 = 0.2464
Goodness-of-fit on F^2	1.036	1.072	1.061
Largest diff. peak and hole/ e. $Å^{-3}$	.619 and 0.465	1.061 and 0.587	1.213 and 0.522

Table 4.5. Selected bond distances (Å) and angles (°) for compounds **20**-**22**

salpen(^{t}Bu)Al($Ph_3PO)_2$Br (**20**)					
Al1-N1	2.092(2)	Al1-N(2)	2.045(2)	Al1-O1	1.8195(16)
Al1-O2	1.8437(17)	Al1-O(3)	1.9241(17)	Al1-O4	1.9516(17)
O1-Al1-O2	89.38(7)			O1-Al1-O4	94.36(7)
O2-Al1-O4	94.14(7)			O1-Al1-O3	93.45(7)
O2-Al1-O3	93.48(7)			O4-Al1-O3	169.14(8)
O1-Al1-N2	179.60(9)			O2-Al1-N2	90.55(8)
O4-Al1-N2	85.25(7)			O3-Al1-N2	86.95(8)
O1-Al1-N1	89.23(8)			O2-Al1-N1	178.58(8)
O4-Al1-N1	86.23(7)			O3-Al1-N1	86.35(7)
N2-Al1-N1	90.85(8)			Al1-O3-P1	170.37(11)
				Al1-O4-P2	153.04(10)
salophen(^{t}Bu)Al($Ph_3PO)_2$Br (**21**)					
Al-N1	1.989(6)	Al-N(2)	1.986 (6)	Al-O1	1.794 (5)
Al-O2	1.804 (5)	Al-O(3)	1.958 (5)	Al-O4	1.950 (5)
O1-Al-O2	93.8 (2)			O1-Al-O4	94.1 (2)
O2-Al-O4	92.6 (2)			O1-Al-O3	93.2 (2)
O2-Al-O3	94.2 (2)			O4-Al-O3	169.7 (2)
O1-Al-N2	173.8 (2)			O2-Al-N2	92.3 (2)
O4-Al-N2	84.9 (2)			O3-Al-N2	87.1 (2)
O1-Al-N1	92.7 (2)			O2-Al-N1	173.4 (2)
O4-Al-N1	87.4 (2)			O3-Al-N1	85.0 (2)

N2-Al-N1	81.2 (2)			Al1-O3-P1	164.0(3)
				Al1-O4-P2	161.0(3)

Salophen(^{t}Bu)Al[$(PhO)_3PO]_2$Br (**22**)

Al1-N1	1.973(6)	Al1-N(2)	1.984(7)	Al1-O1	1.811(6)
Al1-O2	1.798(6)	Al1-O(3)	1.935(6)	Al-O4	1.967(6)
O1-Al1-O2	96.1(3)			O1-Al1-O4	91.0(2)
O2-Al1-O4	91.1(3)			O1-Al1-O3	92.6(2)
O2-Al1-O3	92.6(3)			O4-Al1-O3	174.6(3)
O1-Al1-N2	172.3(3)			O2-Al1-N2	91.5(3)
O4-Al1-N2	89.4(2)			O3-Al1-N2	86.5(2)
O1-Al1-N1	91.6(3)			O2-Al1-N1	172.1(3)
O4-Al1-N1	87.1(2)			O3-Al1-N1	88.7(2)
N2-Al1-N1	80.7(3)			Al1-O3-P1	157.2(4)
				Al1-O4-P2	165.5(4)

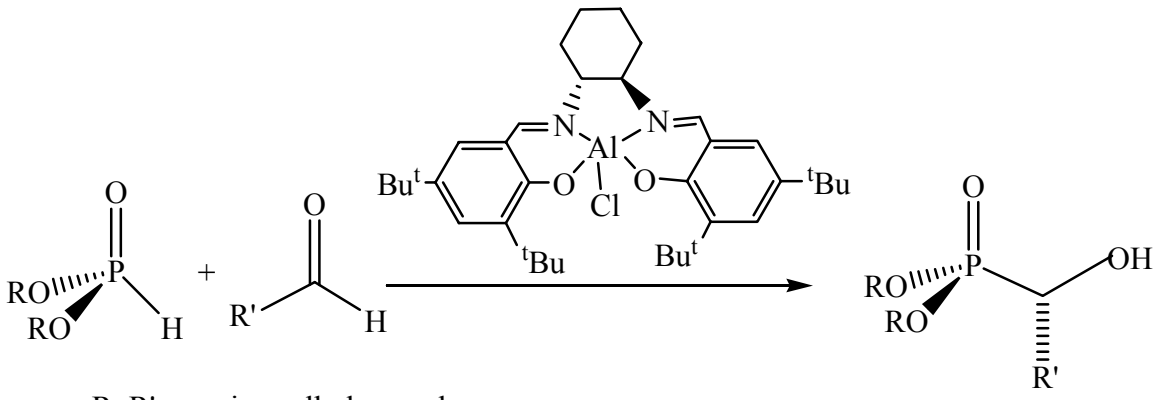

R, R' = various alkyl or aryl groups

Figure 4.1. Phospho transfer reaction with SalenAlCl.

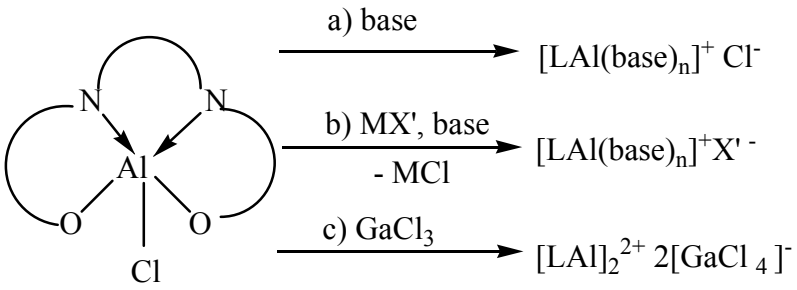

Figure 4.2. Formation of cationic aluminum compounds with Salen ligands.

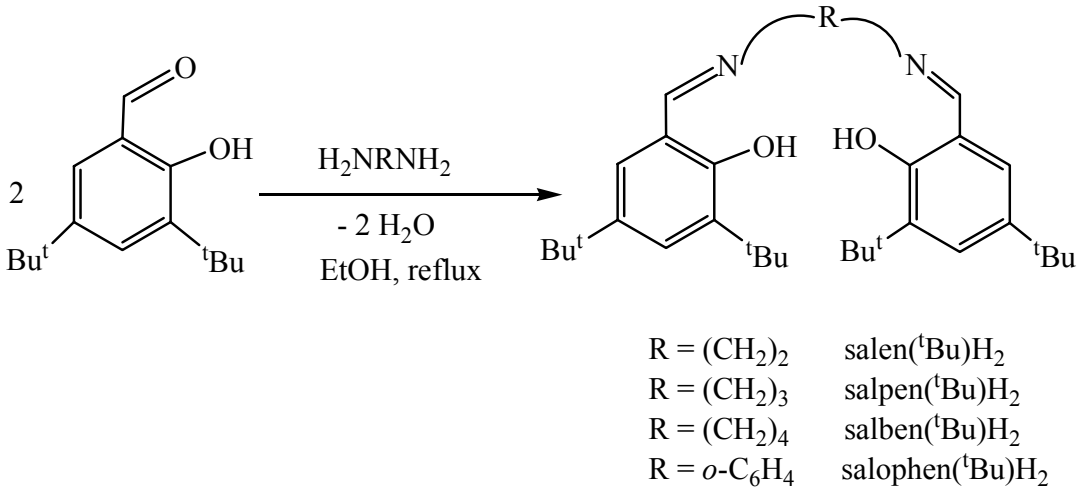

Figure 4.3. Synthesis of Salen(^{t}Bu)H_2 ligands.

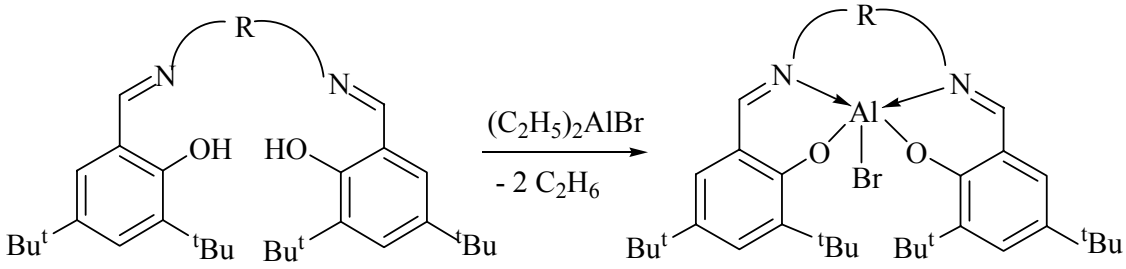

R=$(CH_2)_2$, salen(^{t}Bu)AlBr (**15**)
R=$(CH_2)_3$, salpen(^{t}Bu)AlBr (**16**)
R=$(CH_2)_4$, salben(^{t}Bu)AlBr (**17**)
R=*o*-C_6H_4, salophen(^{t}Bu)AlBr (**18**)

Figure 4.4. Formation of Salen(^{t}Bu)AlBr compounds.

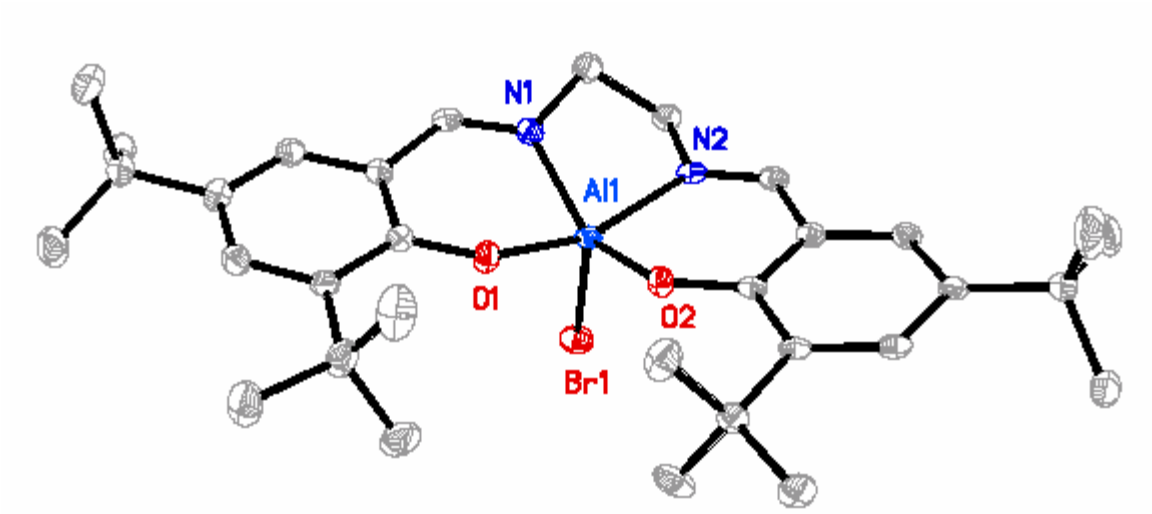

Figure 4.5. Crystal structure of salen(^{t}Bu)AlBr (**15**).

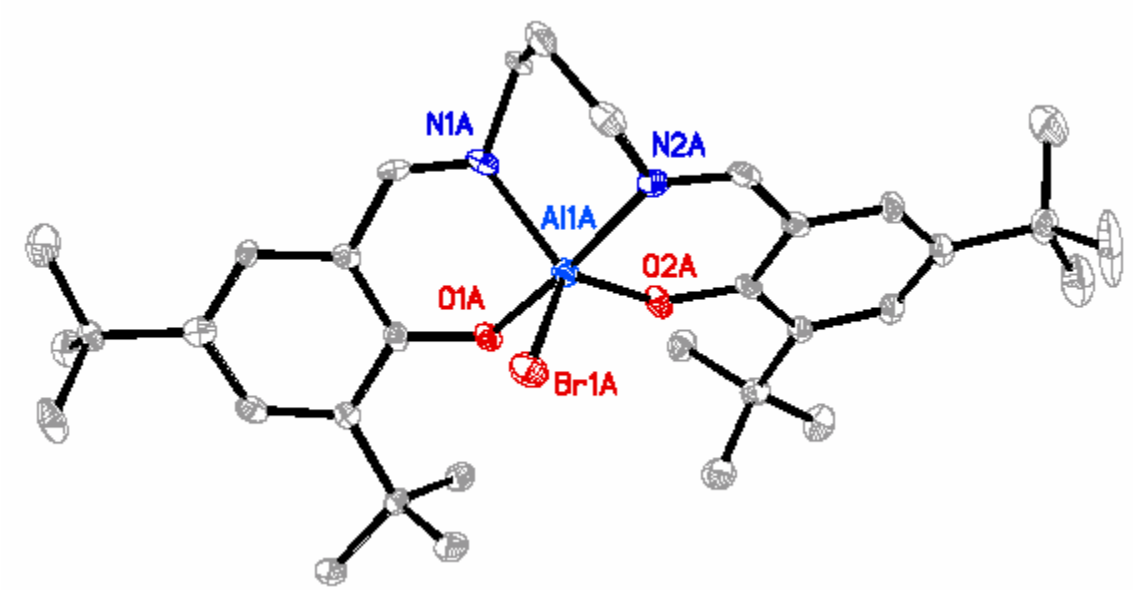

Figure 4.6. Crystal structure of salpen(^{t}Bu)AlBr (**16**). There are two molecules in the asymmetric unit; only one is shown.

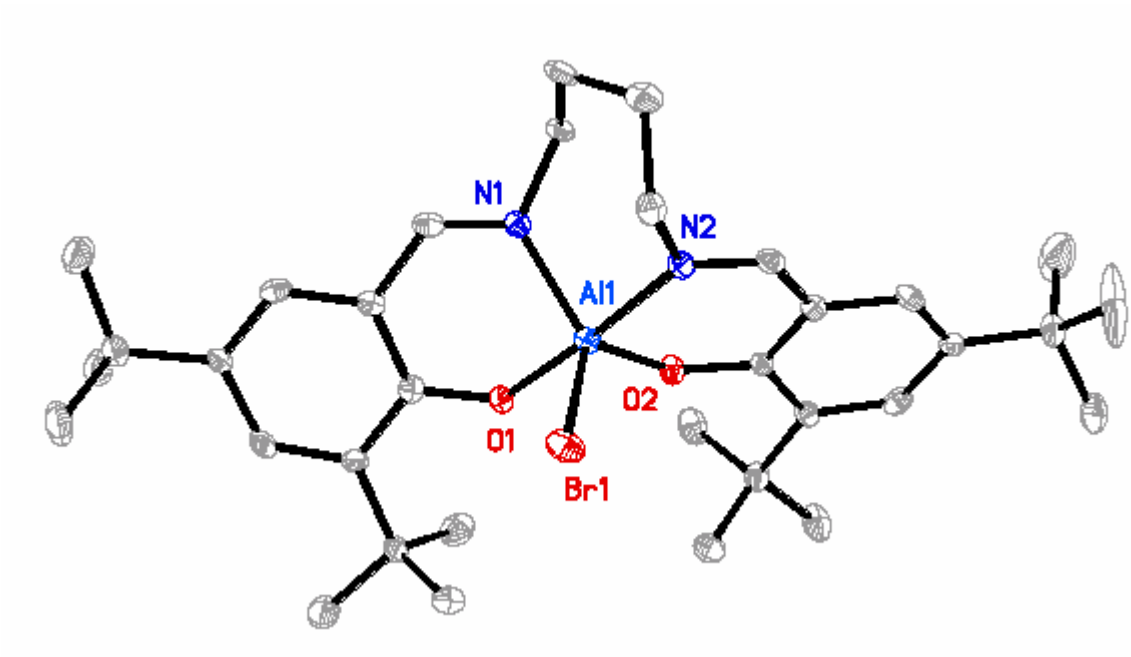

Figure 4.7. Crystal structure of salben(^{t}Bu)AlBr (**17**).

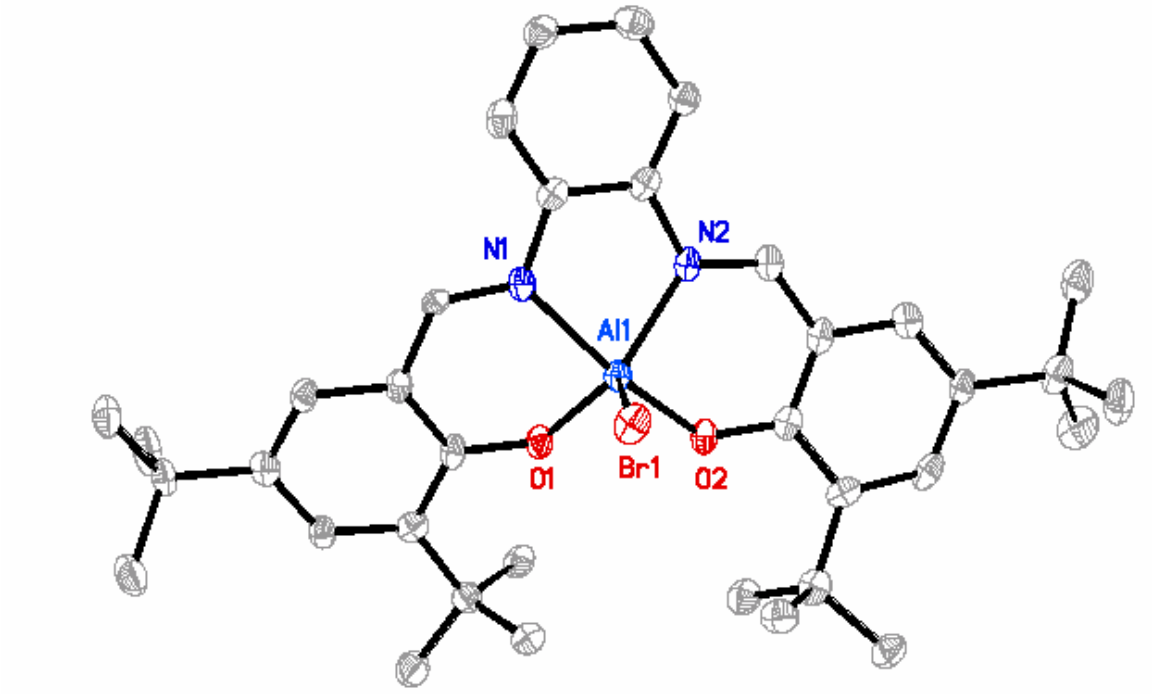

Figure 4.8. Crystal structure of salophen(^{t}Bu)AlBr (**18**).

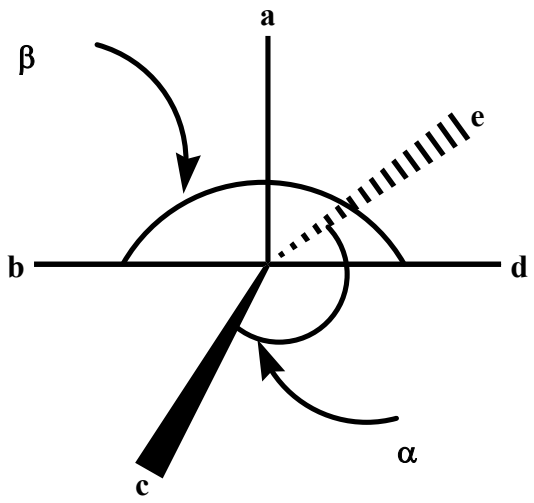

Figure 4.9. "Tau" (τ) diagram. $\tau = (\beta - \alpha)/60$. α (c ─ e) and and β (b ─ d) are the angles opposite to each other in the xy plane where a is along the z-axis. By convention β is the most obtuse angle.

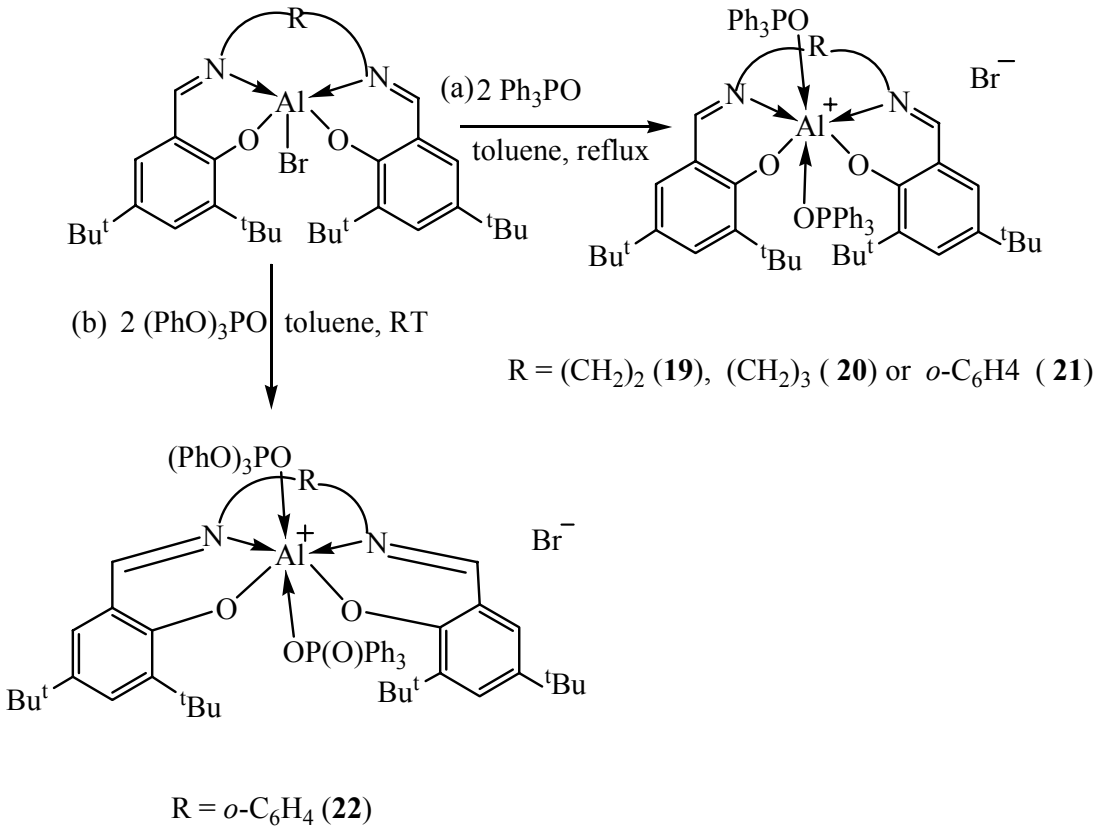

Figure 4.10. Formation of six-coordinate aluminum cations from Salen(^{t}Bu)AlBr compounds.

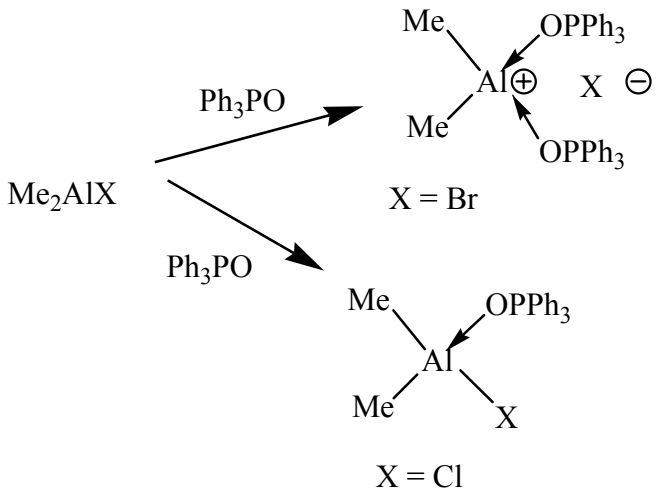

Figure 4.11. Reaction of triphenylphosphine oxide with Me_2AlX.

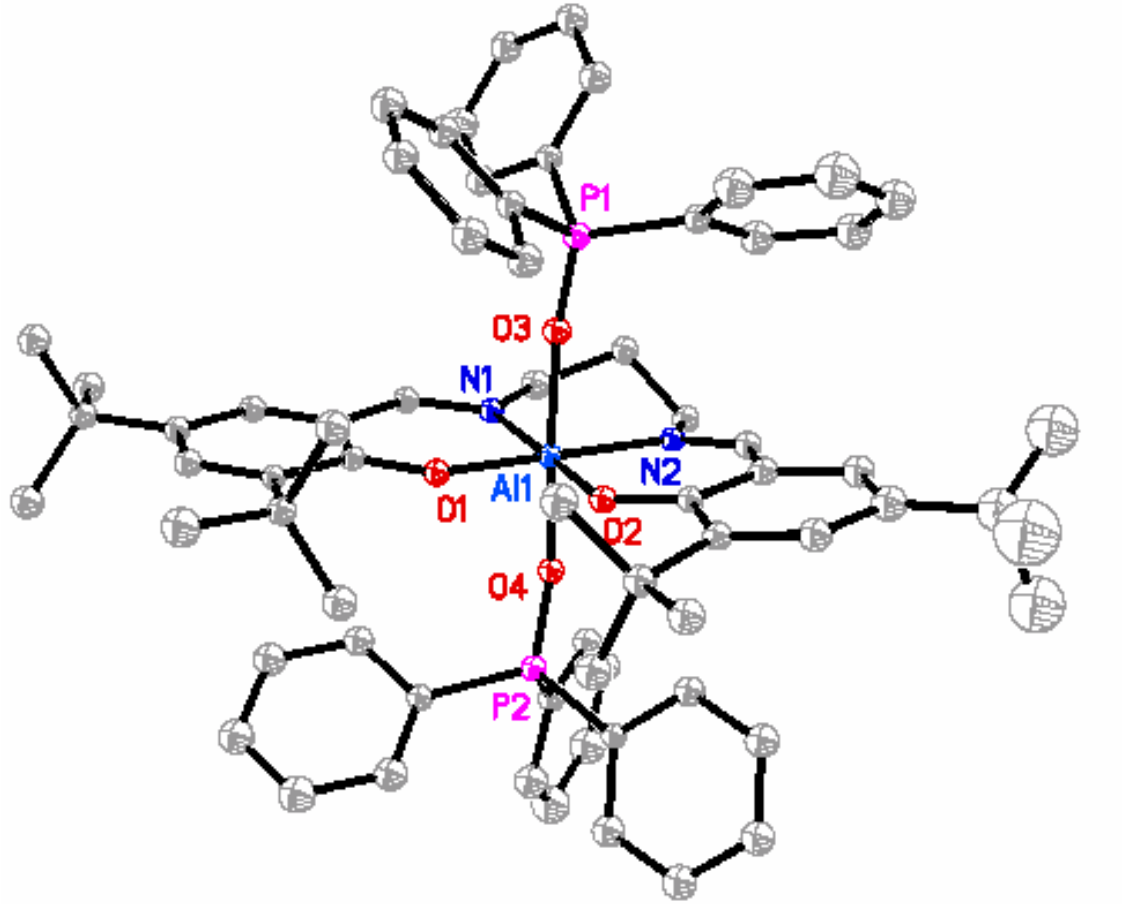

Figure 4.12. Crystal structure of [salpen(^{t}Bu)Al($Ph_3PO)_2$]Br (**20**).

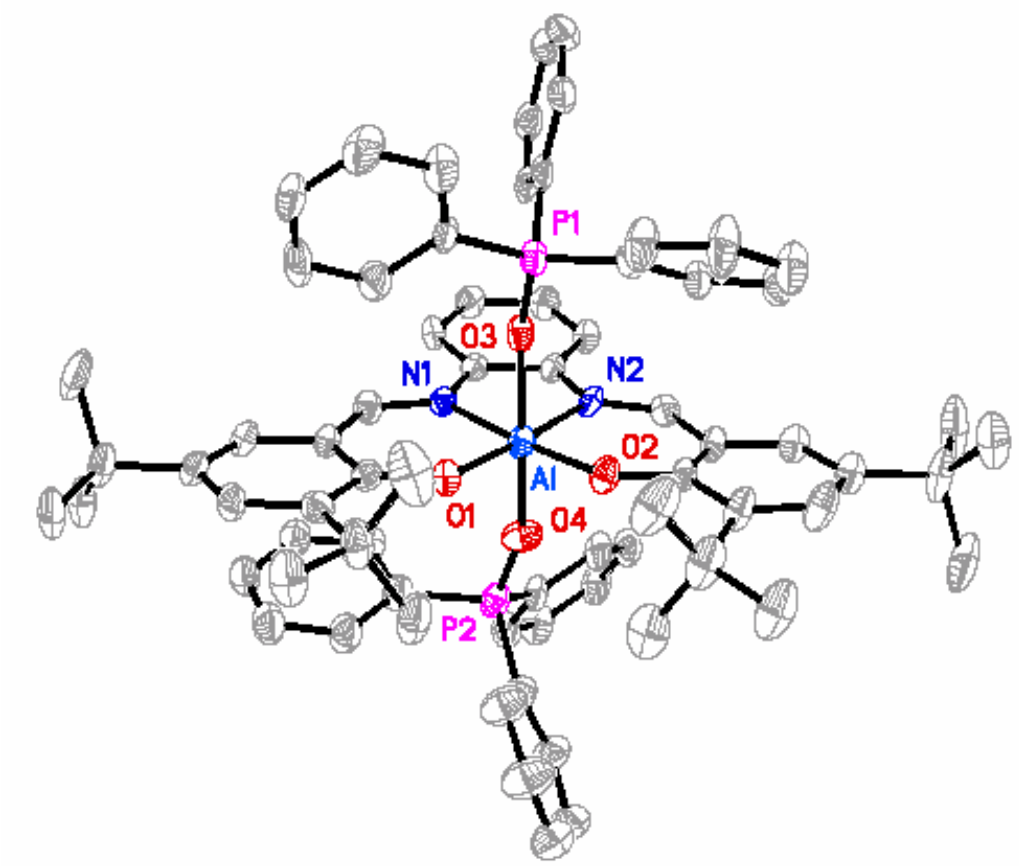

Figure 4.13. Crystal structure of [salophen(^{t}Bu)Al($Ph_3PO)_2$]Br (**21**).

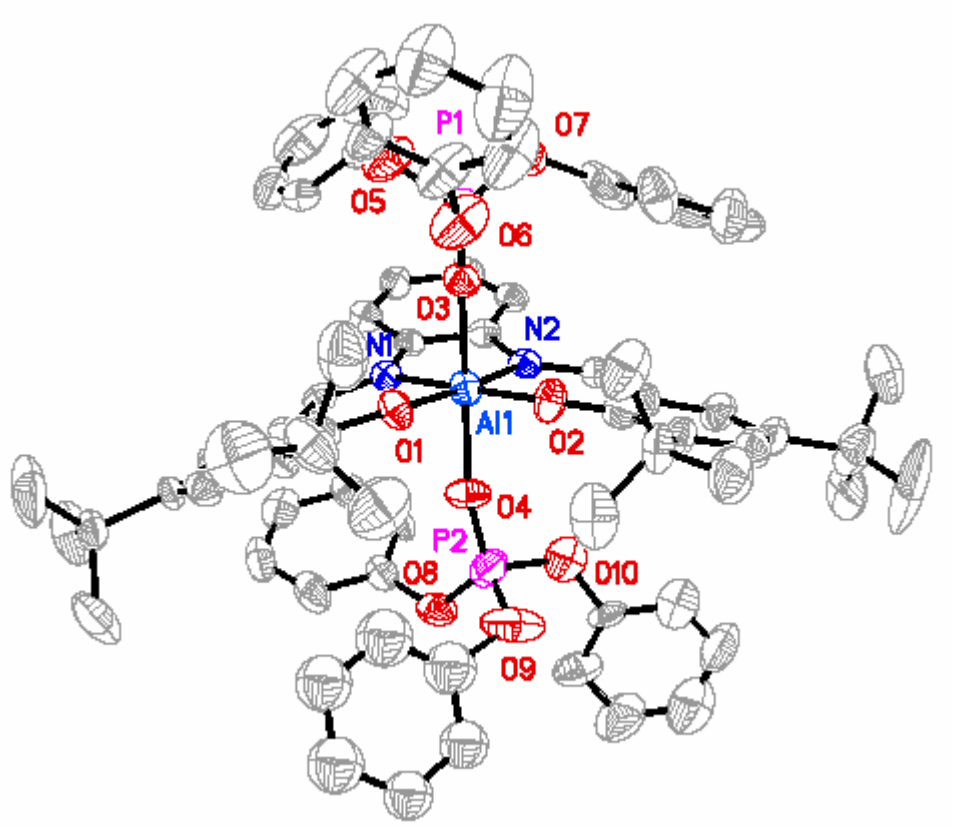

Figure 4.14. Crystal structure of [salophen(^{t}Bu)Al{$(PhO)_3PO$}$_2$]Br (**22**).

CHAPTER 5

Dealkylation of Organophosphates with Salen Aluminum Bromides

5.1. Background

Although extensive research is being carried out on phosphate ester cleavage using various metal compounds in models of biological phosphate hydrolysis (see Chapter 1),[66, 95, 96] the use of group 13 compounds in this field is limited. For example, some phosphate cleavage has been achieved with organoaluminum reagents,[156] and aluminum or gallium amides.[157-159] However, these reagents have not been considered as potential nerve agent or pesticide decontamination reagents, probably due to their limited scope or the high temperatures and the long reaction times required. Recently the use of boron-Schiff base halides has shown promise for the catalytic cleavage of various organophosphates at room temperature, opening the possibility of finding a soft, chemical, catalytic means of destroying or decontamintating nerve gas agents and pesticides.[33-35] In chapter 3 the application of mononuclear boron compounds in the dealkylation of trimethyl phosphate was described and some of them showed very good percent conversion. The Salen aluminum bromide compounds synthesized in chapter 4 could also be promising candidates for phosphate dealkylation since the bromide group in these compounds was demonstrated to be easily displaced by the weak Lewis bases triphenylphosphine oxide and triphenyl phosphate. In this chapter the application of Salen aluminum bromide compounds **15**, **16** and **18** for the dealkylation of various organophosphates will be examined.[203] Also, attempts will be made to isolate and characterize some of the dealkylated compounds.[214]

5.2. Dealkylation of organophosphates with compounds 15, 16 and 18

The compounds salen(^{t}Bu)AlBr (**15**), salpen(^{t}Bu)AlBr (**16**) and salophen(^{t}Bu)AlBr (**18**) dealkylated a series of organophosphate compounds at room temperature to produce alkyl bromide and an unidentified aluminum phosphate compound that remained in solution (Figure 5.1). The dealkylation reaction was carried out in an NMR tube in $CDCl_3$ by using stoichiometric amounts of the Salen aluminum bromide compounds and the phosphate. The percent conversion was calculated from the integration of the remaining phosphate and the alkyl bromide produced (Table 5.1). The percent dealkylation was comparable to the binuclear boron Salen bromide compounds Salen(^{t}Bu)$[BBr_2]_2$ reported before.[33-35] For trimethylphosphate, compound **15**, having an ethylene backbone, showed greater dealkylation activity compared to **16** which has a propylene backbone, and **18** which has an aromatic backbone. For example, with **1** the dealkylation was 89% complete in just 4 hours and 96% complete after 12 hours. However, the difference in Salen ligand backbone does not seem to affect the dealkylation of longer chain phosphates. Another interesting observation is that the percent dealkylation was greater for longer chain phosphates compared to those with shorter chains. For example, with **16,** dealkylation was complete in 2 hours for triethylphosphate and in 30 minutes for tributyl phosphate, as opposed to only 30 % conversion for trimethylphosphate after 2 hours. This is probably due to increased nucleophilicity of the phosphate from the increased number of electron releasing carbon atoms in the alkoxy group.

Previously, it was shown that Salen(^{t}Bu)AlCl compounds readily formed cations through the replacement of chloride by a donor ligand like THF, MeOH or H_2O.[17-22] Cation formation should be more favorable for the Salen bromide compounds because

bromide is a better leaving group. As noted previously in Chapter 4, cations are readily formed when SalenAlBr compounds are combined with triphenylphosphine oxide and triphenylphosphate. Cation formation was also observed for Salen boron bromide compounds with THF.[35] Thus, it is likely that compounds **15, 16** and **18** form cations through coordination of the Lewis basic phosphate to the aluminum with displacement of the bromide anion. This activates the α-carbon of the phosphate for nucleophilic attack of the bromide (Figure 5.1). A similar activation of an ester carbon due to coordination of the phosphoryl oxygen to a cationic center was reported before in the combination of phosphinic esters with metal halides.[215] The cation formation is followed by attack of the bromide on the α carbon and elimination of alkyl bromide. Ultimately, all three ester bonds are cleaved to produce an unidentified phosphate material "[$(SalenAlO)_3PO$]". This mechanism is supported by the following observations:

(i) There is little dealkylation in CD_3OD (Table 5.1). Methanol is a stronger Lewis base than trimethylphosphate and although a cation is formed[18] the phosphate cannot replace the CD_3OD to become activated.

(ii) The dealkylation with Salen(^{t}Bu)AlCl (55% after 24 hours, Table 5.1) is much less compared to the bromide analogue. The Al—Cl bond is stronger than the Al—Br bond which impedes the replacement of chloride with the phosphate and hence the required cation formation.

(iii) The triphenylphosphate coordinated cationic compound **22** was structurally characterized (Chapter 4). Salen aluminum halide compounds do not dealkylate triphenylphosphate. No dealkylation was also found with Salen boron bromide compounds.[35] The reaction stops at the formation of the phosphate-coordinated cation.

(iv) The postulate that the bromide attacks the ester carbon instead of the phosphorus is in agreement with the previous findings that for cleavage of phosphate esters in solution nucleophiles with a high charge density, such as hydroxides and alkoxides, preferentially attack the phosphorus whereas more polarizable nucleophiles like bromides or iodides attack the carbon (Figure 5.2).[215, 216]

Salen(^{t}Bu)AlBr compounds, when added in catalytic amount, were found to accelerate the reaction between trimethylphosphate and stoichiometric amount of BBr_3 (Table 5.2). With BBr_3 only, the dealkylation of trimethyl phosphate is low. However, compounds **15** **16** and **18** in only 10 mol% with BBr_3 increased the extent of dealkylation. For example, with **15** the reaction was 100% complete within only two hours. Although detailed mechanistic studies were not carried out, it is likely that BBr_3 regenerates the catalytic species from the dealkylated phosphate material allowing the repetition of the catalytic cycle. However, the dealkylation was higher for the (Salen(^{t}Bu)AlBr + TMP + BBr_3) system compared to either (Salen(^{t}Bu)AlBr+ TMP) system or (BBr_3 + TMP) system. Thus it is likely that it is not the Salen(^{t}Bu)AlBr compound itself but a species which is formed from the reaction of Salen(^{t}Bu)AlBr and BBr_3 that speeds up the reaction.

In an attempt to get a preliminary idea of the catalytic species, a series of NMR tube experiments involving multinuclear NMR were conducted. Based on this preliminary evidence a catalytic cycle shown in Figure 5.3 is proposed. In the NMR tube reaction system of BBr_3 and salen(^{t}Bu)AlBr (**15**) (1:1) a narrow ^{27}Al peak was observed at δ 79 ppm ($w_{1/2}$ = 507 Hz) which is a significant upfield shift from the broad five-coordinate aluminum peak observed at δ 38 ppm ($w_{1/2}$ = 5183 Hz) for compound **15** and in the range of four-coordinate aluminum.[217] This suggests a severe weakening of the B-Br bond in **15**

by interaction with BBr_3. BBr_3 is known to form BBr_4^- (^{11}B NMR: δ -21.60 ppm) by abstracting Br from $L[BBr_2]_2$ (L = salpen(^{t}Bu)) to form the cationic species $L[BBr_2(BBr)^+]$.[35] The ^{11}B shift in the system (**15** + BBr_3) was observed at δ -0.79 ppm ($w_{1/2}$ = 1038 Hz) which is significantly upfield from the shift observed for boron tribromide (δ 38 ppm), but this shift was not close to the shift of BBr_4^-. Hence, it is likely that instead of the formation of an ion pair, "$[SalenAl]^+[BBr_4]^-$", the bromide bridges both the aluminum and the boron centers and a complex (type **A** shown in figure 5.3) is formed. This would give the ^{11}B shift observed. This gives a partially positive charge to the aluminum and a partially negative charge to the boron. The formation of this complex increases the electrophilicity of the aluminum, which is now a stronger Lewis acid than either neutral salen(^{t}Bu)AlBr (**15**) or BBr_3. Attack of the phosphate on **A** causes cleavage of the Al·····Br bond to form the cationic complex **B.** This is followed by abstraction of the methyl group by the bromide to give the aluminophosphate **C** which on combination with BBr_3 forms a boron phosphate material **D** with the regeneration of the active species **A**. The dealkylation results with salen(^{t}Bu)AlBr for trimethyl phosphate shown in Table 5.2 indicate that the dealkylation reaction is 88 % in 30 minutes but it goes to 100 % conversion within 2 h. On the other hand Table 5.1 indicates that the dealkylation with only salen(^{t}Bu)AlBr (**15**) is only 79 % after 2 hours. Thus it can be assumed that in the presence of both **15** and BBr_3, the reaction speeds up and goes to completion at some point between 30 minutes and 2 hours. This makes one think that there is probably an induction period during which the reaction is slow and during which the formation of the active species **A** is complete. To verify this, BBr_3 was added to **15** in 1:1 ratio and allowed to stand for 1 h to allow the formation of **A**. To this mixture TMP was added and

the ^{1}H NMR taken after 15 minutes showed complete conversion. Thus the formation of complex **A** appears to be responsible for accelerating and taking the dealkylation reaction to completion which is otherwise slower either with **15** or BBr_3. To check if species **A** is being regenerated in the reaction system, BBr_3 was added to a solution containing compound **15** and TMP (3:1) and a peak at 75 ppm ($w_{1/2}$ = 238 Hz) appeared in the ^{27}Al NMR spectra. Appearance of this peak indicates the formation of **A** from the aluminophosphate compound **C** by BBr_3. A similar peak was observed on addition of BBr_3 to the fully characterized aluminum phosphinate compound salen(^{t}Bu)AlOP(O)Ph_2 (**23**) (the synthesis and characterization of **23** is described in the next section). The regeneration of this cationic species is presumably accompanied by the formation of an insoluble boron phosphate material **D** which showed a ^{11}B peak at δ -13.58 ppm ($w_{1/2}$ = 124 Hz), which matched closely to a ^{11}B peak (-13.51 ppm, $w_{1/2}$ = 3 Hz) found in the system (BBr_3 + $(MeO)_3P(O)$) (1:1). The ^{31}P NMR shift (-5.11) present in the salen aluminum-TMP-boron bromide system was different from the ^{31}P shift observed in salen aluminum-TMP system (-14.09 ppm) suggesting that a boron phosphate material and not an aluminum phosphate material is the final dealkylated product. Isolation of the catalytic species and either the boron or aluminum phosphate compound will be required to confirm this cycle. Also, low-temperature studies could tell if the three esters groups are getting dealkylated in a stepwise manner or at the same time. Based on current experiments it was not possible to tell the efficiency of the Salen aluminum bromide compounds as the catalyst. Detailed studies on catalyst loading and determination of turnover frequency will be required for this purpose.

5.3. Formation of aluminum phosphates and phosphinates by dealkylation

Although attempts to isolate the fully dealkylated product "[$(SalenAlO)_3PO$]" by running the dealkylation reaction on a larger scale (mmol) than the NMR tube experiments (0.05 mmol) were not successful, a unique aluminophosphinate and an aluminophosphate compound were isolated and fully characterized. Group 13 phosphates and phosphonates are of potential utility in areas such as catalysis, molecular sieves, ion-exchange resins and adsorption media. [218-220] Aluminophosphate molecular sieves [221] have traditionally been prepared by hydrothermal synthetic methods at temperatures between 100 and 200 ºC where a source of aluminum, e.g., $Al(O^iPr)_3$, is combined with aqueous H_3PO_4.[222, 223] The non-aqueous syntheses of aluminum phosphate molecules and materials have recently been discovered.[73, 157, 158, 224] Previously, the preparation of molecular aluminophosphates by a dealkylation reaction between aluminum amides and phosphoric acid triesters and also by a dealkylsilylation reaction between aluminum chloride and $OP(OSiMe_3)_3$ were reported.[157] Also, aluminum trialkyls undergo adduct formation and subsequent dealkylsilylation to produce molecular aluminophosphates.[158] Most of the aluminophosphate molecules and materials contain four-coordinate aluminum.[79] There are relatively few higher-coordinate aluminum compounds bound to either a phosphate, phosphonate, or phosphinate. One such example is $[(AlO^iPr)_2O_2P(O^tBu)_2]_4$ where the aluminum atom is five-coordinate (Figure 5.4).[225]

Group 13 molecular phosphates and phosphinates are predominantly dimeric and almost all of them have four-coordinate aluminum. Previously, it was reported that six-coordinate aluminum phosphinates may be readily obtained using the tetradentate Salen class of ligand (Figure 5.5).[187, 226] In these chelated phosphinates,

[Salen(^{t}Bu)AlO$_2$P(H)Ph]$_n$, the degree of aggregation was manipulated by changing the length of the ligand "backbone". Some of the compounds revealed unique coupling of the Salen ligand with THF.

The work described in this section shows for the first time the use of Salen aluminum compounds for the dealkylation of phosphinates and phosphates at room temperature in an organic solvent to prepare soluble monomeric aluminum phosphates and phosphinates with five- and six-coordinate aluminum.

5.3.1. Five-coordinate monomeric Salen aluminum phosphinate

Salen(^{t}Bu)AlOP(O)Ph$_2$ (**23**) was prepared by dealkylation of methyldiphenylphosphinate by salen(^{t}Bu)AlBr at room temperature (Figure 5.6). Compound **23** was soluble in organic solvents (toluene and chloroform). It was fully characterized using ^{1}H, ^{13}C, ^{27}Al and ^{31}P NMR, IR and MS (EI, positive). The ^{1}H NMR spectrum of **23** was very close to the corresponding chloride analogues reported in the literature [205] and also the bromide starting materials.[203] There are two singlets for the ^{t}Bu-Ph groups at δ 1.29 and δ 1.58 ppm. Two methylene peaks corresponding to the ethylene backbone protons from the ligand appear at δ 3.64 and δ 4.40 ppm. There is only one imine singlet at δ 8.17 ppm. The ^{27}Al NMR showed a broad peak centered at δ 30 ppm for five-coordinate aluminum which is similar to the shift observed in many other five-coordinate aluminum Salen compounds, e.g., salen(^{t}Bu)AlOSiMe$_3$ (δ 30.5 ppm) and salen(^{t}Bu)AlN$_3$ (δ 31.9 ppm).[199] However, this is upfield from the related chloride analogue (δ 57 ppm).[205] The ^{31}P{H} NMR of **23** contained a single peak at δ 35 ppm. Interestingly, this is considerably downfield compared to dimeric or polymeric Salen aluminum phosphinates (δ 7.08-9.16 ppm). [226]

Compound **23** was recrystallized by slow evaporation of a methanol solution at room temperature under atmospheric conditions to produce **23•MeOH**. The compound was stable in the atmosphere and no nucleophilic displacement of the phosphinate group by methanol or atmospheric moisture was observed. The compound crystallizes in the orthorhombic space group $P2_12_12_1$. The molecular structure is shown in Figure 5.7. There are two molecules in the asymmetric unit; only one is shown in the figure. The crystal data collection parameters are shown in Table 5.3 and the important bond lengths and angles are shown in Table 5.4. Previously, the only structurally characterized examples of Salen aluminum phosphinate compounds, $[Salen(^tBu)Al\{O_2P(H)Ph\}]_n$, were polymeric ($n = \infty$) for salen, salophen and salomphen and dimeric ($n = 2$) for salpen and salben. [187, 188] In these compounds two phosphinate groups bridge between the Salen(^{t}Bu)Al units. They were synthesized by alkane elimination between Salen(^{t}Bu)AlMe and phenylphosphinic acid Ph(H)P(O)OH. Compound **23•MeOH** is the first example of a structurally characterized monomeric aluminum phosphinate compound bound by a Salen ligand. The aluminum atom has a six-coordinate distorted octahedral environment with MeOH and the phosphinate group at the axial positions. The O3-Al-O4 angle is nearly linear (~175º). The Al-O-P linkage is bent with a bond angle of 151º which is considerably narrower than the Al-O-P angle (~ 159º) in $[salen(^tBu)Al\{O_2P(H)Ph\}]_\infty$. [188] The Al-O (ligand) bond distances (~1.80-1.81 Å) are marginally shorter than the Al-O(P) bond distance (~1.87 Å).

5.3.2. Salpen aluminum phosphate ring compound (24)

The compound $[salpen(^tBu)AlO]_2[(BuO)_2PO]_2$ **(24)** resulted from the dealkylation reaction of salpen(^{t}Bu)AlBr with tributylphosphate in toluene at room temperature

(Figure 5.8). Only one of the three butoxy groups on each phosphate molecule underwent dealkylation. The compound is soluble in toluene and chloroform. It was characterized by IR, ^{1}H NMR, ^{27}Al NMR, ^{31}P NMR, Mp and MS. The ^{1}H NMR has peaks corresponding to the ligand and the alkoxy groups of the mono-dealkylated phosphate. The ^{27}Al NMR shows two peaks. The peak at δ -5 ppm corresponds to six-coordinate aluminum. However the peak at δ 40 ppm falls in the region of five-coordinate aluminum. This does not correspond to the solid-state structure of the compound which shows the presence of six-coordinate aluminum only. It could be possible that in solution one phosphate linkage from one of the aluminum atoms dissociates, thus making it five-coordinate. The ^{31}P NMR has a single peak at δ -18 ppm. The TGA curve (Figure 5.9) of **24** shows a weight loss of about 5 % around 100-120 ˚C which is probably due to the entrapped solvent. There is a second weight loss of about further 85 % in the temperature range 300-600 ˚C that is probably due to the thermal oxidation of the organic species leaving behind some inorganic aluminophosphate material. The remaining weight percentage (~ !0 %) is lower than the calculated percentage of $AlPO_4$ (16 %).

Compound **24** crystallizes in the monoclinic space group $P2_1/c$. The molecular structure of **24** (Figure 5.10) contains an aluminum-phosphate ring formed by two salen aluminum units and two mono-dealkylated phosphate units. The crystal data collection parameters are shown in Table 5.3 and important bond lengths and angles are contained in Table 5.4. Two aluminum and two phosphorus atoms are part of an eight-membered Al-O-P ring. The ring P-O bond distances P1-O3 and P1-O4 (1.4827(18) and 1.4778(18) Å respectively) are essentially equal and have double bond character (Table 5.4). The

other P-O distances P1-O5 and P1-O6 are longer (1.5750(19) and 1.5836(18) Å respectively) and in the range of P-O single bonds.

Each phosphorus atom is in a distorted tetrahedral geometry. The biggest distortion is found in the O-P-O bond angle (118.52(11) º) inside the aluminophosphate ring. Each aluminum atom is six-coordinate with a distorted octahedral geometry. The phosphate oxygen atoms occupy two of the equatorial positions. The other two equatorial positions are occupied by one nitrogen atom and one oxygen atom from the ligand. Another pair of nitrogen and one oxygen from the ligand occupy the axial positions. The axial Al-O distance (1.8274(19) Å) is slightly shorter than the equatorial Al-O distances (1.8597(19), 1.8816(19) and 1.8611(19) Å. However, the axial Al-N2 distance (2.001(2) Å) is almost equal to the equatorial Al-N1 distance (2.026(2) Å). The longer Al-N distances compared to Al-O distances are a reflection of larger atomic radius and lower electronegativity of nitrogen. The Al-O-P angles are not equal. Al1-O4-P1 (165.22(12) ˚) is larger than Al1-O3-P1 (150.46(12) ˚.

The crystal packing diagram of **24** (Figure 5.11) shows that the aluminophosphate rings stack on top of each other with alkoxy chains on phosphorus and ligand groups on aluminum extending away from the ring. The distance between two aluminum atoms is 5.108 Å (Figure 5.12) which is comparable to the pore diameter (6.6 Å) of a synthetic layered aluminphosphate templated by 2-methylpiperazine.[227] This distance is also comparable to the pore size of the aluminophosphate material AlPO-5.[218]

5.4. Conclusion

The Salen(^{t}Bu)AlBr compounds **15**, **16** and **18** dealkylate a series of trialkyl phosphates in high percent conversion. They also appeared to promote the reaction between

trimethylphosphate and boron tribromide. The phosphates used in this study could be envisioned as model compounds for organophosphate chemical warfare agents and pesticides. Thus these compounds could be developed into potential nerve gas and pesticide decontamination agents. A mechanism has been proposed for the dealkylation reaction based on literature precedents for similar reactions and initial experimental findings. Although the attempts to isolate and characterize the fully dealkylated phosphate triester of the type $(LAlO)_3PO$ did not succeed these efforts produced two new aluminum phosphinate and phosphate compounds. The dealkylation reaction between salen(^{t}Bu) aluminum bromide and methyldiphenylphosphinate gave the first structurally characterized monomeric Salen aluminum phosphinate. Furthermore the dealkylation reaction of salpen(^{t}Bu)AlBr with tri-butyl phosphate produced an aluminophosphate ring compound. This compound is the first example of an aluminum phosphate with Salen ligands. It contains six-coordinate aluminum which is rare for molecular aluminophosphate compounds. The reaction conditions for all these compounds are very mild. This method could be developed to prepare aluminophosphate ring, cage and chain structures for soluble models of aluminophosphate materials. This is the first example of the intentional use of an aluminum chelate-based dealkylation reaction in forming compounds containing an Al-O-P linkage.

5.5. Experimental

General remarks. All air-sensitive manipulations were conducted using standard bench-top Schlenk line technique in conjunction with an inert atmosphere glove box. All solvents were rigorously dried prior to use. All glassware was rigorously cleaned and dried in an oven at 130ºC overnight prior to use. All other chemicals were purchased

from Sigma-Aldrich. NMR data were obtained on Varian Gemini-200 and Varian VXR-400 instruments. Chemical shifts were reported relative to $SiMe_4$ for ^1H and ^{13}C, 85% H_3PO_4 for ^{31}P and $AlCl_3$ in D_2O for ^{27}Al, and were reported in ppm. Infrared transmission spectra were recorded at room temperature in a potassium bromide pellet on a Fourier-transform Magna-IR ESP 560 spectrometer. Thermogravimetric analyses were performed on a TA Instruments Hi-Res TGA 2950 Analyzer. Elemental analyses were performed on a LECO CHN-2000 Analyzer.

X-ray data were collected on either a Bruker-Nonius X8 Proteum diffractometer (**23**; CuK_α radiation) or a Nonius Kappa-CCD (**24**; MoK_α radiation). All calculations were performed using the software package SHELXTL-Plus.[174, 176] The structures were solved by direct methods and successive interpretation of difference Fourier maps, followed by least-squares refinement. All non-hydrogen atoms were refined with anisotropic thermal parameters. The hydrogen atoms were included using a riding model with isotropic parameters tied to the parent atom.

Dealkylation of phosphates. In a typical experiment salen(^{t}Bu)AlBr (**15**) (30 mg, 0.050 mmol) was dissolved in about 1 mL $CDCl_3$ in a glass vial. The solution was transferred to a NMR tube in which trimethylphosphate (1.96 μL, 0.0170 mmol, density 1.197 g/mL) was added with a syringe. The mixture was shaken and monitored by ^1H NMR. The % dealkylation was calculated from the peak integrations of methyl bromide produced and unchanged phosphate.

Catalytic dealkylation of phosphate. In a typical experiment in a glass vial 15 mg (0.025 mmol) salen(^{t}Bu)AlBr (**15**) was dissolved in about 1 mL $CDCl_3$. The solution was transferred to a NMR tube in which trimethylphosphate (29 μL, 0.25 mmol, density 1.197

g/mL) and boron tribromide (0.25 mL, 0.25 mmol, 1 M solution in hexane) were added with syringe. The mixture was shaken and monitored by ^{1}H NMR. The % dealkylation was calculated from the peak integrations of methyl bromide produced and unchanged phosphate.

Attempts to identify the active species for the catalytic reaction: (a) In a glass vial 60 mg (0.10 mmol) salen(^{t}Bu)AlBr (**15**) was dissolved in about 1 mL $CDCl_3$. The solution was transferred to an NMR tube in which boron tribromide (0.10 mL, 0.10 mmol, 1 M solution in heptane) was added with a syringe. The mixture was shaken, allowed to stand for 30 minutes and NMR was taken. ^{27}Al NMR: δ 79 ppm ($w_{1/2}$ = (507 Hz).^{11}B NMR: δ -0.79 ppm (($w_{1/2}$ = 1038 Hz).

b) In a glass vial 60 mg (0.10 mmol) salen(^{t}Bu)AlBr (**15**) was dissolved in about 1 mL $CDCl_3$. The solution was transferred to an NMR tube in which boron tribromide (0.10 mL, 0.10 mmol, 1 M solution in heptane) was added with a syringe. The mixture was shaken, allowed to stand for 1 h. To this mixture trimethylphosphate (3.9 μL, 0.034 mmol, density 1.197 g/mL) was added with a microsyringe. ^{1}H NMR taken after 15 minutes showed 100 % conversion of trimethyl phosphate.

Attempts to observe the regeneration of the catalytic species: (a) In a glass vial 30 mg (0.05 mmol) salen(^{t}Bu)AlBr (**15**) was dissolved in about 1 mL $CDCl_3$. The solution was transferred to an NMR tube in which trimethylphosphate (1.96 μL, 0.017 mmol, density 1.197 g/mL) was added with a microsyringe. The mixture was shaken, allowed to stand for 24 h. Boron tribromide (0.05 mL, 0.05 mmol, 1 M solution in heptane) was then added to the reaction mixture with syringe and NMR was taken after 20 minutes. ^{27}Al: δ

75 ppm ($w_{1/2}$ = 238 Hz). $^{31}P\{^{1}H\}$: δ -5.11 ppm. ^{11}B: δ 12.28 ($w_{1/2}$ = 475 Hz), -0.56 ($w_{1/2}$ = 1894 Hz), -6.55 ($w_{1/2}$ = 1100 Hz), -13.58 ($w_{1/2}$ = 124 Hz) ppm.

(b) In a glass vial 60 mg (0.080 mmol) salen(^{t}Bu)AlOP(O)Ph_2 (**23**)was dissolved in about 1 mL $CDCl_3$. The solution was transferred to an NMR tube in which boron tribromide (0.08 mL, 0.08 mmol, 1 M solution in heptane) was added with a syringe. The mixture was shaken, allowed to stand for 2 h and NMR was taken. ^{27}Al NMR: δ 76 ppm ($w_{1/2}$ = (290 Hz). Similar peak was observed when BBr_3 was added in excess (**23**:BBr_3 = 1:10).

(c) In an NMR tube trimethyl phosphate (29 μL, 0.25 mmol, density 1.197 g/mL) was dissolved in about 1 mL $CDCl_3$. Boron tribromide (0.25 mL, 0.25 mmol, 1 M solution in hexane) was then added to the reaction mixture with syringe. The reaction mixture was shaken and allowed to stand for 2 h and NMR was taken. ^{11}B: δ -13.51 ppm ($w_{1/2}$ =3 Hz), 37.39 ppm ($w_{1/2}$ = 64 Hz). $^{31}P\{^{1}H\}$: δ -9.08 ppm.

(d) In a glass vial 30 mg (0.050 mmol) salen(^{t}Bu)AlBr (**15**) was dissolved in about 1 mL $CDCl_3$. The solution was transferred to an NMR tube in which trimethylphosphate (1.96 μL, 0.017 mmol, density 1.197 g/mL) was added with a microsyringe. The mixture was shaken, allowed to stand for 12 h and NMR was taken. ^{27}Al: δ 24 ppm ($w_{1/2}$ = 5900 Hz). $^{31}P\{^{1}H\}$: δ -14.09 ppm.

Synthesis of salen(^{t}Bu)AlOP(O)Ph_2 (23). To a rapidly stirred solution of salen(^{t}Bu)AlBr (**15**) (0.50g, 1.8 mmol) in toluene, $Ph_2P(O)OMe$ (0.20 g, 0.85 mmol) was added. The reaction mixture was stirred for 24 hours and then refluxed for 17 hours. Then it was cannula filtered and the pale yellow residue was dried under vacuum. Yield: 0.40 g (65.0%). Mp: 302-304 ºC. ^{1}H NMR ($CDCl_3$): δ 1.29 (s, 18H, C(CH_3)$_3$), 1.59 (s, 18H,

C(CH_3)$_3$), 3.64 (m, 2H, NCH_2), 4.40 (m, 2H, NCH_2), 6.90 (d, 2H, Ph-*H*), 6.99 (m, 5H, Ph-*H*), 7.26 (d, 2H, Ph-*H*), 7.52 (m, 5H, Ph-*H*) 8.17 (s, 2H, N=C*H*); ^{13}C NMR ($CDCl_3$): δ 29.7 (C(*C*H$_3$)$_3$), 31.3 (C(*C*H$_3$)$_3$), 33.9 (*C*CH$_3$)$_3$), 35.6 (*C*CH$_3$)$_3$), 54.7 (N*C*H$_2$), 118.3 (Ph), 127.2 (Ph), 127.4 (Ph), 127.5 (Ph), 129.9 (Ph), 130.8 (Ph), 130.9 (Ph), 131.1 (Ph), 138.4 (Ph), 140.5 (Ph), 162.8 (Ph), 170.3 (N=*C*H); ^{27}Al NMR ($CDCl_3$): δ 30 ($W_{1/2}$ = 1951 Hz). ^{31}P{^{1}H} NMR ($CDCl_3$): δ 35. IR ν/ cm^{-1}: 3053 (w),2955s, 2905m, 2858w, 1643s, 1625s, 1547w, 1536w, 1478m, 1468m, 1441m, 1390m, 1359m, 1259m, 1176s, 1131m, 1071w, 1025, 857w, 847m,786w,753m, 726m, 700m, 605m, 555m. MS (EI, positive): 734(M^+, 17%), 677 (M^+-^{t}Bu, 100%), 517 (M^+ - $Ph_2P(O)O$, 8%). Anal. Calc.for $C_{44}H_{56}O_4N_2Al$: C 71.91, H 7.68, N 3.81. Found: C 71.40**,** H 8.18, N 3.57.

Synthesis of [salpen(^{t}Bu)AlO]$_2$[(BuO)$_2$PO]$_2$ (24). To a rapidly stirred solution of salpen(^{t}Bu)AlBr (**16**) (0.81 g, 1.3 mmol) in toluene, $(BuO)_3PO$ (0.16 g, 0.44 mmol) was added. The yellow reaction mixture was stirred for 48 hours. After filtration and concentration to about one third of its volume and cooling for several days at -30 ºC yellow crystals precipitated which were filtered, washed with hexane (twice) and dried under vacuum. Yield: 0.17 g (52 %). Mp: softens at 196 ºC and melts at 236-238 ºC. ^{1}H NMR ($CDCl_3$): δ 0.65 (m, phosphate $CH_2CH_2CH_2CH_3$), 0.89 (m, phosphate $CH_2CH_2CH_2CH_3$), 1.30 (s, C(CH_3)$_3$), δ 1.32 (s, br, phosphate $CH_2CH_2CH_2CH_3$ and C(CH_3)$_3$), 1.41 (s, C(CH_3)$_3$), 1.46 (s, br, phosphate $CH_2CH_2CH_2CH_3$ and C(CH_3)$_3$), 2.1 (m, $CH_2CH_2CH_2$), 3.4 (m, phosphate $CH_2CH_2CH_2CH_3$), 3.72 (m, NCH_2), 7.20-7.54 (m, Ph-*H*), 8.41 (s, br, N=C*H*), 8.50 (s, br, N=C*H*); ^{13}C NMR ($CDCl_3$, 200 MHz): δ 13.6 (phosphate $CH_2CH_2CH_2CH_3$), 18.3 (phosphate $CH_2CH_2CH_2CH_3$), 27.2 (CH_2), 29.6 (C(*C*H$_3$)$_3$), (29.8 (C(*C*H$_3$)$_3$), 31.5 (C(*C*H$_3$)$_3$), 31.6(C(*C*H$_3$)$_3$), 31.9 (phosphate

$CH_2CH_2CH_2CH_3$), 34.2 ($CCH_3)_3$), 34.3 ($CCH_3)_3$), 35.5 ($CCH_3)_3$), 55.1 (NCH_2), 67.8 ($CH_2CH_2CH_2CH_3$), 118.4 (Ph), 125.6 (Ph), 126 (Ph), 128.1 (Ph), 128.5 (Ph), 129.3 (Ph), 131.4 (Ph),139.4 (Ph), 140.6 (Ph), 166.9 (Ph), 172.0 (N=CH); ^{27}Al NMR ($CDCl_3$): δ -5 ($W_{1/2}$ = 997 Hz), 40 ($W_{1/2}$ = 3704 Hz) . $^{31}P\{^1H\}$ NMR($CDCl_3$): δ -18 (s). IR ν/ cm^{-1}: IR ν/ cm^{-1}: 2957s, 2906s, 2870m, 1620s, 1547m, 1479s, 1467s, 1442s, 1418s, 1391m, 1361m, 1342w, 1326w, 1312w, 1271s, 1259s, 1236m, 1201m, 1174s, 1091w, 1068w, 1028w, 860w, 847m, 786w, 751w, 599w, 568w. MS (MALDI-TOF): 1272 (M^+ - $(BuO)_2PO_2$, 1.9%), 531 (M^+ – 2 $(BuO)_2PO_2$, 100%). Anal. Calc. for $C_{82}H_{132}O_{12}N_4Al_2P_2$: C 66.46, H 8.98, N 3.78. Found: C 65.85**,** H 9.66, N 4.15.

Table 5.1. Dealkylation (%)[a] of organophosphates with compounds **15**, **16** and **18**.

Compound	**15**			**16**			**18**		
	TMP	TEP	TBP	TMP	TEP	TBP	TMP	TEP	TBP
30 minutes	64	14	12	35	75	7	18	7	100
2 hours	79	100	100	44	100	100	30	100	
4 hours	89			44			40		
6 hours	91			56			46		
8 hours	93			58			58		
10 hours	95			62			64		
12 hours	96			67			69		
24 hours	96			69			85		

[a] Calculated from the integration of ^{1}H NMR spectra of alkyl bromide produced and unchanged trialkyl phosphate at room temperature in $CDCl_3$. In CD_3OD after 24 hours **15** showed no dealkylation while **16** and **18** had 4% and 3% dealkylation, respectively. Salen(^{t}Bu)AlCl showed 55% dealkylation of TMP in $CDCl_3$ after 24 hours. TMP = trimethylphosphate, TEP = triethylphosphate, TBP = tributylphosphate.

Table 5.2. Catalytic dealkylation (%) of trimethylphosphate (TMP) with Salen(^{t}Bu)AlBr compounds.[a]

Compound	**15** + TMP + BBr_3 (1:10:10)	**16** + TMP + BBr_3 (1:10:10)	**18** + TMP + BBr_3 (1:10:10)	TMP + BBr_3 (1:1)
30 minutes	88	78	82	58
2 hours	100	92	84	67
6 hours	100	100	95	67
24 hours	100	100	95	81

[a] Calculated from the integration of ^{1}H NMR spectra of methyl bromide produced and unchanged trimethyl phosphate at room temperature in $CDCl_3$.

Table 5.3. Crystallographic data and refinement details for compounds **23·MeOH** and **24**

	Compound **23**	Compound **24**
Empirical formula	$C_{45}H_{60}AlN_2O_5P_2$	$C_{96}H_{148}Al_2N_4O_{12}P_2$
M/ g mol^{-1}	766.90	1666.08
Color	Yellow	Pale yellow
Crystal size/mm	0.22 x 0.10 x 0.10	0.20 x 0.20 x 0.08
Crystal system	Orthorhombic	monoclinic
Space group	P $2_12_12_1$	P 2_1/c
a/ Å	11.6850(2)	10.6546(2)
b/ Å	26.1840(5)	17.6944(3)
c/ Å	28.1148(5)	24.9473(5)
α/ °	90.00	90.00
β/ °	90.00	95.9921(7)
γ/ °	90.00	90.00
V/ Å^3	8602.0(3)	4677.54(15)
ρ_{calc}/ g cm^{-3}	1.184	1.183
Z	8	2
F(000)	3296	1808
Radiation used	Cu-K_α	Mo-K_α
μ /mm $^{-1}$	1.121	0.126
T/ K	90.0(2)	90.0(2)
hkl range	$-14 \leq h \leq 13$, $-11 \leq k \leq 31$, $-33 \leq l \leq 32$	$-12 \leq h \leq 12$, $-21 \leq k \leq 21$, $-29 \leq l \leq 29$
Θ range/ °	2.31 - 68.22	1.41 - 25.00
Reflections measured	48842	91792
Unique reflections (R_{int})	15283 [R(int) = 0.0524]	8238 (0.1476)

Obsd reflections, n [I≥ 2σ (I)]	14037	4803
Refinement method	Full-matrix least-squares on F^2	Full-matrix least-squares on F^2
Refined parameters/restraints	1018/120	538/0
R1 [I > 2σ]	R1 = 0.0408, wR2 = 0.0996	R1 = 0.0566, wR2 = 0.1079
R1 (all data)	R1 = 0.0457, wR2 = 0.1030	R1 = 0.1236, wR2 = 0.1307
Goodness-of-fit on F^2	1.050	0.998
Largest diff. peak and hole/ e. $Å^{-3}$	0.415 and -0.277	0.314 and -0.559

Table 5.4. Selected bond distances (Å) and angles (º) for compounds **23·MeOH** and **24**

Salen(^{t}Bu)AlOP(O)Ph_2 (**23**)			
Al1A-N1A	2.0023(19)	Al1A-O2A	1.8133(16)
Al1A-N2A	1.9977(19)	Al1A-O3A	2.0255(17)
Al1A-O1A	1.8033(16)	Al1A-O4A	1.8729(17)
		O4A-P1A	1.5052(17)
O1A-Al1-O2A	95.97(7)	O3A-Al1A-N1A	88.76(7)
O1A-Al1-O3A	87.18(7)	O3A-Al1A-N2A	82.36(7)
O1A-Al1A-N1A	91.34(7)	O3A-Al1A-O4A	175.39(7)
O2A-Al1A-N2A	91.22(7)	N1A-Al1A-N2A	81.27(8)
O2A-A11A-O3A	89.79(7)	Al1A-O4A-P1A	151.12(11)
[Salpen(^{t}Bu)AlO]$_2$[$(BuO)_2PO]_2$ (**24**)			
Al1-N1	2.026(2)	P1-O3	1.4827(18)
Al1-N2	2.001(2	P1-O4	1.4778(18)
Al1-O1	1.8274(19)	P1-O5	1.5750(19)
Al1-O2	1.8597(19)	P1-O6	1.5836(18)
Al1-O3	1.8816(19)		
Al1-O4	1.8611(19)		
O1-Al1-N1	88.32(9)	O2-Al1-O4	91.34(8)
O1-Al1-N2	176.15(10)	O3-Al1-N1	86.60(9)
O1-Al1-O2	93.01(9)	O3-Al1-N2	87.23(9)
O1-Al1-O3	93.64(8)	O3-Al1-O4	91.40(8)
O1-Al1-O4	93.45(8)	N1-Al1-N2	87.98(9)
O2-Al1-N1	90.45(9)	Al1-O3-P1	150.46(12)

O2-Al1-N2	85.94(9)	Al1-O4-P1	165.22(12)
O2-A1l-O3	172.64(9)	O3-P1-O4	118.52(11)
O3-P1-O5	111.59(10)	O4-P1-O6	110.32(10)
O5-P1-O6	105.78(10)		

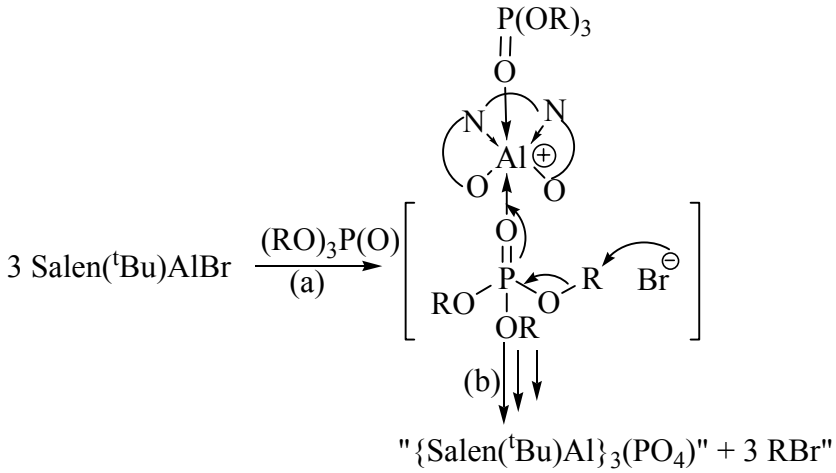

Figure 5.1. Possible dealkylation pathway of organophosphates with Salen((^{t}Bu)AlBr compounds.

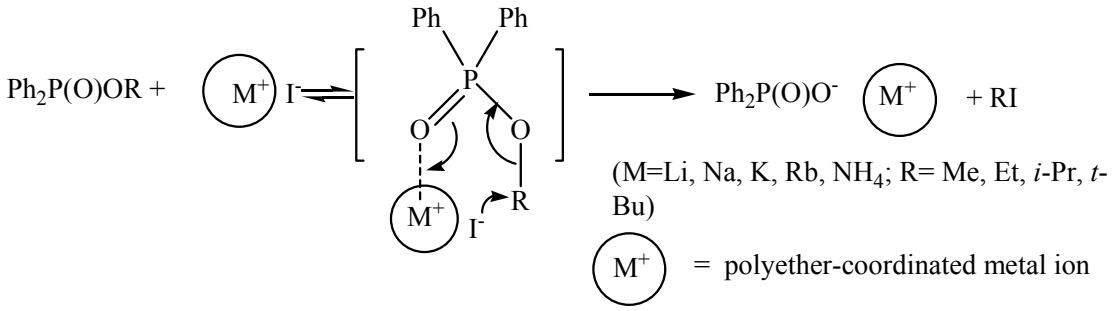

Figure 5.2. Dealkylation of a phosphinate with various iodide salts.

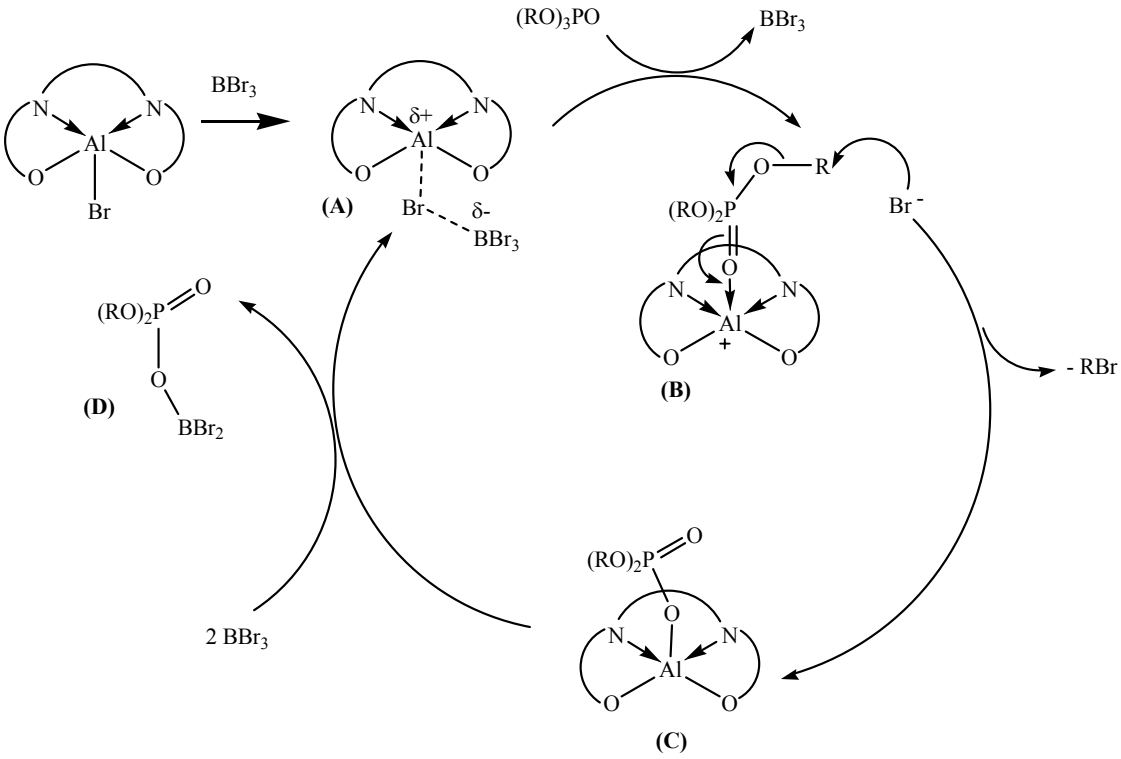

Figure 5.3. Proposed catalytic cycle for dealkylation of trimethylphosphate with excess boron tribromide in the presence of salen(^{t}Bu)AlBr (**15**). For the sake of simplicity only the dealkylation of one ester group is shown.

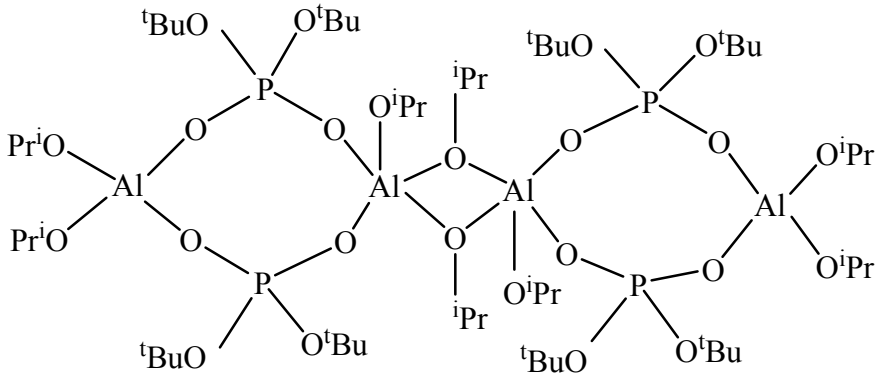

Figure 5.4. Compound $[(AlO^iPr)_2O_2P(O^tBu)_2]_4$ containing a rare five-coordinate aluminum phosphate.

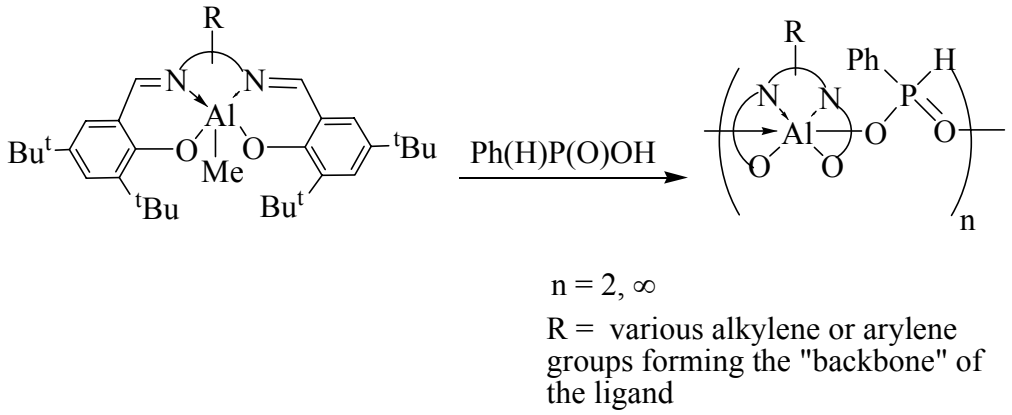

Figure 5.5. Salen aluminum phosphinate compounds formed by alkane elimination reaction.

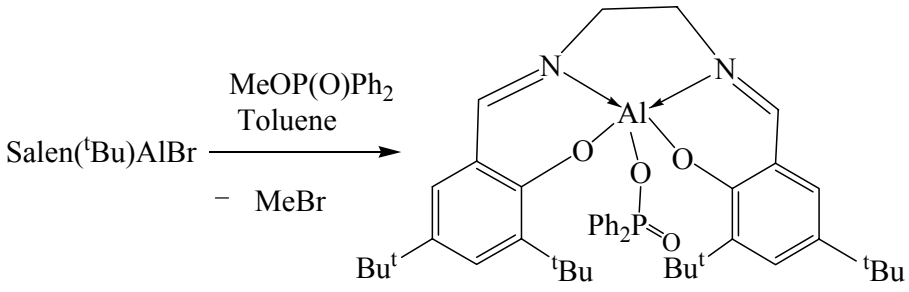

Figure 5.6. Synthesis of salen aluminum phosphinate (**23**).

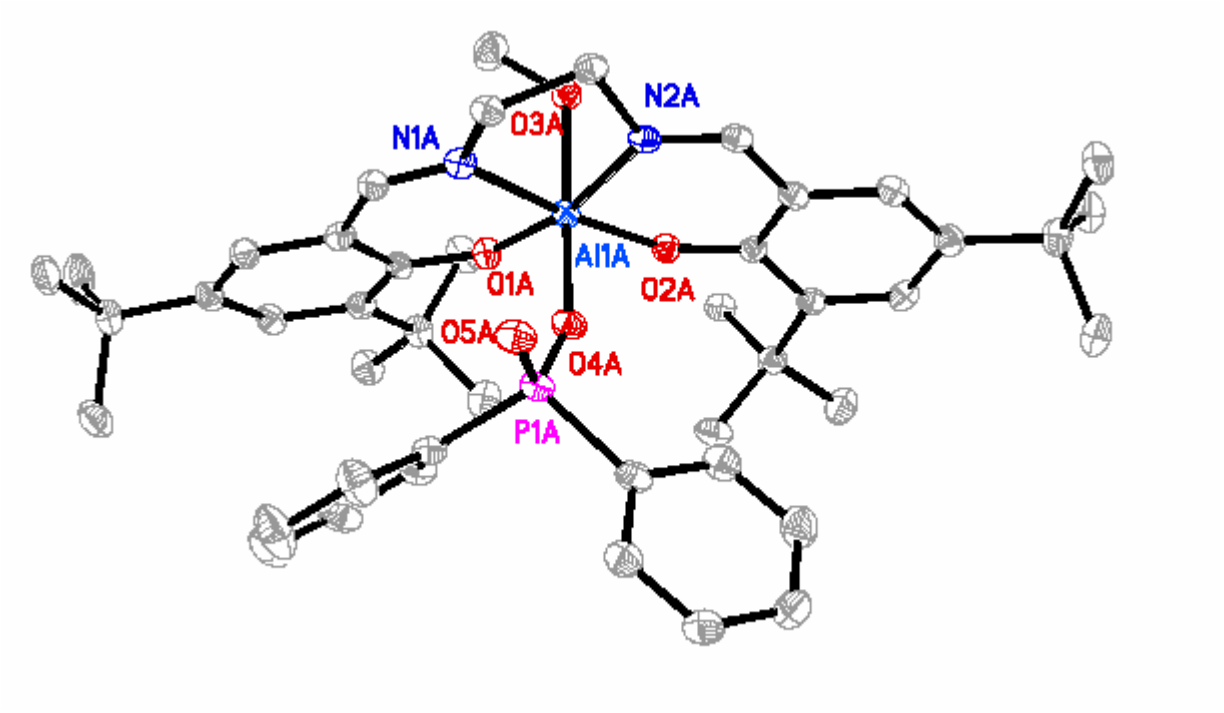

Figure 5.7. Crystal structure of **23•MeOH**.

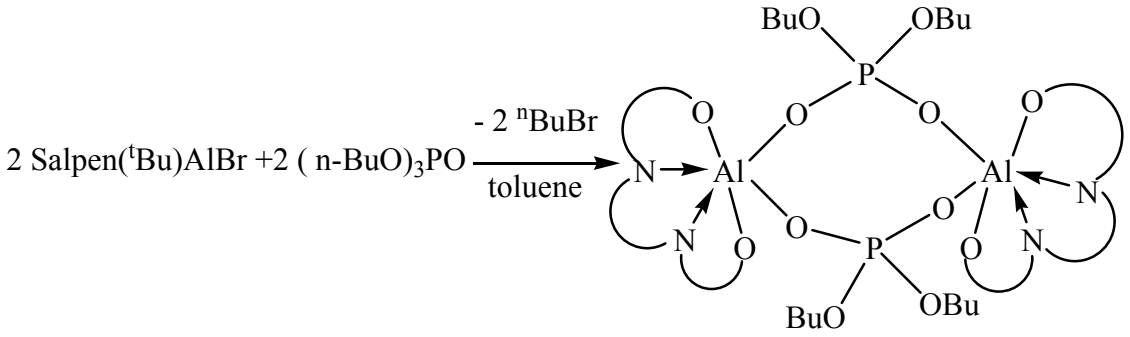

Figure 5.8. Synthesis of compound **24**.

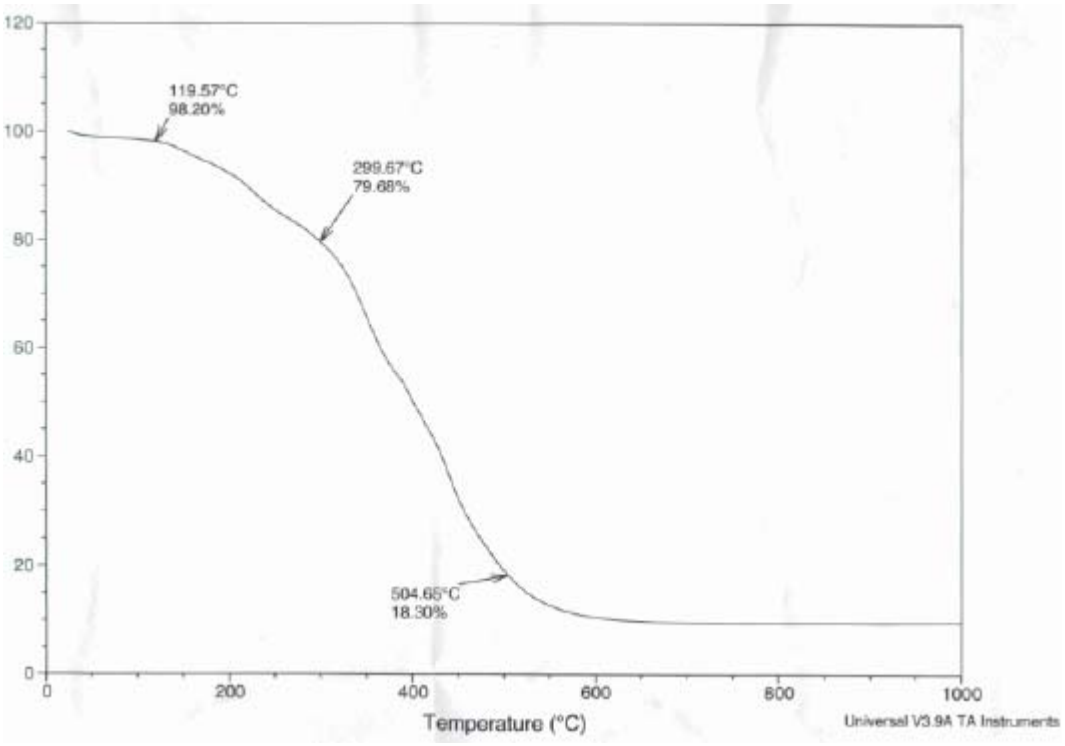

Figure 5.9. TGA of compound **24**.

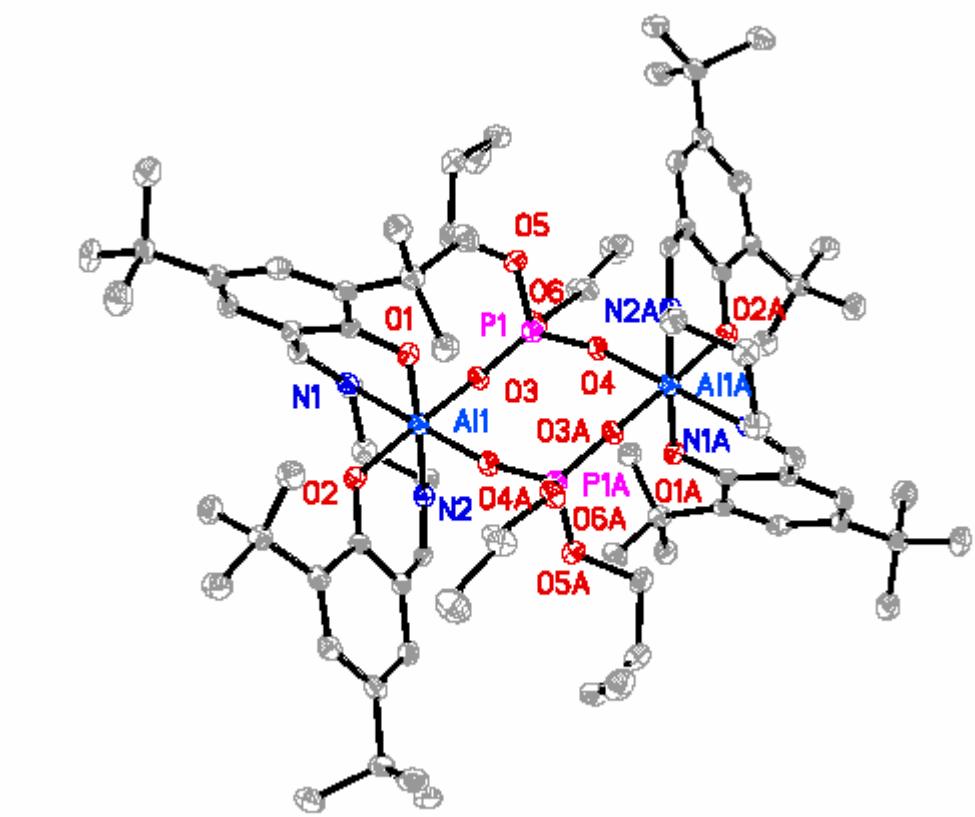

Figure 5.10. Molecular structure of **24**.

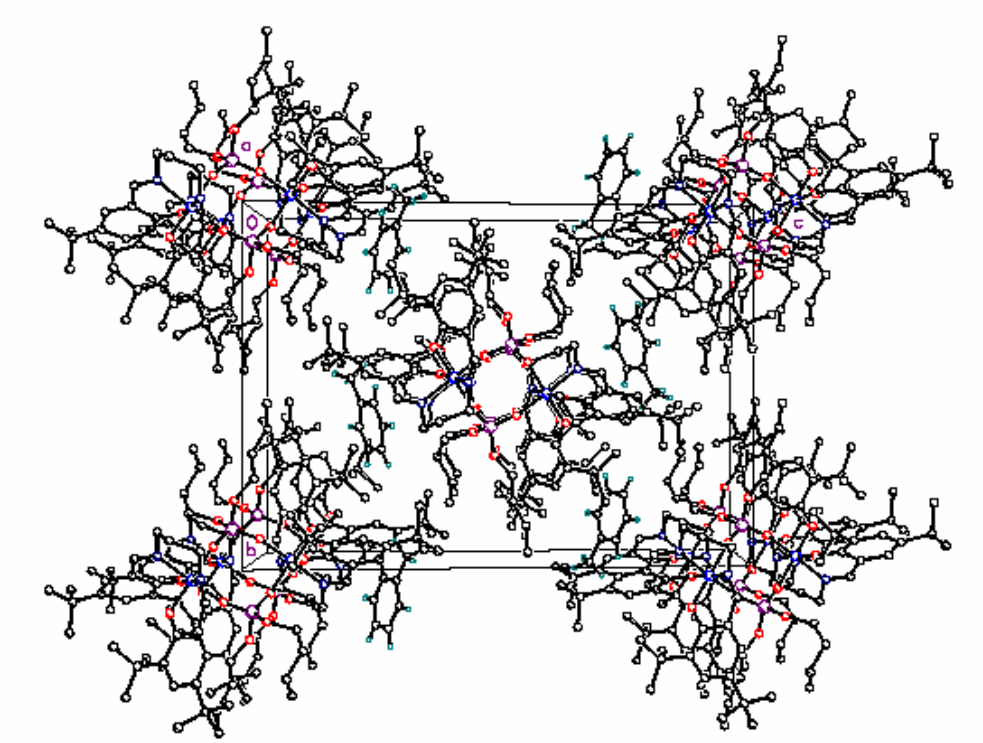

Figure 5.11. Packing diagram of **24** viewed down the *a*-axis.

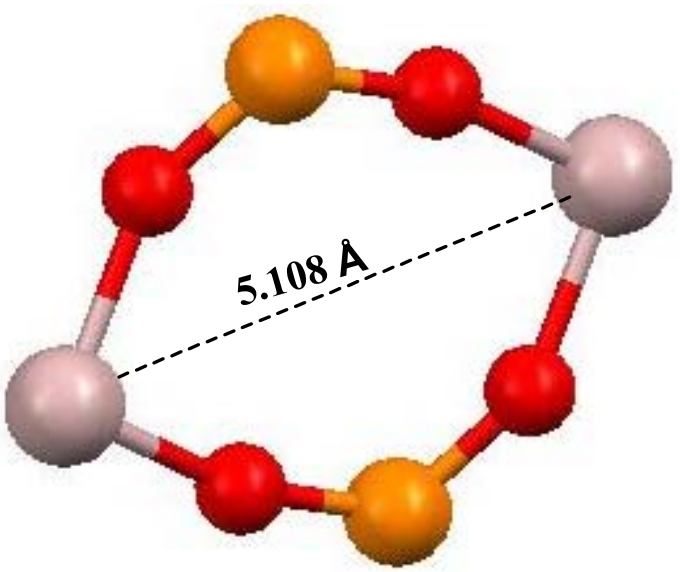

Figure 5.12. Al-O-P ring showing the Al-Al distance.

CHAPTER 6

Conclusion and Future Research

In this dissertation research two group 13 systems, mononuclear boron Schiff base halide compounds based on salicylidenimine ligands, and mononuclear aluminum bromide compounds based on Salen ligands, have been investigated for the dealkylation of organophosphate esters. Some of the mononuclear boron compounds showed very good dealkylation activity. One of the dealkylated products from a phosphate monoester (*t*-butyl diphenylphosphinate) was characterized both spectroscopically and structurally. The Salen aluminum bromide compounds prepared could form cations easily with the weak bases, triphenylphosphine oxide and triphenylphosphate. These compounds were also found to be very active for the dealkylation of a series of phosphates. The good activity of both mononuclear boron and aluminum Schiff base compounds shows that a binuclear chelate compound is not necessary for the dealkylation of phosphate esters. However, the mononuclear boron compounds were prone to hydrolysis and thus comparatively more difficult to synthesize compared to the binuclear compounds. Both mono- and binuclear compounds had to be prepared in a two-step process through the borate precursor from the ligand. On the other hand the synthesis of mononuclear Salen aluminum compounds was a one-step process. These compounds are stable to hydrolysis in sealed containers and can be handled in air for short periods of time. The dealkylated product from both mononuclear boron and mononuclear aluminum systems remain soluble which makes them more suitable for spectroscopic and structural characterization compared to the binuclear system for which the end product is insoluble. The mononuclear Salen aluminum system having the advantage of producing soluble end

product and being fairly stable seems to be the most suitable system for further study. Although no fully dealkylated product from the phosphate triester $P(O)(OR)_3$ could be isolated and characterized, two dealkylated products from the phosphinates, $Ph_2P(O)O^tBu$ in case of mononuclear boron and $Ph_2P(O)OMe$ in case of Salen aluminum compounds, were fully characterized. Their structures represent rare examples of monomeric chelated compounds with terminal phosphinate groups. In another attempt, an aluminophosphate ring compound containing six-coordinate aluminum atoms was synthesized which indicates that dealkylation could be a useful tool to prepare soluble models for aluminophosphate materials.

Although the Schiff base boron and aluminum compounds described in this dissertation dealkylate organophosphates effectively in non-nucleophilic solvents, they might not be very effective in strong donor solvents like methanol or water. The solvent will be a stronger nucleophile compared to the phosphate and thus block the coordinating site of boron or aluminum. One potential way around this problem could be to carry out the reactions in ionic liquids that will be non-coordinating and also help dissolve the boron or aluminum Schiff base halides, which are poorly soluble in water.

Attempts have been made to examine the applicability of Salen(^{t}Bu)AlBr as a catalyst for the reaction between trimethyl phosphate and boron tribromide. It appears that Salen(^{t}Bu)AlBr combines with boron tribromide to form a more active partially cationic species. This partially cationic species seemed to regenerate in the system. However, a detailed mechanistic study and isolation of the catalytic species would be required for any confirmation of the catalytic cycle.

The studies described in this dissertation could be the groundwork on which more expanded studies could be carried out in the future. Future work should be directed towards the isolation and characterization of fully dealkylated products from the phosphate triesters. Also kinetic studies should be undertaken which will help determine the optimum reaction conditions for the system. However, it should be noted that the possible applications of this dealkylation, the destruction of nerve gas agents and pesticides, need to be conducted in water. Thus, the creation of a water stable dealkylation system needs to be achieved before embarking on a detailed mechanistic study. The dealkylation study could be expanded to develop other similar systems which could also prove to be useful for phosphate dealkylation. For example, Salen aluminum iodide could be more useful than the bromide since Al-I bond is weaker than Al-Br bond. Considering the easier removal of bromide compared to chloride by a nucleophile, Salen aluminum bromides have the potential to be better application prospect compared to the widely used Salen aluminum chloride compounds in various Lewis acidic applications.

Beside potential application in nerve agents and pesticide decontamination the dealkylation reaction using boron and aluminum compounds could be used for various organic syntheses. One example is in oligonucleotide synthesis where the phosphate protecting group has to be removed in the last step by breaking a C-O bond. Also, chiral Salen aluminum bromide could be prepared and used for various enantioselective syntheses in which chiral Salen aluminum chlorides are already in use. Some other useful applications might be in ring opening polymerization of oxiranes and cyclic carbonates, and ether cleavage.

Appendix I: Crystal Packing Diagrams

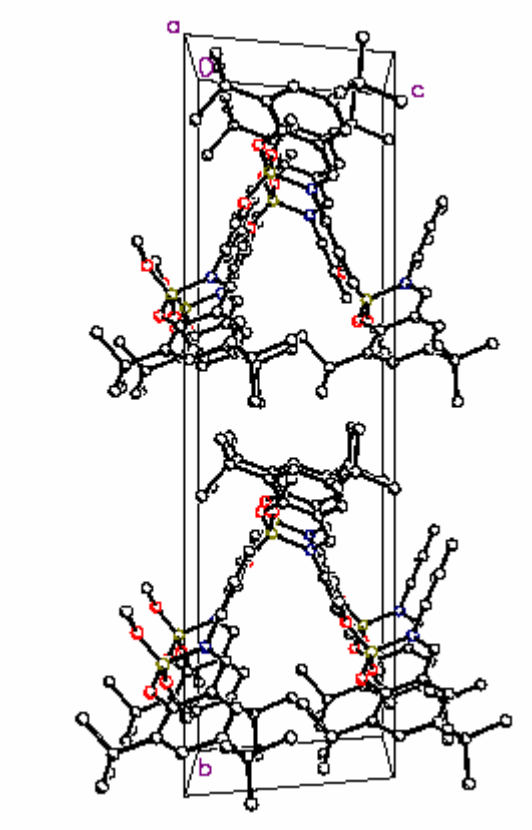

Figure A1. Crystal packing diagram of compound **5** viewed down the *a* axis.

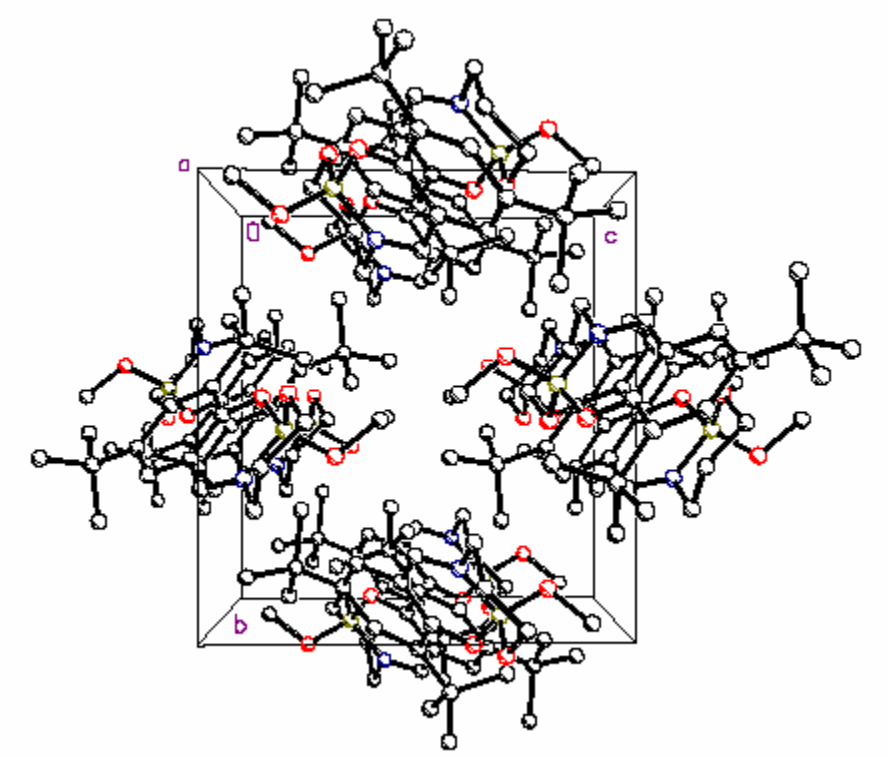

Figure A2. Crystal packing diagram of compound **6** viewed down the *a* axis.

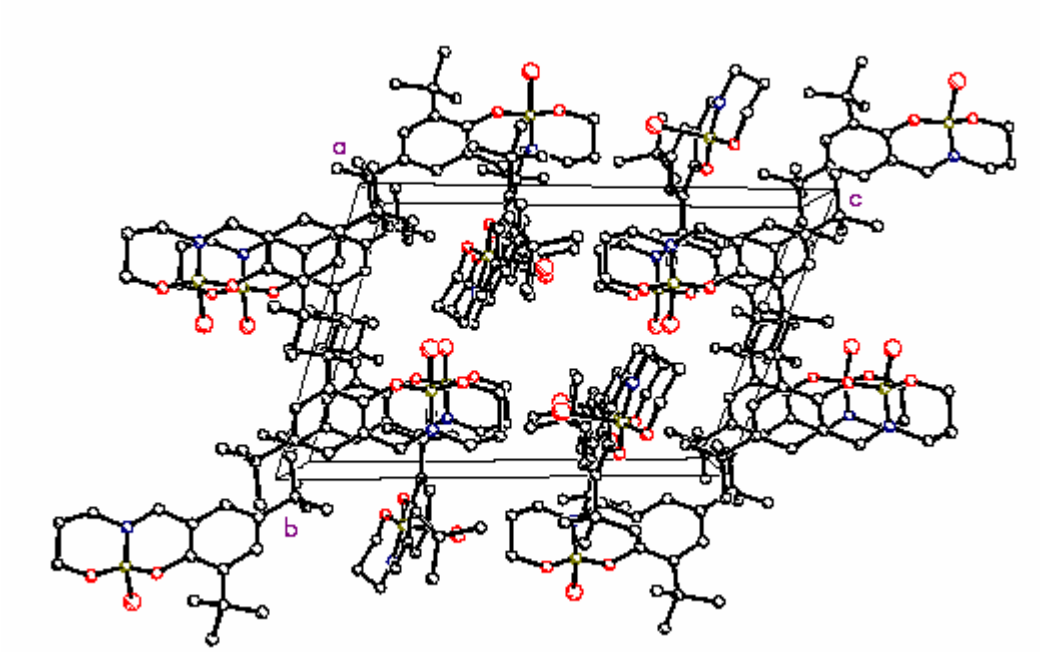

Figure A3. Crystal packing diagram of compound **11** viewed down the *a* axis.

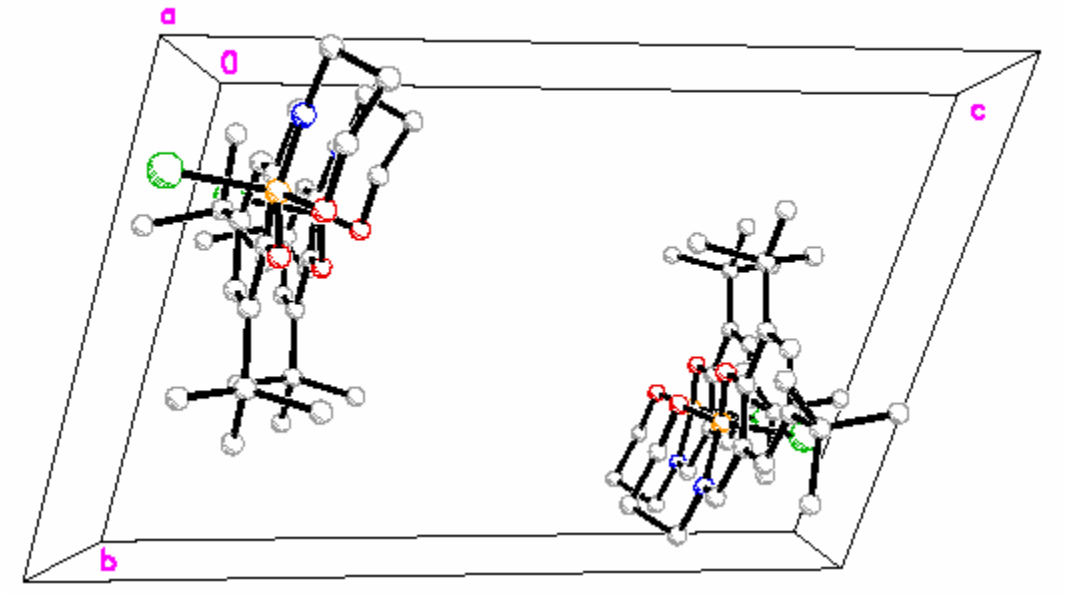

Figure A4. Crystal packing diagram of compound **12** viewed down the *a* axis.

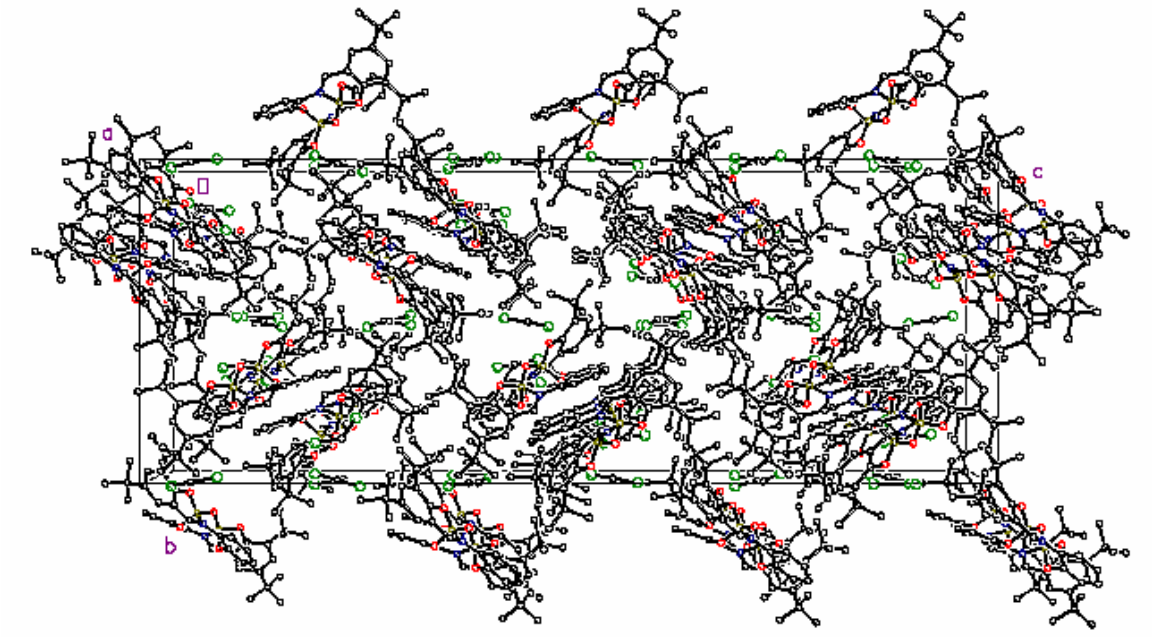

Figure A5. Crystal packing diagram of compound **13** viewed down the *a* axis.

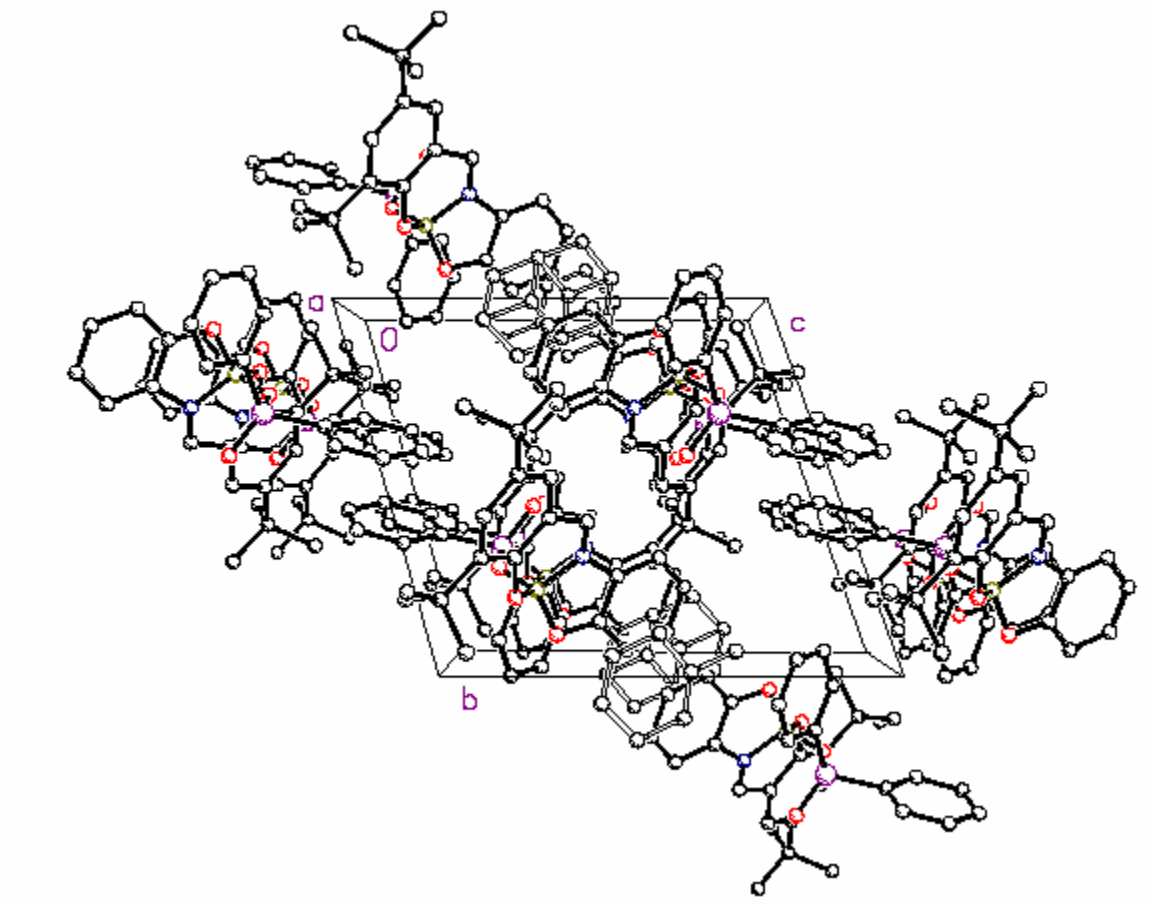

Figure A6. Crystal packing diagram of compound **14** viewed down the *a* axis.

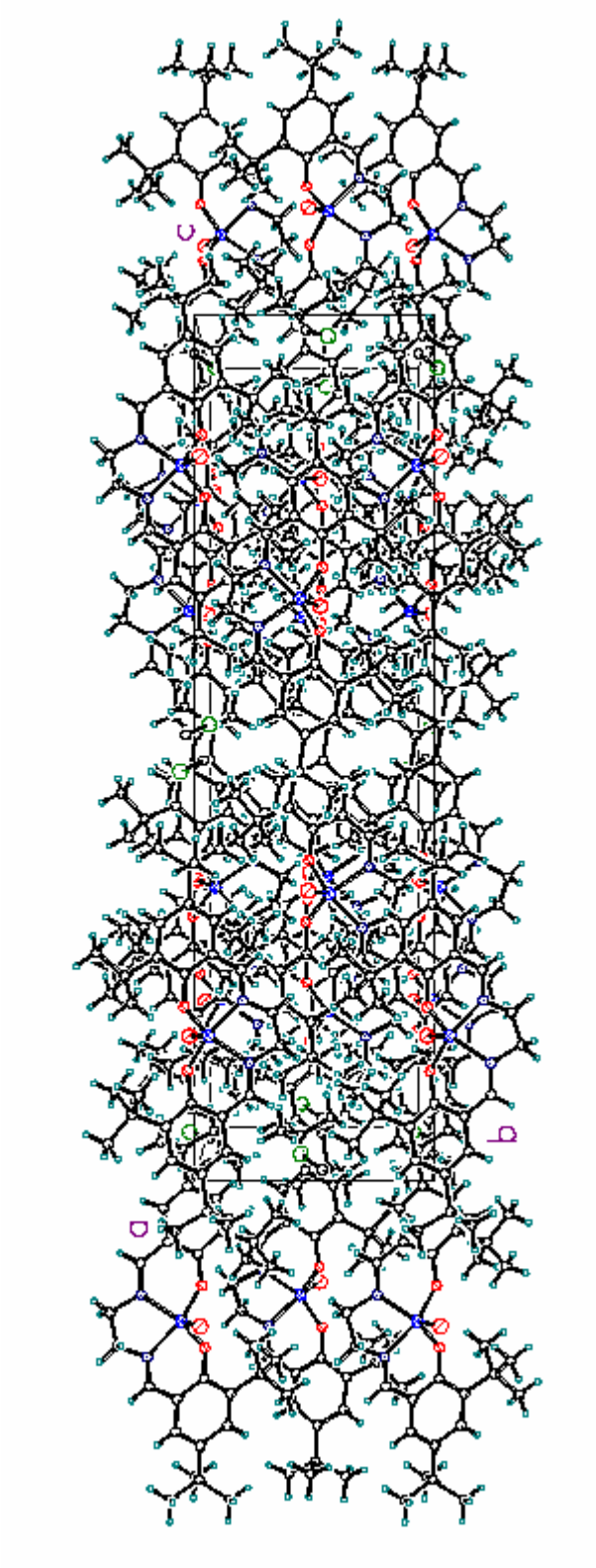

Figure A7. Crystal packing diagram of compound **15** viewed down the *a* axis.

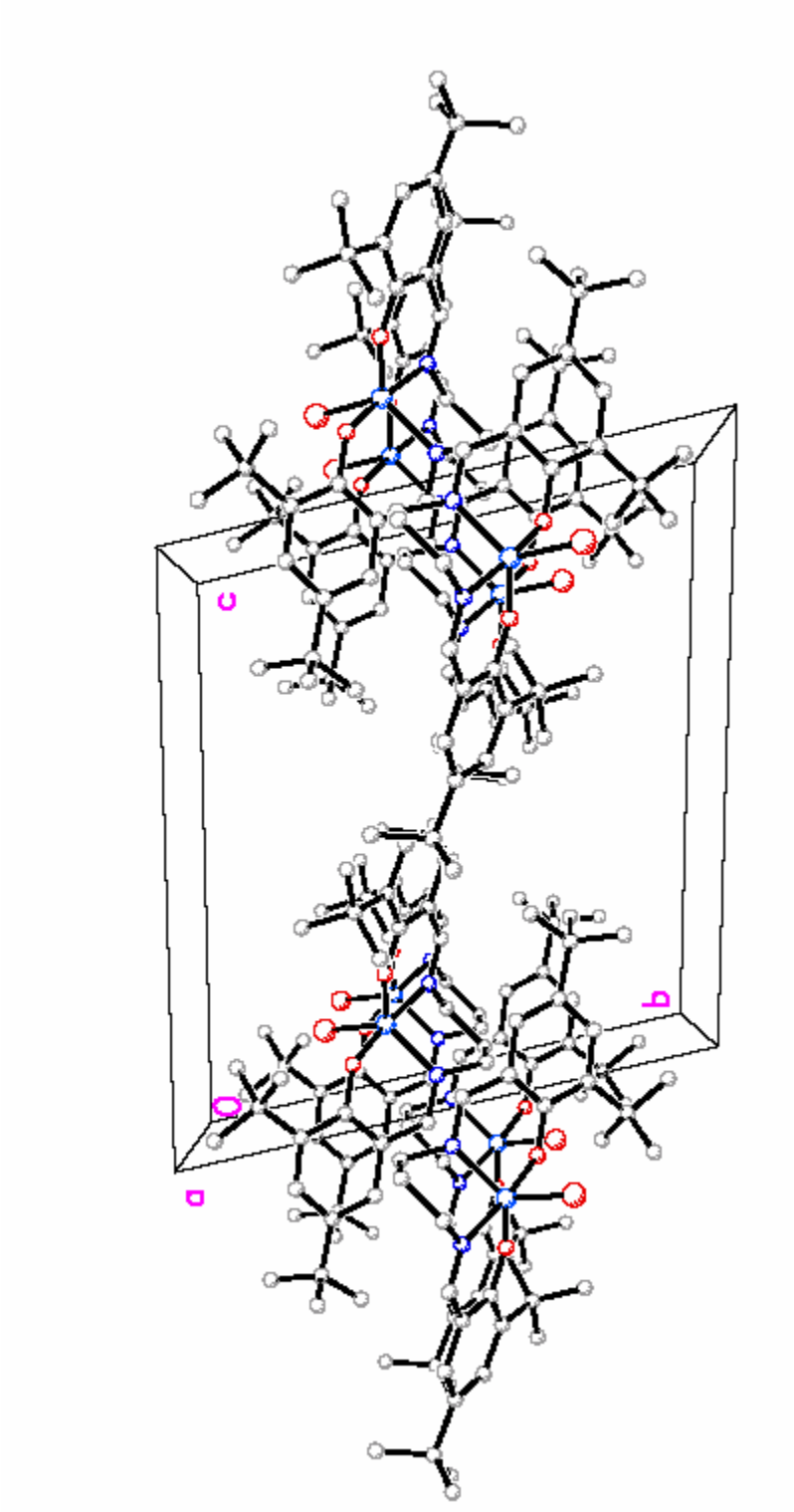

Figure A8. Crystal packing diagram of compound **16** viewed down the *a* axis.

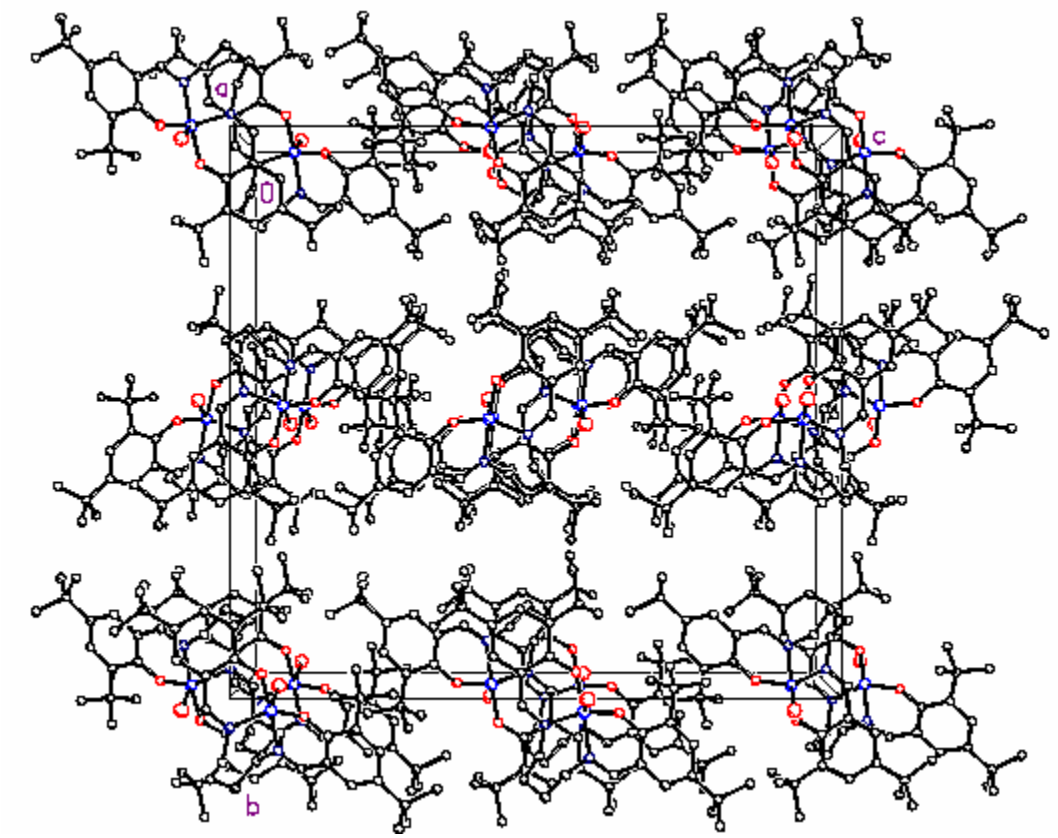

Figure A9. Crystal packing diagram of compound **17** viewed down the *a* axis.

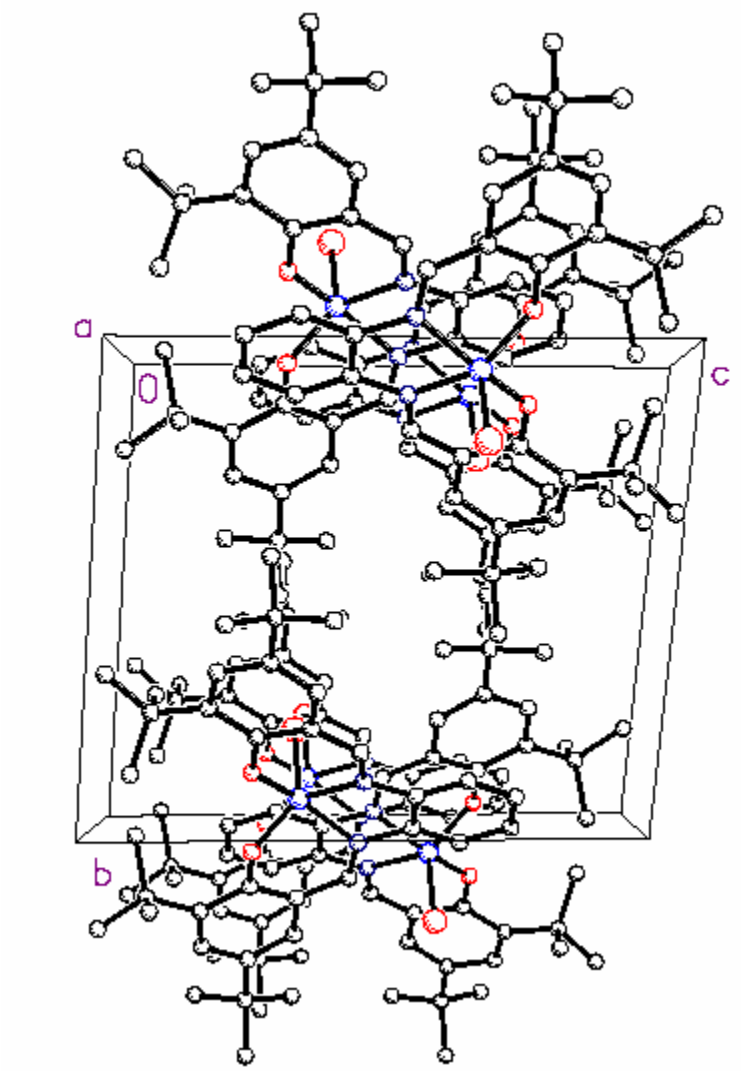

Figure A10. Crystal packing diagram of compound **18** viewed down the a axis.

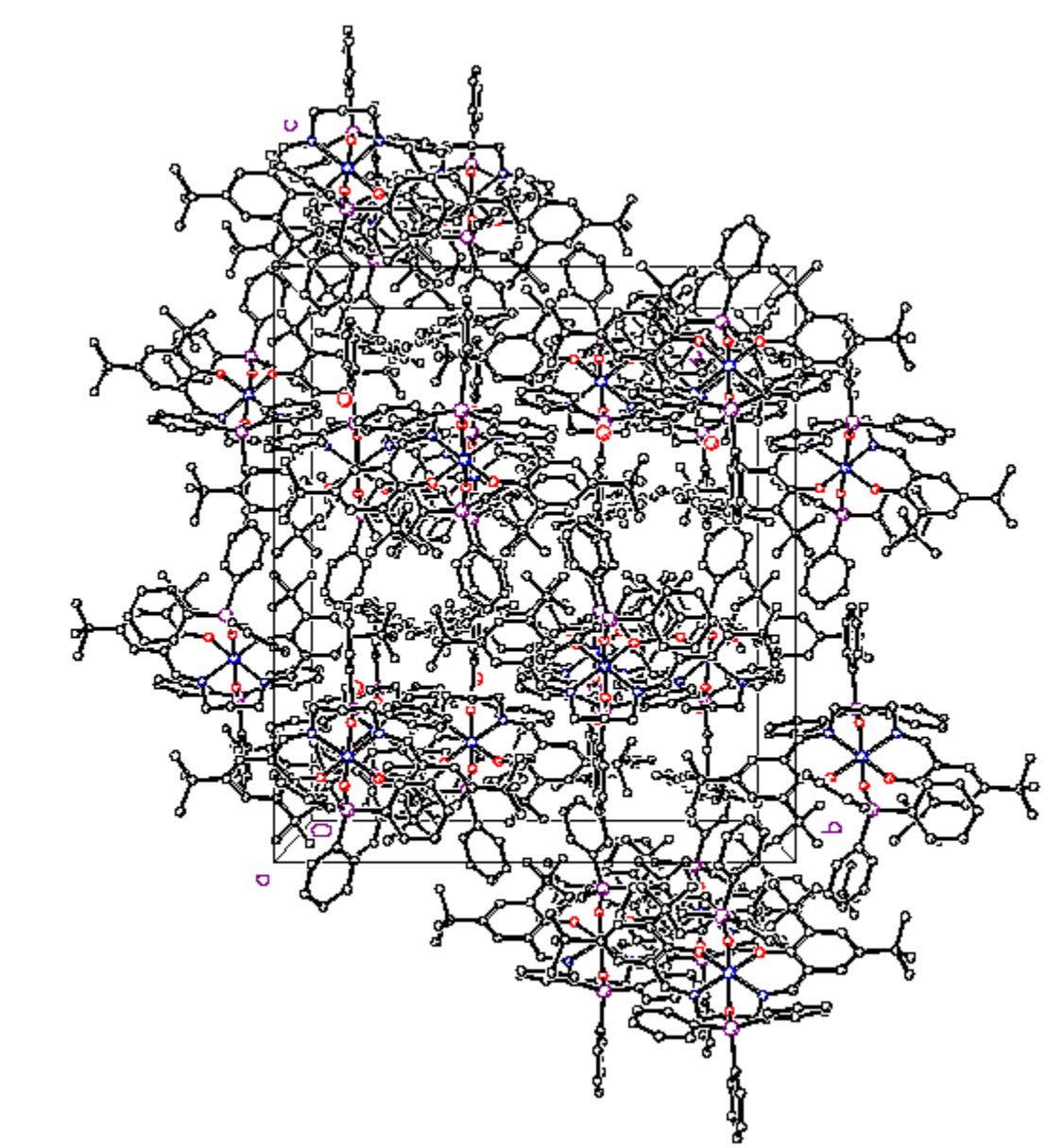

Figure A11. Crystal packing diagram of compound **20** viewed down the *a* axis.

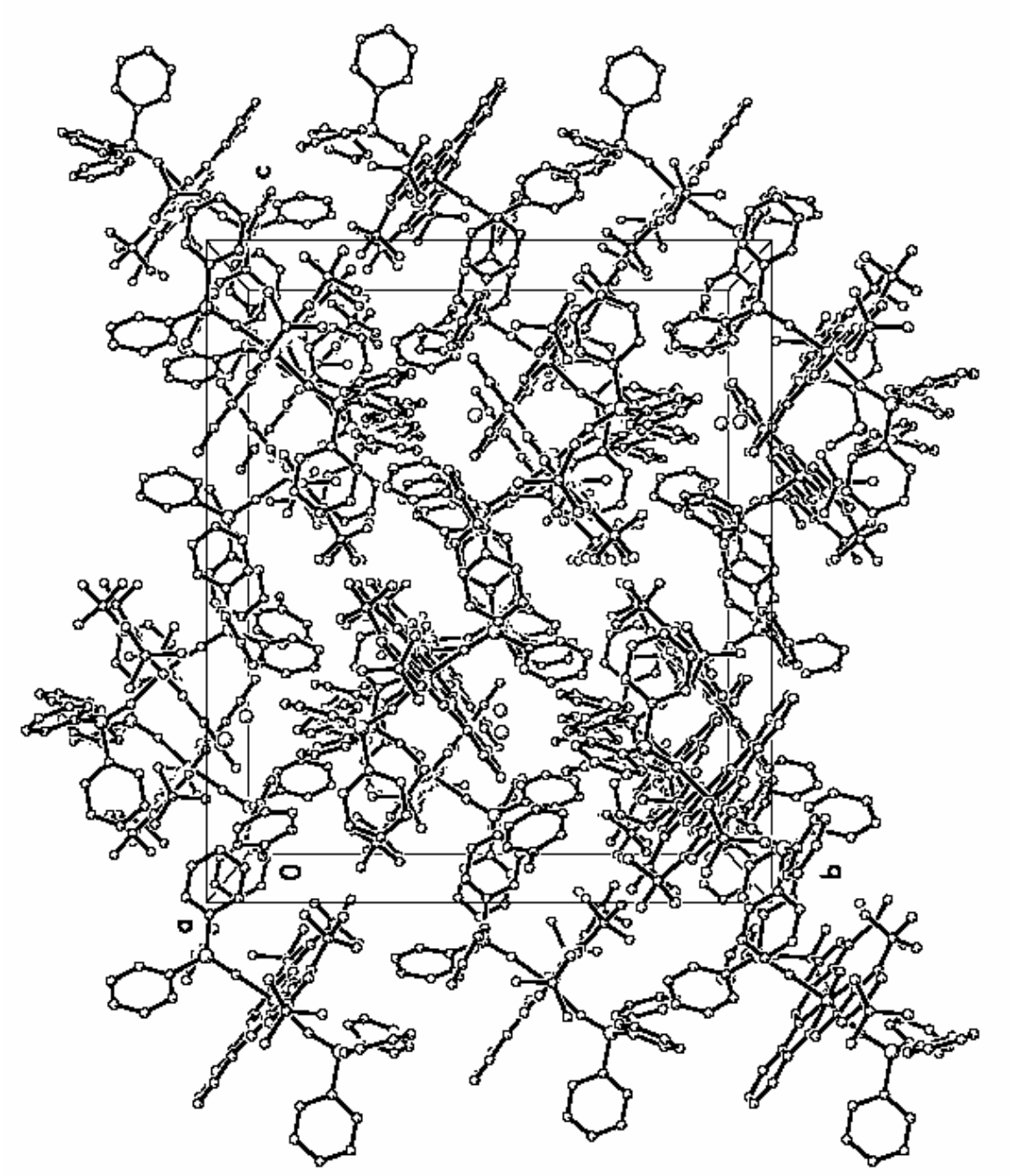

Figure A12. Crystal packing diagram of compound **21** viewed down the a axis.

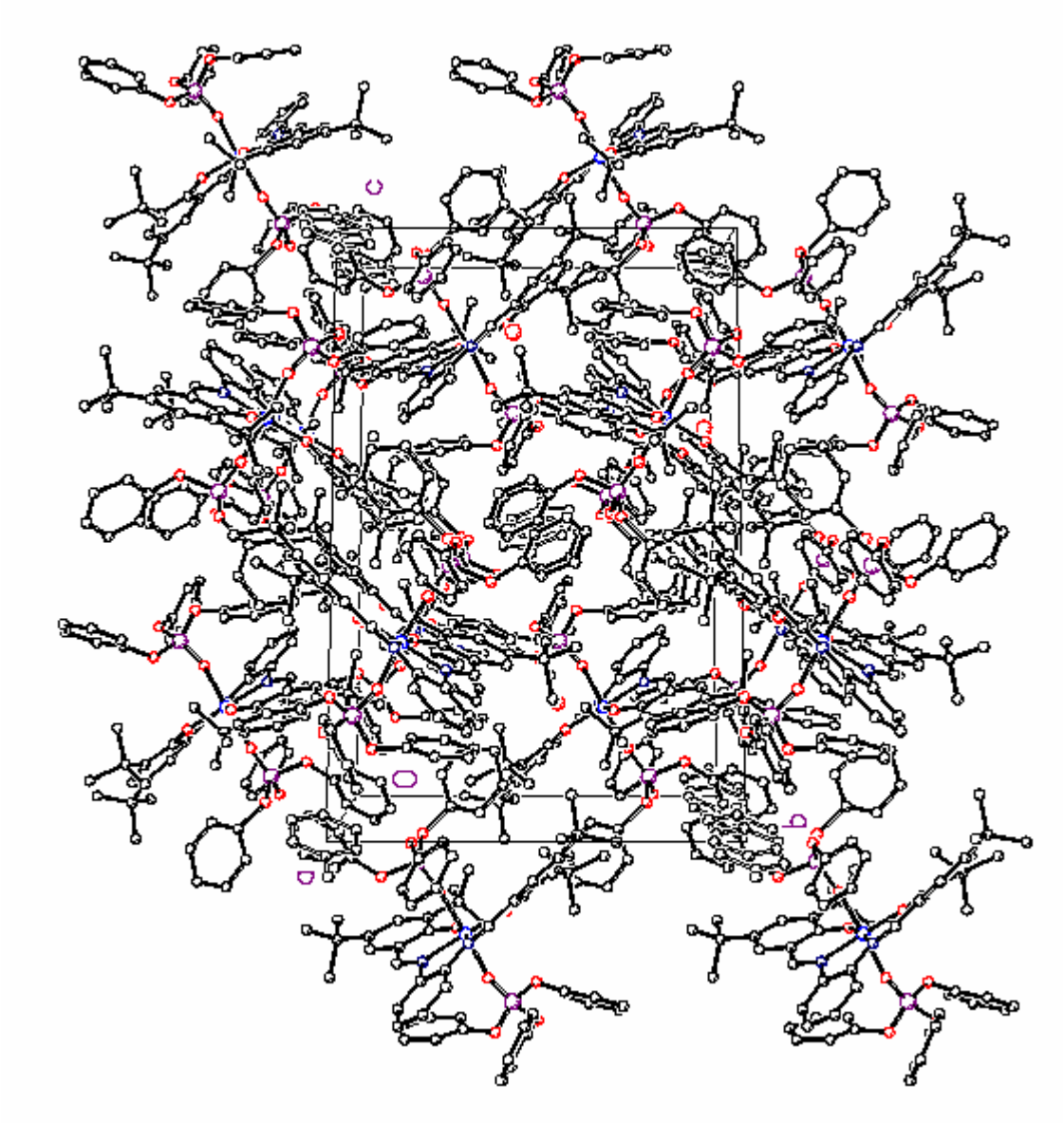

Figure A13. Crystal packing diagram of compound **22** viewed down the *a* axis

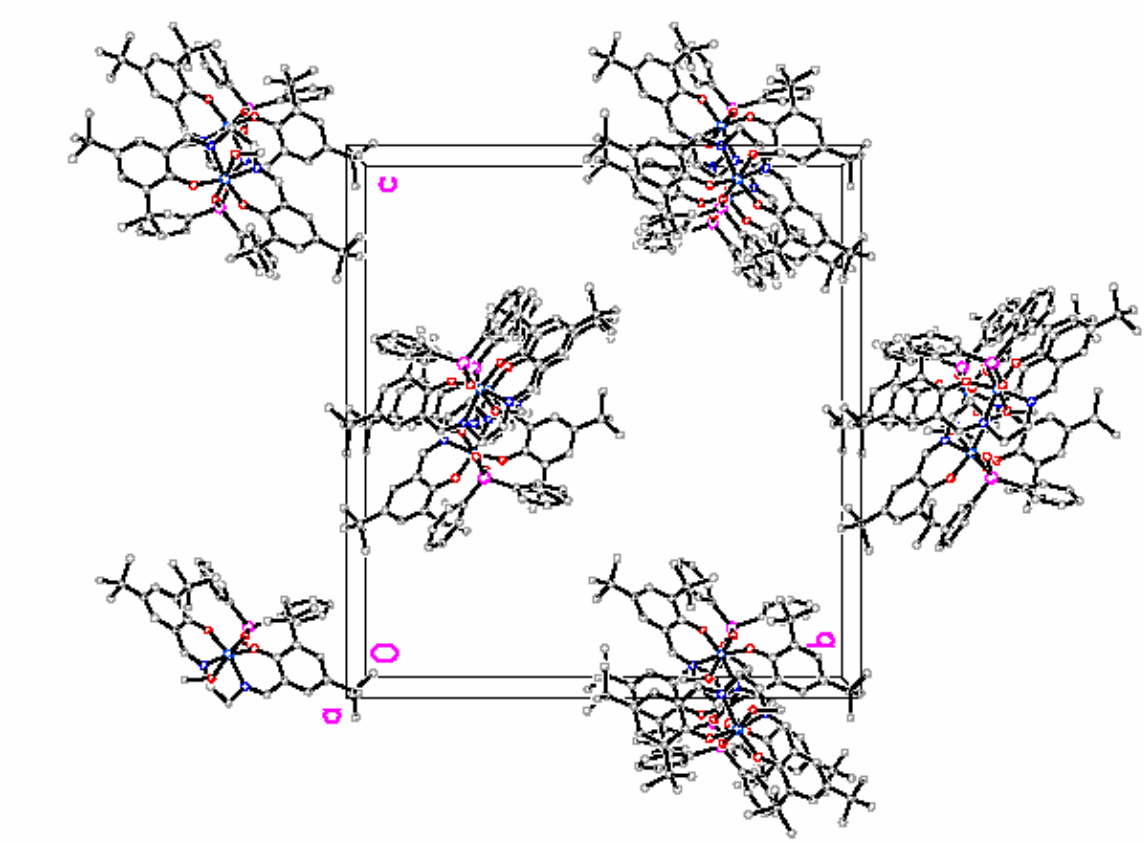

Figure A14. Crystal packing diagram of compound **23.MeOH** viewed down the *a* axis

Appendix II: List of Symbols and Abbreviations

General:

Å	angstrom, 10^{-10} m
Ac	acetate
ATP	adenosine triphosphate
^{n}Bu	*normal*- butyl, $CH_2(CH_2)_2CH_3$
^{t}Bu	*tertiary*-butyl, $C(CH_3)_3$
Calcd	calculated
Cy	cyclohexyl
D	bond dissociation energy
Dec	decomposed
EI	Electron Impact
Et	Ethyl, CH_2CH_3
g	grams
GOF	goodness of fit
h	hours
HMPA	hexamethylphosphoramide
Hz	hertz, s^{-1}
K	Kelvin
M	molar
M^+	molecular ion
Me	methyl, CH_3
mg	milligrams
min	minutes
mL	milliliters
mmol	millimoles
mp	melting point
Ph	phenyl

^{n}Pent	*normal* pentyl, $CH_2(CH_2)_3CH_3$
ppm	parts per million
^{i}Pr	isopropyl, $CH(CH_3)_2$
R	R - factor
R_w	weighted R - factor
s	seconds
Salen	common name for the entire ligand class.
t	time
T	temperature
THF	tetrahydrofuran
^{p}tolyl	*para*- tolyl

For nuclear magnetic resonance spectra:

δ	chemical shift (in parts per million)
d	doublet
m	multiplet
NMR	nuclear magnetic resonance
s	singlet
$w_{1/2}$	width at half height

For infrared spectra:

br	broad
cm^{-1}	wavenumbers
FT IR	Fourier Transform Infrared Spectra
m	medium
s	strong
ν	vibrational frequency (cm^{-1})
w	weak

References

1. Friedel, C.; Crafts, J. M., *Compt. Rend.* **1877,** 84, 1450.
2. Ziegler, K. H., E.; Breil, H.; Martin, H, *Angew. Chem.* **1955,** 67, 541-7.
3. Robinson, G. H., *Coordination Chemistry of Aluminum.* VCH: New York, 1993.
4. Cotton, F. A.; Wilkinson, G.; Bochmann, M.; Murillo, C., *Advanced Inorganic Chemistry, 6th Edition*. 6th ed.; Wiley, New York, N. Y.: 1998; p 27-29.
5. Martell, A. E.; Hancock, R. D.; Motekaitis, R. J., *Coord. Chem. Rev.* **1994,** 133, 39-65.
6. Taylor, M. J., Aluminum and Gallium In *Comprehensive Coordination Chemistry*, Wilkinson, G., Ed. Pergamon Press: 1987; Vol. 3, pp 105-152.
7. Schiff, H., *Ann.* **1864,** Suppl. 3, 343.
8. Ettling, C., *Ann.* **1840,** 35, 241.
9. Holm, R. H.; Everett, G. W., Jr.; Chakravorty, A., *Prog. Inorg. Chem* **1966,** 7, 83-214.
10. Atwood, D. A.; Harvey, M. J., *Chem. Rev* **2001,** 101, 37-52.
11. Hall, D.; Moore, F. H., *Proc. Chem. Soc.* **1960**, 256.
12. O'Connor, M. J.; West, B. O., *Aust. J. Chem.* **1967,** 20.
13. Singer, A. L.; Atwood, D. A., *Inorg. Chim. Acta* **1998,** 277.
14. Sano, T.; Nishio, Y.; Hamada, Y.; Takahashi, H.; Usuki, T.; Shibata, K., *J. Mater. Chem.* **2000,** 10, 157.

15. Ball, S. C.; Cragg-Hine, I.; Davidson, M. G.; Davies, R. P.; Lopez-Solera, M. I.; Raithby, P. R.; Reed, D.; Snaith, R.; Vogl, E. M., *J. Chem. Soc. Chem. Commun.* **1995**, 2147-9.

16. Kerr, J. A.; Stocker, D., W., In *CRC Handbook of Chemsitry and Physics*, 81st ed.; Lide, D. R., Ed. CRC Press: Boca Raton , Florida, 2000-2001.

17. Munoz-Hernandez, M.-A.; McKee, M. L.; Keizer, T. S.; Yearwood, B. C.; Atwood, D. A., *J. Chem. Soc., Dalton Trans.* **2002,** 3, 410-414.

18. Jegier, J. A.; Munoz-Hernandez, M.-A.; Atwood, D. A., *J. Chem. Soc., Dalton Trans.* **1999,** 15, 2583-2587.

19. Atwood, D. A.; Jegier, J. A.; Rutherford, D., *J. Am. Chem. Soc.* **1995,** 117, 6779-80.

20. Atwood, D. A., *Coord. Chem. Rev.* **1998,** 176, 407-430.

21. Munoz-Hernandez, M.-A.; Parkin, S.; Yearwood, B.; Wei, P.; Atwood, D. A., *J. Chem. Cryst* **2000,** 30, 215-218.

22. Liu, S.; Munoz-Hernandez, M.-A.; Atwood, D. A., *J. Organomet. Chem.* **2000,** 596, 109-114.

23. Wei, P.; Atwood, D. A., *Inorg. Chem.* **1998,** 37, 4934-4938.

24. Simpura, I.; Nevalainen, V., *Tetrahedron* **2003,** 59, 7535-7546.

25. Thormeier, S.; Carboni, B.; Kaufmann, D. E., *J. Organomet. Chem.* **2002,** 657, 136-145.

26. Ryu, D. H.; Zhou, G.; Corey, E. J., *J. Am. Chem. Soc.* **2004,** 126, 4800-4802.

27. Sprott, K. T.; Corey, E. J., *Org. Lett.* **2003,** 5, 2465-2467.

28. Ryu, D. H.; Lee, T. W.; Corey, E. J., *J. Am. Chem. Soc.* **2002,** 124, 9992-9993.

29. Hayashi, Y.; Rohde, J. J.; Corey, E. J., *J. Am. Chem. Soc.* **1996,** 118, 5502-5503.

30. Ketter, A.; Glahsl, G.; Herrmann, R., *J. Chem. Res.* **1990**, 278-9.

31. Ovitt, T. M.; Coates, G. W., *J. Am. Chem. Soc.* **1999,** 121, 4072-4073.

32. Radano, C. P.; Baker, G. L.; Smith, M. R., III., *J. Am. Chem. Soc.* **2000,** 122, 1552-1553.

33. Keizer, T. S.; De Pue, L. J.; Parkin, S.; Atwood, D. A., *J. Organomet. Chem.* **2003,** 666, 103-109.

34. Keizer, T. S.; De Pue, L. J.; Parkin, S.; Atwood, D. A., *Can. J. Chem.* **2002,** 80, 1463-1468.

35. Keizer, T. S.; De Pue, L. J.; Parkin, S.; Atwood, D. A., *J. Am. Chem. Soc.* **2002,** 124, 1864-1865.

36. Corbridge, D. E. C., *Phosphorus: An Outline of its Chemistry, Biochemistry and Technology*. 5th ed.; Elsevier: Amsterdam, Netherlands, 1995; Vol. 6, p 51-53.

37. Quinn, L. D., In *A Guide to Organophosphorus Chemistry*, Wiley Interscience: 2000; p 153.

38. Corbridge, D. E. C., *Phosphorus: An Outline of its Chemistry, Biochemistry and Technology*. 5th ed.; Elsevier: Amsterdam, Netherlands, 1995; Vol. 6, p 501.

39. Lassaigne, F., *Justus Liebigs Ann. Chiim* **1820,** 3, 294.

40. Westheimer, F. H., *Science* **1987,** 235, 1173-8.

41. Chambers, J. E.; Oppenheimer, S. F., *Toxicol. Sci.* **2004,** 77, 185-187.

42. Chambers, J. E.; Levi, P. E., *Organophosphates, Chemistry, Fate, and Effects.* 6th ed.; Academic Press: San Diego, 1992.

43. Burgen, A. S. V., *Br. J. Pharmacol.* **1949,** 4, 219-28.

44. Walker, B., Jr. ; Nidiry, J., *Inhal.Toxicol.* **2002,** 14, 975-990.

45. Yang, Y. C.; Baker, J. A.; Ward, J. R., *Chem. Rev* **1992,** 92, 1729-43.

46. Yang, Y.-C., *Acc. Chem. Res.* **1999,** 32, 109-115.

47. Wagner-Jauregg, T.; Hackley, B. E., Jr.; Lies, T. A.; Owens, O. O.; Proper, R., *J. Am. Chem. Soc.* **1955,** 77, 922-929.

48. Ward, J. R.; Hovanec, J. W.; Albizo, J. M.; Szafraniec, L. L.; Beaudry, W. T., *J. Fluorine Chem.* **1991,** 51, 277-82.

49. Gustafson, R. L.; Chaberek, S. J.; Martell, A. E., *J. Am. Chem. Soc.* **1963,** 67, 576-582.

50. Sethunathan, N.; Yoshida, T., *Can. J. Microbiol.* **1973,** 19, 873-875.

51. Racke, K. D.; Coats, J. R., *J. Agric. Food Chem.* **1987,** 35, 94-99.

52. Siddaramappa, R.; Rajaram, K. P.; Sethunathan, N., *Appl. Microbiol.* **1973,** 26, 846-847.

53. Harper, L. L.; McDaniel, C. S.; Miller, C. E.; Wild, J. R., *Appl. Environ. Microbiol.* **1988,** 54, 2586-89.

54. DeFrank, J. J., Organophosphorus cholinesterase inhibitors: detoxification by microbial enzymes. In *Applications of Enzymes Biochemistry*, 9th ed.; Kelly, J. W.; Baldwin, T. O., Eds. Plenum Press: New York, 1991; pp 165-180.

55. Kolakowski, J. E.; Defrank, J. J.; Harvey, S. P.; Szafraniec, L. L.; Beaudry, W. T.; Lai, K. W., James R., *Biocatal. Biotransform.* **1997,** 15, 297-312.

56. Thatcher, G. R. J.; Kluger, R., *Adv. Phys. Org. Chem.* **1989,** 25, 99.

57. Florian, J.; Warshel, A., *J. Phys. Chem. B* **1998,** 102, 719-734.

58. Futatsugi, N.; Hata, M.; Hoshino, T.; Tsuda, M., *Biophys. J.* **1999,** 77, 3287-3292.

59. Bianciotto, M.; Barthelat, J.-C.; Vigroux, A., *J. Am. Chem. Soc.* **2002,** 124, 7573-7587.

60. Cavalli, A.; Carloni, P., *J. Am. Chem. Soc.* **2002,** 124, 3763-3768.

61. Aqvist, J.; Kolmodin, K.; Florian, J., *Chem. Biol.* **1999,** 6, R71-80.

62. Admiraal, S. J.; Herschlag, D., *Chem. Biol.* **1995,** 2, 729-39.

63. Maegley, K. A.; Admiraal, S. J.; Herschlag, D., *Proc. Natl. Acad, Sci. USA* **1996,** 93, 8160-8166.

64. Straeter, N.; Lipscomb, W. N.; Klabunde, T.; Krebs, B., *Angew. Chem. Int. Ed. Engl.* **1996,** 35, 2025-2055.

65. Wilcox, D. E., *Chem. Rev.* **1996,** 96, 2435-2458.

66. Chin, J., *Curr. Opin. Chem. Biol.* **1997,** 1, 514-521.

67. McComb, R. B.; Bowers, G. N., Jr.; Posen, S., *Alkaline Phosphatase*. Plenum Press: N. Y., 1979.

68. Coleman, J. E.; Gettins, P., *Metal Ions in Biology* **1983,** 5, 219-52.

69. Coleman, J. E.; Gettins, P., *Advances in Enzymology and Related Areas of Molecular Biology* **1983,** 55, 381-452.

70. Coleman, J. E., *Annu. Rev. Biophys. Biomol. Struct.* **1992,** 21, 441-83.

71. Bazzicalupi, C.; Bencini, A.; Berni, E.; Bianchi, A.; Fedi, V.; Fusi, V.; Giorgi, C.; Paoletti, P.; Valtancoli, B., *Inorg. Chem.* **1999,** 38, 4115-4122.

72. Applebury, M. L.; Johnson, B. P.; Coleman, J. E., *J. Biol. Chem.* **1970,** 245, 4968-76.

73. Wang, J.; Stieglitz, K. A.; Kantrowitz, E. R., *Biochem.* **2005,** 44, 8378-86.

74. Antanaitis, B. C., *Adv. Inorg. Biochem.* **1983,** 5, 111-36.

75. Doi, K.; Antanaitis, B. C.; Aisen, P., *Struct. Bonding* **1988,** 70, 1-26.

76. Que, L., Jr.; True, A. E., *Prog. Inorg. Chem* **1990,** 38, 97-200.

77. Vincent, J. B.; Olivier-Lilley, G. L., *Chem. Rev.* **1990,** 90, 1447-67.

78. Campbell, H. D.; Zerner, B., *Biochem. Biophys. Res. Commun.* **1973,** 54, 1498-503.

79. Chen, T. T.; Bazer, F. W.; Cetorelli, J. J.; Pollard, W. E.; Roberts, R. M., *J. Biol. Chem.* **1973,** 248, 8560-6.

80. Beck, J. L.; McConachie, L. A.; Summors, A. C.; Arnold, W. N.; De Jersey, J. Z., Burt., *Biochim. Biophys. Acta.* **1986,** 869, 61-8.

81. Fraser, M. J.; Low, R. L., Fungal and mitochondrial nucleases In *Nucleases*, 2nd ed.; Linn, S.; Lloyd, R. S.; Roberts, R. J., Eds. Cold Spring Harbor Laboratory Press: NY, 1993; pp 171-207.

82. Fujimoto, M.; Kuninaka, A.; Yoshino, H., *Agric. Biol. Chem.* **1975,** 39, 1991-7.

83. Potter, B. V. L.; Connolly, B. A.; Eckstein, F., *Biochemistry* **1983,** 22, 1369-77.

84. Ottolenghi, A. C., *Biochim. Biophys. Acta.* **1965,** 106, 510-18.

85. Little, C., *Methods Enzymol.* **1981,** 71, 725-730.

86. Hough, E.; Hansen, L. K.; Birknes, B.; Jynge, K.; Hansen, S.; Hordvik, A.; Little, C.; Dodson, E.; Derewenda, Z., *Nature* **1989,** 338, 357-60.

87. Little, C., *Acta Chem. Scand.* **1981,** B35, 39-44.

88. Little, C.; Aakre, S. E.; Rumsby, M. G.; Gwarsha, K., *Biochem. J.* **1982,** 203, 799-801.

89. Otnaess, A. B., *FEBS Lett.* **1980,** 114, 202-4.

90. Caldwell, S. R.; Raushel, F. M., *Appl. Biochem. Biotechnol.* **1991,** 31, 59-73.

91. Dumas, D. P.; Caldwell, S. R.; Wild, J. R.; Raushel, F. M., *J. Biol. Chem.* **1989,** 264, 19659-65.

92. Lai, K.; Stolowich, N. J.; Wild, J. R., *Arch. Biochem. Biophys.* **1995,** 318, 59-64.

93. Dumas, D. P.; Durst, H. D.; Landis, W. G.; Raushel, F. M.; Wild, J. R., *Arch. Biochem. Biophys.* **1990,** 277, 155-9.

94. Omburo, G. A.; Kuo, J. M.; Mullins, L. S.; Raushel, F. M., *J. Biol. Chem.* **1992,** 267, 13278-83.

95. Bashkin, J. K., *Curr. Opin. Chem. Biol.* **1999,** 3, 752-758.

96. Blasko, A.; Bruice, T. C., *Acc. Chem. Res.* **1999,** 32, 475-484.

97. Jones, D. R.; Lindoy, L. F.; Sargeson, A. M., *J. Am. Chem. Soc.* **1984,** 106, 7807-19.

98. Vance, D. H.; Czarnik, A. W., *J. Am. Chem. Soc.* **1993,** 115, 12165-6.

99. Kaminskaia, N. V.; He, C.; Lippard, S. J., *Inorg. Chem.* **2000,** 39, 3365-3373.

100. Yamami, M.; Furutachi, H.; Yokoyama, T.; Okawa, H., *Inorg. Chem.* **1998,** 37, 6832-6838.

101. Yamami, M.; Furutachi, H.; Yokoyama, T.; Okawa, H., *Chem. Lett.* **1998**, 211-212.

102. Chapman, W. H., Jr.; Breslow, R., *J. Am. Chem. Soc.* **1995,** 117, 5462-9.

103. Molenveld, P.; Kapsabelis, S.; Engbersen, J. F. J.; Reinhoudt, D. N., *J. Am. Chem. Soc.* **1997,** 119, 2948-2949.

104. McCue, K. P.; Morrow, J. R., *Inorg. Chem.* **1999,** 38, 6136-6142.

105. Scrimin, P.; Ghirlanda, G.; Tecilla, P.; Moss, R. A., *Langmuir* **1996,** 12, 6235-6241.

106. Gajda, T.; Duepre, Y.; Toeroek, I.; Harmer, J.; Schweiger, A. S., Juergen; ; Kuppert, D.; Hegetschweiler, K., *Inorg. Chem.* **2001,** 40, 4918-4927.

107. Morrow, J. R.; Buttrey, L. A.; Berback, K. A., *Inorg. Chem.* **1992,** 31, 16-20.

108. Morrow, J. R.; Amin, S.; Lake, C. H.; Churchill, M. R., *Inorg. Chem.* **1993,** 32, 4566-72.

109. Morrow, J. R.; Chin, K. O. A., *Inorg. Chem.* **1993,** 32, 3357-61.

110. Morrow, J. R.; Buttrey, L. A.; Shelton, V. M.; Berback, K. A., *J. Am. Chem. Soc.* **1992,** 114, 1903-5.

111. Amin, S.; Morrow, J. R.; Lake, C. H.; Churchill, M. R., *Angew. Chem. Int. Ed. Engl.* **1994,** 33, 773-5.

112. Schneider, H. J.; Rammo, J.; Hettich, R., *Angew. Chem. Int. Ed. Engl.* **1993,** 32, 1716-19.

113. Breslow, R.; Huang, D. L., *Proc. Natl. Acad, Sci. USA* **1991,** 88, 4080-3.

114. Takasaki, B. K.; Chin, J., *J. Am. Chem. Soc.* **1993,** 115, 9337-8.

115. Takasaki, B. K.; Chin, J., *J. Am. Chem. Soc.* **1995,** 117, 8582-5.

116. Bazzicalupi, C.; Bencini, A.; Bianchi, A.; Fusi, V.; Giorgi, C.; Paoletti, P.; Valtancoli, B.; Zanchi, D., *Inorg. Chem.* **1997,** 36, 2784-2790.

117. Modro, A. M.; Modro, T. A., *Can. J. Chem.* **1993,** 71, 469-72.

118. Mentz, M.; Modro, A. M.; Modro, T. A., *J. Chem. Soc. Chem. Commun.* **1994,** 1537-38.

119. Mentz, M.; Modro, A. M.; Modro, T. A., *Can. J. Chem.* **1994,** 72, 1933-36.

120. Takeuchi, Y.; Demachi, Y.; Yoshii, E., *Tet. Lett.* **1979**, 1231-32.

121. Morita, T.; Okamoto, Y.; Sakurai, H., *Bull. Chem. Soc. Jpn.* **1981,** 54, 267-73.

122. Borisov, S. N.; Voronkov, M. G.; Lukevics, E., *Organosilicon Derivatives of Phosphorus and Sulfur.* Plenum: New York, 1971; p 4.

123. Rabinowitz, R., *J. Org. Chem.* **1963,** 28, 2975-78.

124. Blackburn, G. M.; Ingleson, D., *J. Chem. Soc., Perkin Trans. 1* **1980**, 1150-153.

125. Morales-Rojas, H.; Moss, R. A., *Chem. Rev.* **2002,** 102, 2497-2521.

126. Hampl, F.; Mazac, J.; Liska, F.; Srogl, J.; Kabrt, L.; Suchanek, M., *Collect. Czech. Chem. Commun.* **1995,** 60, 883-893.

127. Simanenko, Y. S.; Karpichev, E. A.; Prokop'eva, T. M.; Lattes, A.; Popov, A. F.; Savelova, V. A.; Belousova, I. A., *Russ. J. Org. Chem.* **2004,** 40, 206--218.

128. Fanti, M.; Mancin, F.; Tecilla, P.; Tonellato, U., *Langmuir* **2000,** 16, 10115-10122.

129. Jaeger, D. A.; Bolikal, D., *J. Org. Chem.* **1985,** 50, 4635-4637.

130. Moss, R. A.; Swarup, S.; Hendrickson, T. F.; Hui, Y., *Tet. Lett.* **1984,** 25, 4079-82.

131. Moss, R. A.; Alwis, K. W.; Shin, J. S., *J. Am. Chem. Soc.* **1984,** 106, 2651-55.

132. Moss, R. A.; Ihara, Y., *J. Org. Chem.* **1983,** 48, 588-92.

133. Scrimin, P.; Tecilla, P.; Tonellato, U., *J. Org. Chem.* **1991,** 56, 161-166.

134. Chandrasekhar, V.; Deria, P.; Krishnan, V.; Athimoolam, A.; Singh, S.; Madhavaiah, C.; Srivatsan, S. G.; Verma, S., *Bioorg. Med. chem. Lett.* **2004,** 14, 1559-1562.

135. Manea, F.; Houillon, F. B.; Pasquato, L.; Scrimin, P., *Angew. Chem. Int. Ed. Engl.* **2004,** 43, 6165-6169.

136. Reutov, V. A.; Gukhman, E. V.; Kafitulova, E., *Russ. J. Gen. Chem.* **2003,** 73, 1441-1444.

137. Qian, B.; Baek, S. W.; Smith, M. R., III., *Polyhedron* **1999,** 18, 2405-2414.

138. Yamashita, M.; Kamura, K.; Yamamoto, Y.; Akiba, K.-Y., *Chem. Eur. J.* **2002,** 8, 2976-2979.

139. Miyazaki, Y.; Yoshimura, K.; Miura, Y.; Sakashita, H. I., Katsutoshi., *Polyhedron* **2003,** 22, 909-916.

140. Gonzalez, A.; Granell, J.; Piniella, J. F.; Alvarez-Larena, A., *Tetrahedron* **1998,** 54, 13313-13322.

141. Kliegel, W.; Metge, J.; Rettig, S. J.; Trotter, J., *Can. J. Chem.* **1998,** 76, 1082-1092.

142. Kliegel, W.; Metge, J.; Rettig, S. J.; Trotter, J., *Can. J. Chem.* **1998,** 76, 389-399.

143. Hopfl, H.; Hernandez, N. P.; Lima, S. R.; Santillan, R. F., Norberto., *Heteroatom Chem.* **1998,** 9, 359-368.

144. Hohaus, E., *Fresenius Z. Anal. Chem.* **1983,** 315, 696-9.

145. Atwood, D. A.; Jegier, J. A.; Remington, M. P.; Rutherford, D., *Aust. J. Chem.* **1996,** 49, 1333-1338.

146. Wei, P.; Atwood, D. A., *Inorg. Chem.* **1997,** 36, 4060-4065.

147. Wei, P.; Atwood, D., *Chem. Commun.* **1997**, 1427-1428.

148. Wei, P.; Keizer, T.; Atwood, D. A., *Inorg. Chem.* **1999,** 38, 3914-3918.

149. Sanchez, M.; Sanchez, O.; Hopfl, H.; Ochoa, M.-E.; Castillo, D.; Farfan, N.; Rojas-Lima, S., *J. Organomet. Chem.* **2004,** 689, 811-822.

150. Sanchez, M.; Hopfl, H.; Ochoa, M. E.; Farfan, N.; Santillan, R.; Rojas, S., *Inorg. Chem.* **2001,** 40, 6405-12.

151. Modro, T. A., *J.Chem. Soc. Chem. Commun.* **1980,** 5, 201-202.

152. Gauvry, N.; Mortier, J., *Synthesis* **2001**, 553-554.

153. Blanksby, S. J.; Ellison, G., *Acc. Chem. Res.* **2003,** 36, 255-263.

154. Zhao, Q.; Sitrin, R., *Anal. Biochem.* **2001,** 295, 76-81.

155. Sturgess, A. W.; Rush, K.; Charbonneau, R. J.; Lee, J. I.; West, D. J.; Sitrin, R. D.; Hennessey, J. P., Jr., *Vaccine* **1999,** 17, 1169-1178.

156. Kitagawa, Y.; Hashimoto, S.; Iemura, S.; Yamamoto, H.; Nozaki, H., *J. Am. Chem. Soc.* **1976,** 98, 5030-31.

157. Pinkas, J.; Wessel, H.; Yang, Y.; Montero, M. L.; Noltemeyer, M.; Froeba, M.; Roesky, H. W., *Inorg. Chem.* **1998,** 37, 2450-2457.

158. Pinkas, J.; Chakraborty, D.; Yang, Y.; Murugavel, R.; Noltemeyer, M.; Roesky, H. W., *Organometallics* **1999,** 18, 523-528.

159. Pinkas, J.; Loebl, J.; Dastych, D.; Necas, M.; Roesky, H. W., *Inorg. Chem.* **2002,** 41, 6914-6918.

160. Ember, L., *Chem. Eng. News.* **1999,** 77, 11.

161. Ember, L., *Chem. Eng. News.* **2003,** 81, 26-27.

162. Hileman, B., *Chem. Eng. News.* **2000,** 78, 11.

163. Strater, N.; Klabunde, T.; Tucker, P.; Witzel, H.; Krebs, B., *Science* **1995,** 268, 1489-92.

164. Klabunde, T.; Straeter, N.; Froehlich, R.; Witzel, H.; Krebs, B., *J. Mol. Biol.* **1996,** 259, 737-748.

165. Dietrich, M.; Muenstermann, D.; Suerbaum, H.; Witzel, H., *Eur. J. Biochem.* **1991,** 199, 105-13.

166. Aquino, M. A. S.; Lim, J. S.; Sykes, G., *J. Chem. Soc. Dalton Trans.* **1992**, 2135-6.

167. Grieco, P. A.; Hiroi, K.; Reap, J. J.; Noguez, J. A., *J. Org. Chem.* **1975,** 40, 1450-1453.

168. Olah, G., *Friedel-Crafts and Related Reactions*. Interscience: New York, 1963; Vol. 4.

169. Vaultier, M.; Carboni, B., Boron In *Comprehensive Organometallic Chemistry II A Review of the Literature 1982-1994* Wilkinson, G.; Stone, G. A.; Abel, E. W., Eds. Elsevier: Oxford, U.K., 1995; Vol. 11.

170. Tas, E.; Kasumov, V. T.; Sahin, O.; Ozdemir, M., *Trans. Met. Chem.* **2002,** 27, 442-446.

171. Bent, H. A., *Chem. Rev.* **1961,** 61, 275-311.

172. Hopfl, H., *J. Organomet. Chem.* **1999,** 581, 129-149.

173. Sanchez, M.; Keizer, T. S.; Parkin, S.; Hopfl, H.; Atwood, D. A., *J. Organomet. Chem.* **2002,** 654, 36-43.

174. Sheldrick, G. M. *SHELXS97 and SHELXL97*, University of Göttingen, Germany: Göttingen, 1997.

175. Sheldrick, G. M. *SHELXTL-plus*, Siemens Analytical X-ray Instruments Inc.: Madison, Wisconsin, 1997.

176. Sheldrick, G. M. *SHELXTL*, version 5.0; Bruker AXS Inc.: Madison, Wisconsin, 1998.

177. Siemens *R3m Software*, version 4.0; Siemens Analytical X-ray Instruments Inc.: Madison, Wisconsin, 1990.

178. Clearfield, A., *Chem. Mater.* **1998,** 10, 2801-2810.

179. Clearfield, A., *Inorganic Ion Exchange Materials*. CRC Press, Inc.: Boca Raton, Fla., 1982.

180. Lugmair, C. G.; Tilley, T. D., *Inorg. Chem.* **1998,** 37, 1821-1826.

181. Clearfield, A.; Sharma, C. V. K.; Zhang, B. P., *Chem. Mater.* **2001,** 13, 3099-3112.

182. Shah, S. A. A.; Dorn, H.; Gindl, J.; Noltemeyer, M.; Schmidt, H. G.; Roesky, H. W., *J. Organomet. Chem.* **1998,** 550, 1-6.

183. Dorn, H.; Vejzovic, E.; Lough, A. J.; Manners, I., *Can. J. Chem.* **2002,** 80, 1650-1654.

184. Swamy, K. C. K.; Veith, M.; Huch, V.; Mathur, S., *Inorg. Chem.* **2003,** 42, 5837-5843.

185. Shihada, A. F.; Weller, F., *Z. Anorg. Alg. Chem.* **2001,** 627, 638-644.

186. Swamy, K. C. K.; Said, M. A.; Nagabrahmanandachari, S.; Poojary, D. M.; Clearfield, A., *Dalton Trans.* **1998**, 1645-1651.

187. Wang, Y.; Parkin, S.; Atwood, D., *Chem. Commun.* **2000**, 1799-1800.

188. Wang, Y.; Parkin, S.; Atwood, D., *Inorg. Chem.* **2002,** 41, 558-65.

189. Hahn, F. E.; Schneider, B.; Reier, F. W., *Z. Naturforsch.* **1990,** 45B, 134-140.

190. Browning, D. J.; Corker, J. M.; Webster, M., *Acta Cryst.* **1996,** C52, 882-884.

191. Quinn, L. D., In *A Guide to Organophosphorus Chemistry*, Wiley Interscience: 2000; p 197.

192. Corbridge, D. E. C., *The Structural Chemistry of Phosphorus.* Elsevier: Amsterdam, Netherlands, 1974.

193. Walawalkar, M. G.; Murugavel, R.; Roesky, H. W.; Schmidt, H. G., *Organometallics* **1997,** 16, 516-518.

194. Hill, M. S.; Atwood, D. A., *Main Group Chem.* **1998,** 2, 191-202.

195. Duxbury, J. P.; Cawley, A.; Thornton-Pett, M.; Wantz, L.; Warne, J. N. D.; Greatrex, R.; Brown, D.; Kee, T. P., *Tet. Lett.* **1999,** 40, 4403-4406.

196. Sammis, G. M.; Danjo, H. J.; Jacobsen, E. N., *J. Am. Chem. Soc.* **2004,** 126, 9928-9929.

197. Taylor, M. S.; Jacobsen, E. N., *J. Am. Chem. Soc.* **2003,** 125, 11204-11205.

198. Vanderwal, C. D.; Jacobsen, E. N., *J. Am. Chem. Soc.* **2004,** 126, 14724-14725.

199. Munoz-Hernandez, M.-A.; Keizer, T. S.; Wei, P.; Parkin, S.; Atwood, D. A., *Inorg. Chem.* **2001,** 40, 6782-6787.

200. Magesh, C. J.; Makesh, S. V.; Perumal, P. T., *Bioorg. Med. chem. Lett.* **2004,** 14, 2035-2040.

201. Atwood, D. A.; Jegier, J. A.; Rutherford, D., *Inorg. Chem.* **1996,** 35, 63-70.

202. Munoz-Hernandez, M.-A.; Sannigrahi, B.; Atwood, D. A., *J. Am. Chem. Soc.* **1999,** 121, 6747-6748.

203. Mitra, A.; DePue, L. J.; Parkin, S.; Atwood, D. A., *J. Am. Chem. Soc.* **2006,** 128, 1147-1153.

204. Deng, L.; Jacobsen, E. N., *J. Org. Chem.* **1992,** 57, 4320-4323.

205. Rutherford, D.; Atwood, D. A., *Organometallics* **1996,** 15, 4417-4422.

206. Atwood, D. A.; Hill, M. S.; Jegier, J. A.; Rutherford, D., *Organometallics* **1997,** 16, 2659-2664.

207. Dzugan, S. J.; Goedken, V. L., *Inorg. Chem.* **1986,** 15, 2858-64.

208. Addison, A. W.; Rao, T. N.; Reedijk, J.; Van Rijn, J.; Verschoor, G. C., *J. Chem. Soc. Dalton Trans.* **1984**, 1349-56.

209. El-Bahraoui, J.; Wiest, O.; Feichtinger, D.; Plattner, D. A., *Angew. Chem. Int. Ed. Engl.* **2001,** 40, 2073-2076.

210. Marlin, D. S.; Olmstead, M. M.; Mascharak, P. K., *Inorg. Chem.* **2001,** 40, 7003-7008.

211. Jegier, J. A.; Atwood, D. A., *Inorg. Chem.* **1997,** 36, 2034-2039.

212. Atwood, D. A.; Rutherford, D., *Organometallics* **1995,** 14, 3988-95.

213. Corbridge, D. E. C., *Phosphorus: An Outline of its Chemistry, Biochemistry and Technology*. 5th ed.; Elsevier: Amsterdam, Netherlands, 1995; Vol. 6, p 1147.

214. Mitra, A.; Parkin, S.; Atwood, D. A., *Inorg. Chem.* **in press**.

215. Albanese, D.; Landini, D.; Maia, A., *J. Org. Chem.* **2001,** 66, 3249-3252.

216. Lum, R. C.; Grabowski, J. J., *J. Am. Chem. Soc.* **1992,** 114, 8619-27.

217. Delpuech, J. J., Aluminum-27. In *NMR of Newly Accessible Nucl*, Laslo, P., Ed. Academic Press: New York, 1983; Vol. 2, pp 153-195.

218. Thomas, J. M.; Raja, R.; Sankar, G.; Bell, R. G., *Acc. Chem. Res.* **2001,** 34, 191-200.

219. Hartmann, M.; Kevan, L., *Chemical Reviews* **1999,** 99, 635-663.

220. Kongshaug, K. O.; Fjellvag, H.; Lillerud, K. P., *Microporous and Mesoporous Materials* **1999,** 32, 17-28.

221. Wilson, S. T.; Lok, B. M.; Messina, C. A.; Cannan, T. R.; Flanigen, E. M., *J. Am. Chem. Soc.* **1982,** 104, 1146-1147.

222. Wilson, S. T., Zeolite Science and Practice In *Studies in Surface Science and Catalysis*, vanBekkum, H.; Flanigen, E. M.; Jansen, J. C., Eds. Elsevier: Amsterdam, 1991; Vol. 58, p 137.

223. Song, Y.; Li, J. Y.; Yu, J. H.; Wang, K. X.; Xu, R. R., *Topics in Catalysis* **2005,** 35, 3-8.

224. Medina, M. E.; Iglesias, M.; Gutierrez-Puebla, E.; Monge, M. A., *J. Mater. Chem.* **2004,** 14, 845-850.

225. Lugmair, C. G.; Tilley, T. D.; Rheingold, A. L., *Chem. Mater.* **1999,** 11, 1615-1620.

226. Wang, Y.; Bhandari, S.; Mitra, A.; Parkin, S.; Moore, J.; Atwood, D. A., *Z. Anorg. Allg. Chem.* **2005,** 631, 2937-2941.

227. Tuel, A.; Gramlich, V.; Baerlocher, C., *Microporous and Mesoporous Mater.* **2002,** 56, 119-130.

Vita

Amitabha Mitra was born in Sylhet, Bangladesh on September 6, 1974. He obtained his Secondary School Certificate from Pabna Zilla School in 1989 and Higher Secondary School Certificate from Pabna Edward College in 1991. He received the Bachelor of Science degree (Honors in Chemistry) from the St. Xavier's College, Calcutta, India, in 1995, and the Bachelor of Technology degree in Polymer Science and Technology from the University of Calcutta, India, in 1998. He held the position of a lecturer at the Shahjalal University of Science and Technology, Sylhet, Bangladesh from 1998 to 2000. He joined the Graduate program in Chemistry at the University of Kentucky, in Spring, 2001, and started his Ph.D. research in the group of Dr. David Atwood in the following summer. He is a member of the American Chemical Society. He has accepted a position as a postdoctoral research fellow in the group of Prof. Robert West at the University of Wisconsin, Madison.

List of publications:

1. Mitra, A.; Parkin, S.; Atwood, D. A., First example of a borate-bridged dimeric aluminum Schiff-base complex containing five-coordinate metal centers. *Main Gr. Chem.* **2005,** 4, (1), 91-96.
2. Mitra, A.; Atwood, D. A., Phosphate ester cleavage with binuclear boron chelates. *ACS Symp. Ser.* **2005,** 917, 389-408.

3. Mitra, A.; Atwood, D. A., Polysiloxanes and polysilanes. In *Encyclopedia of Inorganic Chemistry*, 2nd ed.; King, R. B., Ed. Wiley Interscience: Chichester, England, **2005**; pp 4593-4610.
4. Wang, Y.; Bhandari, S.; Mitra, A.; Parkin, S.; Moore, J.; Atwood, D. A., Ambient-condition nano-alumina formation through molecular control. *Z. Anorg. Allg. Chem.* **2005,** 631, (13-14), 2937-2941.
5. Mitra, A.; DePue, L. J.; Parkin, S.; Atwood, D. A., Five-coordinate aluminum bromides: synthesis, structure, cation formation and cleavage of phosphate ester bonds. *J. Am. Chem. Soc.* **2006,** 128, (4), 1147-1153.
6. Mitra, A.; Harvey, M. J.; Proffitt, M. K.; DePue, L. J.; Parkin, S.; Atwood, D. A., Binuclear Salan borate compounds with three-coordinate boron atoms. *J. Organomet. Chem.* **2006,** 691, (3), 523-528.
7. Mitra, A.; Parkin, S.; Atwood, D. A., Aluminum phosphinate and phosphates of Salen ligands. *Inorg. Chem.* **2006,** 45, (10), 3970-3975.
8. Mitra, A.; Wei, P.; Atwood, D. A., Tripodal saltrenAl(^{i}Bu)(Cl). *Main Gr. Chem.*(in press).
9. Mitra, A.; Atwood, D. A., Aluminium. In *Comprehensive Organometallic Chemistry III: From Fundamentals to Applications*, Crabtree, R. H., Ed. Elsevier: Oxford, U.K. (in press).
10. Mitra, A.; DePue, L. J.; Struss, J. E.; Patel, B. P.; Parkin, S.; Atwood, D. A., Mononuclear Schiff base boron halides: synthesis, characterization and dealkylation of organophosphate esters. *Inorg. Chem*. (in press).